MESOSCOPIC FUEL CONSUMPTION AND EMISSION MODELING

By

Huanyu Yue

Dissertation submitted to the Faculty of the
Virginia Polytechnic Institute and State University
In partial fulfillment of the requirements for the degree of

Doctor of Philosophy
in
Civil and Environmental Engineering

Hesham A. Rakha, Chair
Antonio A. Trani
Hojong Baik
Kyoungho Ahn
Montasir M. Abbas

March 25, 2008
Blacksburg, Virginia

Key Words: Fuel consumption and emission modeling, ITS evaluation, Mesoscopic modeling, INTEGRATION, High Emitter

MESOSCOPIC FUEL CONSUMPTION AND EMISSION MODELING

Huanyu Yue

ABSTRACT

The transportation sector is a major contributor to U.S. fuel consumption and emissions. Consequently, assessing the environmental impacts of transportation activities is essential for air-quality improvement programs. Current state-of-the-art models estimate vehicle emissions based on typical urban driving cycles. Most of these models offer simplified mathematical expressions to compute fuel consumption and emission rates based on average link speeds while ignoring transient changes in a vehicle's speed and acceleration level as it travels on a highway network. Alternatively, microscopic models capture these transient effects; however, the application of microscopic models may be costly and time consuming. Also, these tools may require a level of input data resolution that is not available. Consequently, this dissertation attempts to fill the void in energy and emission modeling by a framework for modeling vehicle fuel consumption and emissions mesoscopically. This framework is utilized to develop the VT-Meso model using a number of data sources. The model estimates average light-duty vehicle fuel consumption and emission rates on a link-by-link basis using up to three independent variables, namely: average travel speed, average number of stops per unit distance, and average stop duration.

The mesoscopic model utilizes a microscopic vehicle fuel consumption and emission model that was developed at Virginia Tech to compute mode-specific fuel consumption and emission rates. This model, known as VT-Micro, predicts the instantaneous fuel consumption and emission rates of HC, CO and NO_x of individual vehicles based on their instantaneous speed and acceleration levels. The mesoscopic model utilizes these link-by-link input parameters to construct a synthetic drive cycle and compute average link fuel consumption and emission rates. After constructing the drive cycle, the model estimates the proportion of time that a vehicle typically spends cruising, decelerating, idling and accelerating while traveling on a link. A series of fuel consumption and emission models are then used to estimate the amount of fuel consumed and emissions of HC, CO, CO_2, and NO_X emissions for each mode of operation. Subsequently, the total fuel consumed and pollutants emitted by a vehicle while traveling along a segment are estimated by summing across the different modes of operation and dividing by the distance traveled to obtain distance-based average vehicle fuel consumption and emission rates. The models are developed for normal and high emitting vehicles.

The study quantifies the typical driver deceleration behavior for incorporation within the model. Since this model constructs a drive cycle which includes a deceleration mode, an accurate characterization of typical vehicle deceleration behavior is critical to the accurate modeling of vehicle emissions. The study demonstrates that while the deceleration rate typically increases as the vehicle approaches its desired final speed, the use of a constant deceleration rate over the entire deceleration maneuver is adequate for environmental modeling purposes.

Finally, the study validates the model on a freeway and urban arterial network. The results demonstrate that the model provides accurate estimates of vehicle fuel consumption and emission rates and is adequate for the evaluation of transportation operational projects.

ACKNOWLEDGEMENTS

First of all, I would especially like to express my sincere gratitude to my adviser, Dr. Hesham Rakha, for his generous time and commitment. I am very much thankful to him for the guidance and the encouragement he provided for my academic study and personal issues. Without his help, I could not have completed my study. I am greatly indebted to him for the financial assistance that he provided to me for completing my graduate study.

I also would like to express my sincere appreciation to Dr. Kyoungho Ahn and Dr. Ihab EI-Shawarby, who gave me invaluable academic advice. My thankfulness also goes to Dr. Antonio Trani, Dr. Hojong Baik, and Dr. Montasir Abbas, for serving as my committee members and giving support to me whenever needed.

To thank my friends at Virginia Tech, thank you for the great memories.

And finally, sincere gratitude goes to my parents and my brother. Their endless love for me always encourages me to make progress.

ATTRIBUTION

Several colleagues and coworkers aided in the writing and research behind several of the chapters of this dissertation. A brief description of their background and their contributions are included here.

Prof. Hesham A. Rakha - Ph.D. (Department of Civil Engineering, Virginia Tech) is the primary Advisor and Committee Chair. Prof. Rakha provided extensive guidance toward all the chapters of this dissertation and advice on the research. Furthermore, Prof. Rakha provided necessary software and hardware equipments for the research.

Chapter 3: VT-Meso Model for Estimating Hot Stabilized Light Duty Vehicle Fuel Consumption and Emission Rates

Francois Dion - Ph.D. (Department of Civil Engineering, University of Waterloo) currently at University of Michigan Transportation Research Institute was a research scientist in the author's group and contributed to this chapter in terms of discussing VT-Mesoscopic model framework.

TABLE OF CONTENT

LIST OF TABLES

LIST OF FIGURES

Chapter 1 : INTRODUCTION

Increase in car ownership in the US, population growth, and the increase in the average annual miles traveled per person has resulted in deterioration in the air quality in many metropolitan areas. The Clean Air Act Amendments of 1990 (CAAA) and the Intermodal Surface Transportation Efficiency Act of 1991 (ISTEA) place great emphasis on the use of transportation controls to meet air quality standards in nonattainment areas. Specifically, these regulations ensure that only highway projects that do not degrade the air environment are implemented.

The transportation sector is the dominant source of U.S. fuel consumption and emissions. Specifically, transportation accounts for 60 percent of the total petroleum consumed, and highway vehicles account for nearly three-fourths of the total transportation use NRC 1995. A reduction in fuel consumption will lead to reduction in carbon dioxide emissions. To make matters worse, the fuel economy of an average new light duty vehicle sold in the US has declined from 9.3 km/L (22.1 mi/gallon) in 1987-1988 to 8.36 km/L (20.4 mi/gallon) in 2001 (Hellman and Heavenrich 2001).

The transportation sector is the source of 41 percent of the Hydrocarbon (HC) emissions, 79 percent of carbon monoxide (CO) emissions, and 51 percent of Oxides of Nitrogen (NO_x) emissions (EPA 1996). Highway vehicles, which contribute more than one-third of the total nationwide emissions, are the largest source of transportation-related emissions (Nizich and United States. Environmental Protection Agency. Office of Air Quality Planning and Standards. 1994). Highway motor vehicles contribute 29 percent of HC emissions, 60 percent of CO emissions, and 31 percent of NO_X emissions.

1.1 Problem Definition

Macroscopic transportation planning models and macroscopic vehicle fuel consumption and emission models are currently the primary tools for evaluating the regional impacts of transportation projects. In typical applications, a transportation planning model such as TRANPLAN (The Urban Analysis Group 1992), MINUTP (The Seider Group 1997) or EMME/2 (INRO Consultants 1996) is first used to determine the average speed and total vehicle-miles of travel for the network or facility being considered. Then, an emission model such as MOBILE6 (EPA 1994) or EMFAC (CARB 1991) is used to compute the average fuel consumption and emission rates for the facility. Within this step, a base emission rate reflecting fuel consumption and emission measurements that were gathered in a laboratory using pre-defined test drive cycles is first selected for the facility considered. This base rate is then modified to account for differences in average speeds between the laboratory and real-world cycles, as well as for differences in temperature, vehicle load, fleet composition, accrued mileage of vehicles within the fleet, type of fuel used, and vehicle operating conditions. Total fuel consumption and emissions are finally obtained by multiplying the resulting rates by the estimated vehicle miles traveled on the facility.

In the macroscopic approach, single fuel consumption and emission rates are produced for each average speed input. These rates are produced under the assumptions that all vehicles pollute similarly for the same average speed and vehicle-miles traveled and that variations in driver

behavior can be neglected (An, Barth et al. 1997). This presents a problem when the drive cycles encountered in the field differ from those assumed within the models, since estimated emission rates may not correspond to actual emissions. A particular problem occurs when comparing drive cycles with identical average speeds, as identical emission rates would then be estimated for all cycles despite differences in the second-by-second speed profiles. For example, Table 1-1 presents the fuel consumption and emission rates of hydrocarbon (HC), carbon monoxide (CO) and oxides of nitrogen (NO_X) for three scenarios exhibiting identical average speeds that were estimated using microscopic models analyzing speed profiles on a second-by-second basis. The only difference between the three scenarios is the number of stops made along the traveled link and the resulting cruise speeds to maintain the same average travel speed. All other parameters affecting the drive cycles, such as deceleration and acceleration rates, were held constant. As can be observed, significant differences exist in fuel consumption and emission rates despite the identical average speeds, thus indicating a need to look beyond the average speed as a single explanatory variable.

Table 1-1: Impact of Vehicle Stops on Fuel Consumption and Emissions

	Scenario 1	Scenario 2	Scenario 3
Trip length (km)	2.0	2.0	2.0
Average speed (km/h)	50.0	50.0	50.0
Number of stops	0	1	2
Cruise speed (km/h)	50.0	55.3	63.3
Fuel consumed (L)	0.175	0.204	0.250
HC emissions (mg)	163.2	202.7	290.3
CO emissions (mg)	2778.0	3638.7	5775.5
NO_x emissions (mg)	215	415.1	745.6

1.2 Research Objective

The primary objective of this dissertation is to develop a modal fuel consumption and emissions model that attempts to make predictions using a limited number of easily measurable input parameters. The model also allows the modeler to calibrate two additional input parameters, namely: typical driver deceleration and acceleration rates. This model is more accurate than current macroscopic models but less data intensive than microscopic models. This model can be used to perform quick evaluations of alternative scenarios without requiring detailed data or modeling as demanded by the use of microscopic models.

1.3 Research contributions

This dissertation develops mesoscopic fuel consumption and emission models for light-duty normal vehicles, trucks, and heavy-duty vehicles under cold start and hot stabilized conditions. Furthermore, models are developed for high emitting vehicles with some engine malfunction.

This model uses average travel speed, number of vehicle stops per unit distance, and average stopped delay to construct synthetic drive cycles for the roadway segments considered, and then predicts average fuel consumption and emission rates by analyzing the deceleration, idling, acceleration and cruising portions of the cycle. It is anticipated that the mesoscopic model will provide significant practical and methodological benefits to local transportation planners and traffic engineers to estimate fuel consumption and pollutants. The model will assist in the evaluation of various transportation operational projects including Intelligent Transportation System (ITS) investments. More specifically, this research effort makes the following contributions.

- Develops a framework for modeling vehicle emissions mesoscopically,
- Characterizes typical driver deceleration behavior for environmental modeling,
- Develops mesoscopic energy and emission models for normal light-duty cars, trucks, and heavy-duty vehicles under cold start and hot-stabilized conditions,
- Develops mesoscopic energy and emission models for vehicles with engine malfunctions, namely high emitting vehicles.

1.4 Dissertation Layout

The dissertation is divided into seven chapters. Chapter 2 provides an overview of the state-of-the-art vehicle fuel consumption and emission models. This chapter reviews various existing fuel consumption and emission models. Furthermore, the factors affecting fuel consumption and emission rates are discussed. Chapter 3 utilizes the proposed framework to develop mesoscopic vehicle fuel consumption and emission models for normal light-duty vehicles. Chapter 4 characterizes typical driver deceleration behavior for environmental modeling. The typical driver deceleration rate is used as input to the VT-Meso model. In chapter 5, the model is expanded to predict vehicle fuel consumption and emissions for hot stabilized high-emitting vehicles. In chapter 6, the INTEGRTION simulation package was used to generate different drive cycles. The outputs from INTEGRATION were used as inputs to the VT-Meso model. Subsequently, the VT-Meso model estimates were compared against estimates from a microscopic vehicle fuel consumption and emissions model. Finally, Chapter 7 provides a summary of the findings and the conclusions of the research effort.

Chapter 2 : LITERATURE REVIEW

This chapter begins by summarizing the current environment standards and regulations, which is the motivation for this research effort. This section then summarizes the current state-of-the-art and state-of-practice vehicle fuel consumption and emission models and model development efforts. In addition, the assumptions, domain of application, and shortcomings of these models are discussed. The objective of this chapter is to provide the reader with a background of the current state-of-art and current state-of-practice in vehicle fuel consumption and emission modeling.

2.1 Emission Standards and Regulations

Since the early 40's air pollution received great attention in the United States. Many regulations and standards were enacted during last 60 years. With the emergence of the new technologies emissions per VMT for new cars and light trucks decreased by roughly 90 percent from the uncontrolled level by 1988. Total VMT, however, increased 2.3 percent annually during 1970s and 1980s due to the increase of number of vehicles, thereby offsetting some of the improvements (Atkinson 1990).

2.1.1 Air Pollution Control of 1995

The first federal legislation regarding air pollution is The Air Pollution Control Act of 1955. Additional research and education on air pollution were suggested by this Act. This Act mandated and provided funds for federal research in air pollution. This Act also authorized the federal government to provide technical assistance to state government. However, this Act did not enact any restriction on polluters.

2.1.2 Clean Air Act

The Clean Air Act (CAA) replaced the Air Pollution Act of 1955, the Clean Air Act was signed in 1963. The first major amendment was made to it in 1970. Four major regulatory programs were initiated by this amendment: the National Ambient Air Quality Standards (NAAQS), State Implementation Plans (SIPs), New Source Performance Standards (NSPS), and National Emission Standards for Hazardous Air Pollutants (NESHAPs). To implement of the Clean Air Act, the Environmental Protection Agency (EPA) was created in 1971. The clean Air Act of 1970 was amended in 1977. The 1977 CAA Amendments provided a longer and realistic time frame for the areas that achieve not attained NAAQS to achieve compliance with the NAAQS. The Clean Air Act was amended again in 1990.

The NAAQS provide threshold concentrations for six pollutants: carbon monoxide (CO), .lead (pb), nitrogen dioxide (NO_2), ozone (O_3), particulate matter (PM-10), and sulfur dioxide (SO_2) (NRC 1995). The NAAQS are comprised of a primary standard for each criteria pollutant. The 1970 Amendment imposed automobile standards for 1975 models to achieve clean air by setting the 0.41 gram per mile HC standard and the 3.4 grams per mile CO standard. These standards were not achieved and the government delayed the HC standard until 1980 and the CO standard until 1981 in the Clean Air Act of 1977.

The 1990 Clean Air Act Amendment established criteria for attaining and maintaining the NAQQS by defining geographic regions within the US that do not meet the NAAQS and are classified as nonattainment areas. Depending on the percentage by which the ambient concentration of pollutants is greater than the NAAQS, the classifications are marginal, moderate, serious, severe, and extreme. Table 2-1 shows the NAAQS classification of level of Nonattainment for Ozone and CO. Every nonattainment area is required to take certain action within a set time frame to attain the NAAQS.

Table 2-1: Classification of Level of Nonattainment of NAAQS for Ozone and CO, Source: (NRC 1995)

Pollutant	Classification	Design Value (ppm)	Attainment Deadline
Ozone	Marginal	0.121 up to 0.138	11/15/1993
	Moderate	0.138 up to 0.160	11/15/1996
	Serious	0.160 up to 0.18	11/15/1999
	Severe 1	0.18 up to 0.19	11/15/2005
	Severe 2	0.19 up to 0.28	11/15/2007
	Extreme	0.28 and above	11/15/2010
CO	Moderate	9.1 up to 12.7	12/31/1995
	Marginal	12.8 up to 16.4	12/31/1995
	Serious	16.5 and above	12/31/2000

The 1990 Clean Air Act Amendment required that areas of moderate or worse ozone classification must submit revision to State Implementation Plans (SIPs). For these areas ozone should be reduced by at least 15 percent during this period, and the ozone emissionshould be reduced by three percent every year until attainment is achieved. Furthermore, severe and extreme areas are required to adopt transportation control measures (TCMs).

The SIP need to be approved by EPA and after the draft SIP is approved by EPA, the SIP is included in the Code of Federal Regulations (Title 40, Part 52) and becomes federally enforceable. If a transportation plan or project does not meet conformity requirements, transportation officials must modify the plan or project to offset the negative emission impacts, or modify the SIP to offset the plan or project emissions. The plan or project can not advance in case these actions can not be accomplished. If a SIP needs to be revised, the EPA will take relumaking on SIP revision. Failure to create and implement a SIP to meet the CAAA requirements will result in such sanctions enforced as withholding Federal Highway Funding, or withholding grants for air pollution planning, or two-to-one emission offsets for major stationary sources.

2.1.3 Intermodal Surface Transportation Efficiency Act (ISTEA)

Following the CAAA of 1990, the 1991 Intermodal Surface Transportation Efficiency Act (ISTEA) allowed transfer of highway funds to transit and other cleaner transportation modes and enhance the planning responsibilities of MPOs that were responsible for conformity analysis. Two programs were established by ISTEA to set aside funding for environmental activities: Congestion Mitigation and Air Quality Improvement (CMAQ) and Surface Transportation Program (STP). The objective of AMAQ is to provide alternatives to conventional highway travel, reduce vehicle miles traveled (VMT). CMAQ assists states to comply with federal air quality standards by funding transportation projects that lower emissions, this program will assist nonattainment areas to achieve the NAAQS. Under STP states must reserve 10% of their funding for environmentally related transportation projects.

2.1.4 California Standards

California emission standards are the strictest in the country. California's standard set emission levels for five categories of vehicles: (1) conventional vehicles (CVs); (2) transitional low-emission vehicles (TLEVs); (3) low-emission vehicles (LEVs); (4) ultra-low emission vehicles (ULEVs); and (5) zero-emission vehicles (ZEVs). All automobile manufacture may be forced to meet more stringent emission standards if the more stringent standard becomes widely accepted; even though different regions have different air quality conditions (NRC 1995). The marketing cars should comply with California Standards, which means that the regulations in California may drive research and development of new control technologies which could be used nationally. Since November 2000 EPA tried to push California standards nationwide, which was stated in EPA November 2000 Advance Notice of Proposed Rulemaking (ANPR).

2.2 Vehicle Fuel Consumption and Emissions Modeling

Many approaches have been developed to estimate vehicle fuel consumption and emission rates. Based on the scale of the input variables the current-state-of-art and current-state-of-practice models can be divided into three categories: microscopic models, mesoscopic models, and macroscopic models. Microscopic models use instantaneous speed and acceleration data to estimate vehicle fuel consumption and emission rates, the estimations from microscopic models are instantaneous rates as well. Macroscopic models use aggregate network or link-based parameters to estimate network-wide or link-based fuel consumption and emission rates. Mesoscopic models use scales that lie between the macroscopic scale and microscopic scale.

2.2.1 Microscopic Vehicle Fuel Consumption and Emissions Models

Instantaneous fuel consumption models are derived from a relationship between the fuel consumption rates and the instantaneous vehicle power. Second-by-second vehicle characteristics and road conditions are required in order to estimate fuel consumption. Due to the disaggregate characteristics of the fuel consumption data, these models are usually used to evaluate individual transportation projects. Instantaneous fuel consumption models can be used in microscopic traffic simulation packages to estimate fuel consumption based on instantaneous speeds and accelerations of individual vehicles.

VT-Microscopic Vehicle Fuel Consumption and Emission Model

Rakha and Ahn developed a microscopic vehicle fuel consumption and emission model (Ahn, Trani et al. 1999, Rakha, Van Aerde et al. 2000, Ahn, Rakha et al. 2002). This model, known as VT-Micro, predicts the instantaneous fuel consumption and emission rates of HC, CO, NO_X and CO_2 of individual vehicles based on their instantaneous speed and acceleration levels. The instantaneous speed/acceleration data and fuel consumption and emission measurements were collected by the Oak Ridge National Lab (ORNL) for eight light-duty vehicles and light-duty trucks. Speed and acceleration variation have significant impacts on vehicle fuel consumption and emissions. This model is intent to capture the effects of these two important factors.

Equation [2-1] describes the general format of the equations used by the VT-Micro models to predict the instantaneous fuel consumption and emission rates of individual vehicles.

$$MOE_e = \begin{cases} \sum_{i=0}^{3}\sum_{j=0}^{3} \exp\left(k_{i,j}^{e} \cdot v^i \cdot a^j\right) & \text{for } a \geq 0 \\ \sum_{i=0}^{3}\sum_{j=0}^{3} \exp\left(l_{i,j}^{e} \cdot v^i \cdot a^j\right) & \text{for } a < 0 \end{cases} \qquad [2\text{-}1]$$

where: MOE_e = Instantaneous fuel consumption or emission rate (L/s or mg/s),
a = Instantaneous acceleration of vehicle (km/h/s),
v = Instantaneous speed of vehicle (km/h),
$k^e_{i,j}$ = Vehicle-specific acceleration regression coefficients for MOE_e, and
$l^e_{i,j}$ = Vehicle-specific deceleration regression coefficients for MOE_e.

Two sets of coefficients are used for this equation: coefficients for accelerating, idling, and cruising and coefficients for decelerating. This split was implemented in the microscopic models to account for differences in emission rate sensitivity to speed between acceleration and deceleration modes of operation of vehicles. Another important feature is the use of natural logarithms to ensure that non-negative fuel consumption and emission rates are produced by the models.

Figure 2-1 illustrates the evaluation results for a composite vehicle having the average characteristics of the eight ORNL test vehicles. This figure shows that VT-Micro model is able to follow very closely the trends in increasing fuel consumption with higher speeds and sharper acceleration, this model provide good fit in terms of the absolute values of vehicle fuel consumption and emission rates. The model estimates vehicle fuel consumption to within 2.5 percent of actual measured field values. The model has been incorporated within INTEGRATION, a microscopic traffic simulation package, to further demonstrate its application to traffic engineering and management studies.

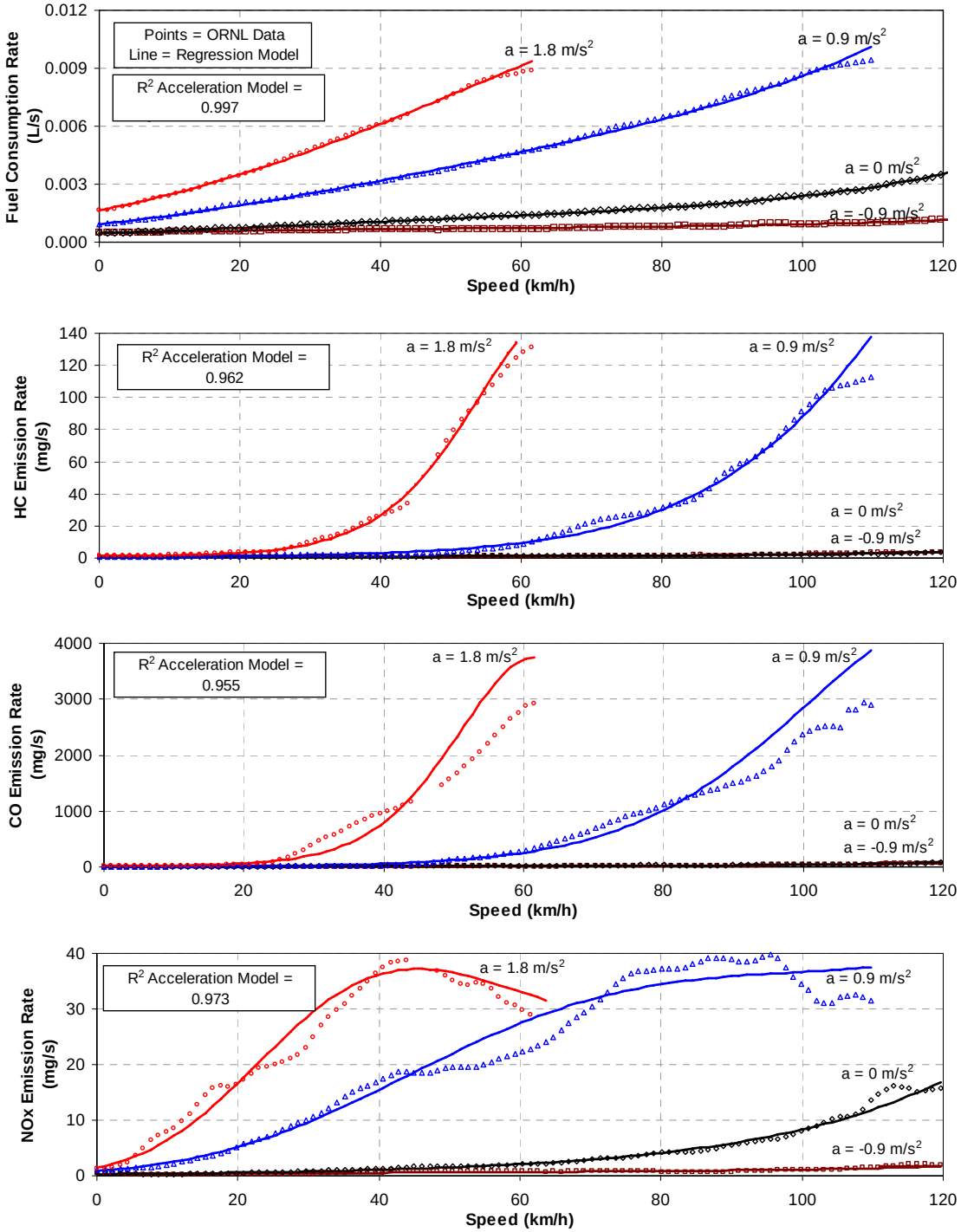

Figure 2-1: VT-Microscopic Models for ORLN Composite Vehicle (Ahn, Rakha et al. 2002)

CMEM Model

An *et al.* (An, Barth et al. 1997) developed a modal emissions model, which is based on a simple parameterized physical approach and consists of six modules that predict engine power, engine speed, air/fuel ratio, fuel use, engine-out emissions, and catalyst pass fraction. This model was built from in-house dynamometer test on 300 real-world vehicles. Three dynamic variables, second-by-second speed, grade, and accessory use (such as air conditioning), were used as the input operating variables. The instantaneous emissions were modeled as the product of three components: fuel rate (FR), engine-out emissions indexes ($g_{emission}/g_{fuel}$), and catalyst pass fraction (CPF):

$$tailpipe\,emissions = FR \cdot \left(\frac{g_{emission}}{g_{fuel}} \right) \cdot CPF \qquad [2\text{-}2]$$

where,

FR = fuel-use rate in grams/s;
$g_{emissions}/g_{fuel}$ = grams of engine-out emissions per grams of fuel consumed; and
CPF = the catalyst pass fraction, defined as the ratio of tailpipe to engine-out emission.

The modal emissions model is composed of six modules: engine power demand, engine speed, air-fuel ratio, fuel rate, engine-out emissions, and catalyst pass fraction.

Engine Power Demand Module

$$P_{tract} = A \cdot v + B \cdot v^2 + C \cdot v^3 + M \cdot a + M \cdot g \cdot v \cdot \sin\theta$$
$$P = \frac{P_{tract}}{\eta_{tf}} + P_{acc} \qquad [2\text{-}3]$$

where,

P_{tract} = total tractive power (kw),
A = coefficient of rolling resistance
B = coefficient of speed-correction to rolling resistance
C = coefficient of air-drag factor
v = speed (m/sec)
a = acceleration (m/s^2),
g = the gravitational constant (9.81 m/s^2)
θ = the road grade angle,
P = the engine power output,
η_{tf} = the combined efficiency of the transmission and final drive,
P_{acc} = the engine power demand associated with the operation of vehicle accessories, such as air conditioning, power steering and brakes, and electrical loads.

For the engine speed module engine speed is simply to express it in vehicle speed, using gear ratios and a shift schedule to determine up- or downshift. In the air/fuel ratio module the air/fuel ratio is from three regions: lean, staichiometric, and rich.

Fuel rate Module

$$FR \approx \phi(kNV + \frac{P}{\eta})\frac{1}{44} \quad [2\text{-}4]$$

where,

k = the engine friction factor,
N = engine speed (revolutions per second),
V = engine displacement (liter),
$\eta \approx 0.4$ = a measure of indicated efficiency

Engine-out emissions Module

$$ECO \approx \left[C_0\left(1-\phi^{-1}\right)+a_{CO}\right]FR$$
$$EHC \approx a_{HC}FR + r_{HC}$$
$$ENO_x = a_{1NOx}\left(FR - FR_{NOx}\right)\phi < 1.05$$
$$ENO_x = a_{2NOx}\left(FR - FR_{NOx}\right)\phi \geq 1.05 \quad [2\text{-}5]$$

Catalyst Pass Fraction Module

$$CPF\left(ei\right) = 1 - \varepsilon_{ei} \cdot \exp\left\{\left[-b_{ei} - c_{ei} * \left(1-\phi^{-1}\right)\right] * FR\right\} \quad [2\text{-}6]$$

where,

ei = either CO or HC emissions,
ε_{ei} = the maximum catalyst CO or HC efficiency,
FR = the fuel rate (gram/second),
b_{ei} = the stoichoimetric CPF coefficients, and
c_{ei} = the enrichment CPF coefficient.

2.2.2 Macroscopic Vehicle Fuel Consumption and Emissions Models

Macroscopic models use average aggregate network parameters to estimate network-wide energy consumption and emission rates. Microscopic models estimate instantaneous vehicle fuel consumption and emission rates that are aggregated to estimate network-wide measures of effectiveness. Modal models estimate vehicle emissions for different operating modes.

Elemental Model

Elemental Model, which sued average speed, was proposed by Herman and coworkers (Chang, Evans et al. 1981; Evans and Herman 1978), it is a simple theoretically-based model expressing fuel consumption in urban conditions as a linear function of the average trip time per unit distance (reciprocal of average speed). This model is expressed as:

$$\Phi = K_1 + K_2 T, V < 55\ km/hr \quad [2\text{-}7]$$

Where,

Φ: fuel consumption per unit distance
T: average travel time per unit distance, and
V(=1/T): average speed

K_1 and K_2 are the model parameters. K_1 (in mL/km) represents to the vehicle mass. K_2 (in mL/sec) is a function of vehicle average speed.

In average speed models, fuel consumption rates are a function of trip time, trip distance, and average speed. Since these models do not adequately take into account aerodynamic drag resistance at high speeds, they should only be used for average speeds of less than 50 km/h. (Akcelik 1985).

Watson Model

Watson et al. (Waston, Milkins et al. 1980) used average speed to develop a fuel consumption model. The model incorporates the changes in the positive kinetic energy during acceleration as a predictor variable, namely,

$$F = K_1 + K_2/V_s + K_3 V_s + K_4 PKE \quad [2\text{-}8]$$

Where,
F = fuel consumed (L/km)
V_s = space mean speed (km/hr)

The term PKE represents the sum of the positive kinetic energy changes during acceleration in m/s^2, and is calculated as follows:

$$PKE = \sum \left(V_f^2 - V_i^2\right) / \left(12.960 X_s\right) \quad [2\text{-}9]$$

where,
V_f = final speed (km/hr) f
V_i = initial speed (km/hr) i
X_s = total section length (km)

When the average speeds are high enough, the aerodynamic effects on fuel consumption become significant. This occurs at average speeds over 55 km/h (Evans, Herman et al. 1976). It is easier to achieve steady-state speed requirement under highway driving conditions.

MOBILE and EMFAC Model

MOBILE and the EMission FACtors (EMFAC) EMFAC model are two emission models that are commonly utilized in the United States. MOBILE6 model was developed by the EPA, and the current version of MOBILE model is MOBILE6.2. The EMFAC model was developed by California Air Resources Board's (CARB's). EMFAC model is used only in the state of California, while MOBILE model is used in all other states. MOBILE and EMFAC has been used by state and local agencies for transportation planning and conformity analysis.

MOBILE model estimates are a function of vehicle's average speed, the vehicle's technology, the vehicle's age, the ambient temperature, fuel parameters, and the vehicle's operating mode (NRC 1995). Eight pollutants can be estimates by MOBILE6 model: hydrocarbons (HC), carbon monoxide (CO), oxides of nitrogen (NOx), carbon dioxide (CO_2), particulate matter (PM), sulfur dioxide (SO_2), ammonia (NH3), and six hazardous air pollutants (HAP). The CO_2 emission estimate from MOBILE6 is unlike other MOBILE6 emission estimates, CO_2 emission rate is not affected by speed, temperature, gasoline type. This rate is based on vehicle type only. The current version of EMFAC model is EMFAC2007. EMFAC2007 can be used to estimate hydrocarbons (HC), carbon monoxide (CO), oxides of nitrogen (NOx), carbon dioxide (CO_2), particulate matter (PM), fuel consumption, oxides of sulfur (SO_X), and lead (pb).

MOBILE6 and EMFAC emission rate are a function of vehicle average travel speed. Adjustment are used for different temperatures, gasoline types, humidity, and etc. basic emission rates are derived from emissions tests conducted under standard conditions such as temperature, fuel, and driving cycle. Speed Correction Factor (SCF) is used when vehicle average travel speed is different from the average travel speed from the standard testing drive cycle. SCF was derived based on emission rates from a limited number of testing driving cycles.

2.2.3 Mesoscopic Vehicle Fuel Consumption and Emissions Models

The input variables to mesoscopic model are more disaggregate than macroscopic model and more aggregate than microscopic model. Generally, mesoscopic models use a few explanatory variable to estimate vehicle fuel consumption and emissions.

Akcelik Model

Akcelik and co-workers (Akcelik 1985; Richardson and Akcelik 1981) proposed a model which separately estimates the fuel consumed in each of the three portions of an urban driving cycle, namely, during cruising, idling, and deceleration-acceleration cycle. Hence, the fuel consumed along an urban roadway section is estimated as:

$$F = f_1 X_s + f_2 d_s + f_3 h \qquad [2\text{-}10]$$

where,

F = average fuel consumption per roadway section (mL),
X_s = total section distance (km),
d_s = average stopped delay per vehicle (secs),
h = average number of stops per vehicle,
f_1 = fuel consumption rate while cruising (mL/km),
f_2 = fuel consumption rate while idling (mL/sec),
f_3 = excess fuel consumption per vehicle stop (mL).

MEASURE Model

The Mobile Emission Assessment System for Urban and Regional Evaluation (MEASURE) was developed by researchers at The Georgia Institute of Technology. The MEASURE model is a GIS-based modal emissions model process that predicts modal vehicle operations and generates mesoscopic estimates of HC, CO, and NOx (Bachman, Sarasua et al. 1996; Bachman, Sarasua et

al. 2000). MEASURE model is compatible with most of the traditional four-step travel demand models. This model includes two major modules: start emissions module and on-road emission module.

Emission rates were derived based on a refined tree-based regression analysis of vehicle emission test data from EPA and California Air Resource Board. Emission rates are a function of pollutant, vehicle model year, vehicle fuel delivery technology, high or normal emitter vehicle, and modal variables.

For start emission module, the vehicle registration data was used to get vehicle cold and hot-start characteristics distribution. The start emission estimates will be based on start characteristics distribution and start emission rates.

On-Road emission module estimate vehicle emission based different operating modes: idle, cruise, acceleration, and deceleration. Vehicle operating modes are constructed based on average travel speed, roadway characteristics, traffic flow, and volume to capacity ratio. Outputs from microscopic traffic simulation package or travel demand models, roadway, traffic control conditions, traffic conditions, and facility type are used to develop statistical distribution of vehicle activity data. Vehicle activity data, fleet composition characteristics, operating conditions, and emission rates were used to get emission estimates

2.3 Summary

This chapter reviews the current state-of-the-art in vehicle fuel consumption and emission models. In addition, the chapter described the factors affecting fuel consumption and emissions. These factors are categorized as travel, driver, highway network, and vehicle related factors. Various approaches and modeling efforts for quantifying transportation fuel consumption and emission impacts were presented. Macroscopic models lack the level of resolution that is required to evaluate alternative traffic-operational projects on the environments; and the application of microscopic models may be costly and time consuming for some applications.

Chapter 3 : VT-MESO MODEL FOR ESTIMATING HOT STABILIZED LIGHT DUTY VEHICLE FUEL CONSUMPTION AND EMISSION RATES

Hesham Rakha, Huanyu Yue, and Francois Dion

ABSTRACT

Currently, macroscopic vehicle fuel consumption and emission models are used for evaluating the environmental impacts of proposed transportation projects. These models used average travel speed to estimate network wide vehicle fuel consumption and emissions. These models would produce identical emission estimates for all drive cycles exhibiting identical average speeds, regardless of the specific speed profile associated with each drive cycle. In an attempt to overcome this limitation of current state-of-the-art procedures, this paper presents a mesoscopic model that estimates light duty vehicle fuel consumption and emission rates on a link-by-link basis based on up to three independent variables, namely: average travel speed, number of vehicle stops per unit distance, and average stop duration. The model uses these variables to construct synthetic drive cycles for the roadway segments considered, and then predicts average fuel consumption and emission rates by analyzing the deceleration, idling, acceleration and cruising portions of the cycle. Two optional input variables, acceleration power and deceleration rate, can be calibrated to reflect various driver behaviors. Within each mode of operation, fuel consumption and emission rates are determined using relationships that are derived from instantaneous microscopic models. The model also allows the modeler to calibrate two additional input parameters, namely typical driver deceleration and acceleration rates. The proposed model is finally demonstrated to successfully predict trends in vehicle fuel consumption, HC emission rate, and HC emission rate, as well as trends of CO and NO_x emissions to a lesser degree.

KEYWORDS: Vehicle Emissions, Vehicle Fuel Consumption, Traffic Modeling, and Intelligent Transportation Systems.

3.1 INTRODUCTION

Transportation planners and Federal Agencies currently rely on the combination of macroscopic transportation planning models and macroscopic vehicle emission models to evaluate the regional impacts of proposed transportation projects. These impacts are typically evaluated using a two-step process involving the successive use of a transportation planning and a vehicle emission model. In the first step, a transportation planning model such as TRANPLAN (The Urban Analysis Group 1992), MINUTP (The Seider Group 1997) or EMME/2 (INRO Consultants 1996) is used to determine the average speed and total vehicle-miles of travel for an entire network, or at best for each link in the network. In the second step, an emission model such as MOBILE6 EPA 1994 or EMFAC (CARB 1991) is then used to compute the average fuel consumption and emission rates for the facility. Within this step, a base emission rate reflecting fuel consumption and emission measurements that were gathered in a laboratory using pre-defined test drive cycles is first selected for the facility considered. This base rate is then modified to account for differences in average speeds between the laboratory and real-world cycles, as well as for differences in temperature, vehicle load, fleet composition, accrued mileage of vehicles within the fleet, type of fuel used, and vehicle operating conditions. Total regional emissions are finally obtained by multiplying the respective vehicle miles of travel with the estimated vehicle emission rate.

When used to perform evaluations, macroscopic emission models usually only provide a single emission rate for each average speed level. This rate is produced while assuming that all vehicles pollute similarly under an average range of speeds and vehicle-miles traveled and that variations in driver behavior can be neglected (An, Barth et al. 1997). This assumption present a problem when the drive cycles encountered in the field differ from those assumed in the models. A particular problem occurs when comparing drive cycles with identical average speeds, as identical emission rates would then be estimated for all cycles despite differences in the second-by-second speed profiles. Table 3-1 presents the fuel consumption and emission rates of hydrocarbon (HC), carbon monoxide (CO) and oxides of nitrogen (NO_X) for three scenarios exhibiting identical average speeds that were estimated using microscopic models analyzing speed profiles on a second-by-second basis. The only difference between the three scenarios is the number of stops made along the traveled link and the resulting cruise speeds to maintain the same average travel speed. All other parameters affecting the drive cycles, such a deceleration and acceleration rates, were held constant. As can be observed, significant differences exist in fuel consumption and emission rates despite the identical average speeds, thus indicating a need to look beyond the average speed as a single explanatory variable.

3.1.1 Proposed Approach

One approach in considering the impact of having different drive cycles with similar average speed is to estimate the fuel consumption and emissions of individual vehicles based on their unique time series of instantaneous speeds and accelerations. Rakha et al. (Rakha, Van Aerde et al. 2000), Ahn et al. (Ahn, Rakha et al. 2002), Rakha et al. (Rakha, Ahn et al. 2003), and Rakha et al. (Rakha, Ahn et al. 2003) provide examples of such an approach. Unfortunately, the application of microscopic models to the estimation of vehicle fuel consumption and emissions may be too costly and time consuming for many practical applications. In addition, these tools

may require more data than can be collected, or a level of accuracy that cannot be achieved with available data. Consequently, a need remains to develop fuel consumption and emission models that are less data intensive.

An and Ross (An and Ross 1993) further developed a modal model that predicts fuel consumption by mathematically modeling the engine operation and estimating a vehicle's fuel consumption rate within each mode of operation. The trip parameters considered as input include the average speed, average peak speed, braking time, idling time, and number of stops per unit distance. These parameters allow the model to account for various drive cycle patterns. However, the authors also acknowledged that their model remained unwieldy for many applications, essentially due to the fact that the average peak speed and fraction of time braking may be difficult to estimate. While a simpler model relying only on average speed, free-flow speed, and the portion of time stopped was also developed by the authors, it is not clear if this simpler model can be extended to predict vehicle emissions. In particular, the combination of parameters in the simplified model do not allow for the consideration of various acceleration and deceleration rates. This is particularly important when considering vehicle emissions because pollutant emission rates are more sensitive to changes in acceleration rates than fuel consumption rates (Rakha and Ding 2003).

In response to the need to develop vehicle fuel consumption and emissions models that are more accurate than current macroscopic model but also less data intensive that microscopic model, this paper proposes a unique mesoscopic model that estimates vehicle fuel consumption and emission rates using a limited number of easily measurable input parameters. These parameters include the average trip speed, number of stops per unit distance, and average stop duration.

3.1.2 Paper Layout

The remainder of this paper is divided into six sections. The first section presents an overview of the proposed mesoscopic model, while the second section describes the data and the underlying microscopic fuel consumption and emission models that were utilized to develop the proposed mesoscopic model. The third section follows with a description of how typical drive cycles are constructed using the provided traffic information. The fourth section then describes the formulae that were derived for computing vehicle fuel consumption and emissions associated with a given drive cycle. Finally, the fifth section compares the mesoscopic estimates against those produced by MOBILE5a and the underlying microscopic model, while the sixth and last section provides some conclusions and recommendations for future research.

3.2 Overview of Mesoscopic Model

Figure 3-1 indicates how the proposed model can be used to estimate the network-wide impacts of transportation improvement projects. As indicated, the model is primarily intended for use after the demand for a given transportation network has been predicted and link-by-link information about average travel speed, number of stops and stop duration has been obtained. From this point, an application of the model on a link-by-link basis would then yield information about average fuel consumption and emission rates per vehicle-kilometer for each link in the network. Link total fuel consumption and emissions would then be obtained by multiplying the ave-rages fuel consumption and emission rates for each link by the link's estimated amount of

vehicle-kilometers of travel. Finally, system-wide averages would be obtained by summing the estimates for each link within the network.

Figure 3-1 further details the process used to estimate average vehicle fuel consumption and emissions rates for a given roadway segment. The first step involves the construction of a synthetic drive cycle based on the trip parameters of average speed, average number of stops, and average delay per stop on the segment under consideration. After constructing the drive cycle, the model estimates the proportion of time that a vehicle typically spends cruising, decelerating, idling and accelerating while traveling on the link. A series of fuel consumption and emission estimation models are then used to determine the amount of fuel consumed and emissions of HC, CO and NO_X emitted by a vehicle during each mode of operation. Subsequently, the total fuel consumed and pollutants emitted by the vehicle while traveling along the segment considered are estimated by summing the corresponding estimates across the different modes of operation and dividing the results by the distance traveled to obtain distance-based average vehicle fuel consumption and emission rates.

At this point, it must be understood that the proposed model is intended not only for predicting the fuel consumption and emissions of fleets of vehicles, but also for the analysis of individual vehicles. As will be shown later, specific vehicles or different fleet compositions could be analyzed by simply generating new sets of regression coefficients. The focus of this paper is therefore only to present a mesoscopic emission modeling framework and to demonstrate its effectiveness in modeling vehicle emissions and not to present a definitive model. While extensions to the model are recommended in the conclusions section, the basic structure of the model would remain the same.

3.2.1 Underlying Microscopic Model

The proposed mesoscopic model utilizes a microscopic vehicle fuel consumption and emission model that was developed at Virginia Tech to compute mode specific fuel consumption and emission rates (Rakha, Van Aerde et al. 2000; Ahn, Rakha et al. 2002, Rakha, Ahn et al. 2003; Rakha, Ahn et al. 2004). This model, known as VT-Micro, predicts the instantaneous fuel consumption and emission rates of HC, CO and NO_X of individual vehicles based on their instantaneous speed and acceleration levels. It was developed to bridge the gap between traffic model simulator outputs, transportation planning models, and environmental impact models. The initial intent behind the development of this model was not to capture all the elements that affect vehicle fuel consumption and emission rates, but simply to develop a model in which vehicle dynamics are explicit enough to account for speed and acceleration variations, two elements that have been shown to have significant impacts on vehicle fuel consumption and emission rates.

Equation [3-1] describes the general format of the equations used by the VT-Micro models to predict the instantaneous fuel consumption and emission rates of individual vehicles.

$$MOE_e = \begin{cases} \sum_{i=0}^{3}\sum_{j=0}^{3} \exp\left(k_{i,j}^{e} \cdot v^i \cdot a^j\right) & \text{for } a \geq 0 \\ \sum_{i=0}^{3}\sum_{j=0}^{3} \exp\left(l_{i,j}^{e} \cdot v^i \cdot a^j\right) & \text{for } a < 0 \end{cases} \quad [3\text{-}1]$$

where: MOE_e = Instantaneous fuel consumption or emission rate (L/s or mg/s),

a = Instantaneous acceleration of vehicle (km/h/s),
v = Instantaneous speed of vehicle (km/h),
$k^e_{i,j}$ = Vehicle-specific acceleration regression coefficients for MOE_e, and
$l^e_{i,j}$ = Vehicle-specific deceleration regression coefficients for MOE_e.

As can be observed, Equation [3-1] defines the use of two sets of coefficients, one set for acceleration and one set for deceleration. This split was implemented in the microscopic models to account for differences in emission rate sensitivity to speed between acceleration and deceleration modes of operation of vehicles. Another important feature is the use of natural logarithms to ensure that non-negative fuel consumption and emission rates are produced by the models.

The general format of Equation [3-1] was first developed by testing the ability of various regression models to adequately model the observed steady-state fuel consumption and emission behaviors of eight vehicles that were tested by the Oak Ridge National Laboratory (ORNL) in 1995 (West, McGill et al. 1997). These test vehicles ranged from model year 1988 to model year 1995 and were deemed representative of typical light-duty vehicles in use at the time of the testing. For each vehicle, fuel consumption and emission rates for hot-stabilized, steady-state operation were obtained through both field measurements and dynamometer testing. Vehicles were first tested on-road to obtain realistic road loads and determine engine conditions as a function of vehicle speed and acceleration. The engine conditions were then duplicated on a chassis dynamometer while making fuel consumption and emission measurements. The regression models that were developed based on the ORNL data resulted in very good fits. As an example, Figure 3-2 illustrates the evaluation results for a composite vehicle having the average characteristics of the eight ORNL test vehicles. As can be observed, the figure indicates an ability to follow very closely the trends in increasing fuel consumption with higher speeds and sharper acceleration, as well as relatively good agreements between the predicted and observed emission trends for the pollutant considered.

Further refinement and validation of the microscopic models were more recently made using data that had been collected by the EPA in 1997. This second dataset included dynamometer fuel consumption and emission measurements under ambient conditions for 43 normal-emitting light-duty vehicles and 17 normal-emitting light-duty trucks. A comparison of the fuel consumption and emission rates produced by the microscopic models against in-laboratory measurements made on a dynamometer using the ARTA drive cycle for various groups of vehicles within the EPA database further confirmed the validity of the microscopic model, as described in Rakha *et al.,* (Rakha, Ahn et al. 2003) and Rakha *et al.*, (Rakha, Ahn et al. 2004).

Since the above datasets considered only normal light-duty vehicles operated under hot stabilized conditions and ignored the effects of additional engine loads on vehicle fuel consumption and emission rates, such as the effect of vehicle start and air conditioning usage, these limitations are thus reflected not only in the resulting microscopic models, but also the proposed mesoscopic model that are developed based on the microscopic model. Further research is however currently underway to expand the microscopic models to include high emitting vehicles, capture vehicle start effects, and model diesel engine vehicle emissions. Once these developments are completed, adjustments could then be made to the proposed mesoscopic model to expand its prediction capabilities.

3.2.2 Synthetic Drive Cycle Construction

This section describes how typical drive cycles are constructed using selected trip information. The section first presents the general approach behind the synthetic drive cycle construction and follows with more detailed description of the model assumptions to characterize the deceleration, idling, acceleration and cruising modes of operation of a vehicle. It should be emphasized that the objective of the paper is to present a general framework for the development of a model and that is continuously evolving and expanding to capture a number of vehicle, traffic, and driver behavior factors.

3.2.3 General Approach

As indicated in the introduction, the proposed mesoscopic model relies on three input variables, namely the average trip speed, the number of vehicle stops, and the stopped delay, to construct a representative drive cycle along a given roadway segment. Currently, the model does not distinguish between freeway and arterial facilities in constructing a drive cycle; however, further enhancements to the model will investigate the potential of considering different facility types in constructing drive cycles.

As an example, Figure 3-3 demonstrates how a drive cycle can be constructed using the three mentioned input parameters. In this case, it is assumed that a vehicle makes on average three stops of a given duration over the segment considered. To account for those three stops, the trip speed profile is constructed by fitting three identical stop-and-go cycles over the entire segment considered. Within each cycle, the cruise speed is computed to maintain the same trip time (identical average speed). While the above drive cycle generation does not obviously model actual driving profiles, as actual profiles would not show such perfect repetitiveness, it should be kept in mind that the objective of the model described in this paper is not to produce precise estimates of vehicle fuel consumption and emissions, but rather to provide quick and reasonable estimates for cases in which actual drive cycles are not available. If drive cycles were available, then a microscopic model would be more suitable for such an application.

Vehicle Deceleration

The model currently assumes that drivers decelerate at a constant rate that can be set by the user. Specifically, the model allows the user to specify the deceleration rate in the range of -2.00 m/s^2 to -0.25 m/s^2 in increments of 0.25 m/s^2.

The assumption that drivers decelerate at a constant rate was made to simplify the development of the initial model. In reality, different drivers are likely to decelerate at different rates. Individual drivers are also likely to apply rates that vary with speed and/or the distance from the obstacle ahead. For example, it is often observed that drivers often increase their braking level as they come closer to an obstacle ahead. However, while the model currently assumes constant deceleration rates, variable rates could be considered. Once determined, typical variable deceleration rates could be implemented by simply using the appropriate rates when using the underlying microscopic models to calculate the total fuel consumed and pollutants emitted during a given deceleration prior to generating the model's prediction equations. Research is currently underway to characterize typical driver deceleration behavior.

Vehicle Idling

A vehicle is assumed to be idling when it reaches a speed of 0 km/h. This mode of operation is only considered when the input parameters to the model specify that at least one full stop occur within the segment considered. If the user specifies a number of stops that is less than one, the model will then assume that a partial stop only occur and thus that a vehicle decelerates only to a given speed before starting to accelerate again.

Vehicle Acceleration

In the modeling of vehicle acceleration, the model considers a vehicle dynamics model that was initially developed by Rakha et al. (Rakha, Lucic et al. 2001) and Rakha and Lucic (Rakha and Lucic 2002) for modeling truck acceleration behavior and that was later applied to the modeling of light-duty passenger cars by Snare (Snare 2002) and Rakha et al. (Rakha, Snare et al. 2004). As indicated by Equation [3-2], the model is based on the principle that the acceleration of a vehicle is proportional to the resulting force applied to it. The model predicts acceleration rates that decrease with increasing speeds. The decreased acceleration rates are a result of two factors. First, the vehicle tractive effort (F) decreases with vehicle speed. Second, the aerodynamic and rolling resistance forces increase with vehicle speeds. It should be noted that the acceleration factor (α) is used to reduce the vehicle acceleration level to reflect the fact that drivers do not typically use the full power of a vehicle while accelerating, as is discussed by Snare (Snare 2002). The acceleration factor (α) accounts for the fact that drivers do not utilize the full power of the vehicle while accelerating, as derived by Rakha and Snare (Rakha, Snare et al. 2004). Specifically, Snare and Rakha indicate that drivers accelerate at 62.5 percent of the maximum acceleration on average, with aggressive drivers accelerating at 85 percent of the available power and passive drivers accelerating at only 40 percent. Since the intent of the model is to evaluate typical driving behavior, it was thus determined that typical accelerations should be considered by the model instead of maximum feasible accelerations. In particular, assuming that vehicles accelerate at their maximum potential can lead to gross overestimation of vehicle fuel consumption and emission rates.

$$a = \alpha\left(\frac{F - R}{M}\right) \qquad [3\text{-}2]$$

where: a = Vehicle instantaneous acceleration (m/s^2)
F = Residual force (N),
R = Total resistance force (N), and
M = Vehicle mass (kg).
α = Fraction of the maximum acceleration that is utilized by the driver.

Equations[3-3], [3-4], and [3-5] further indicate how the effective tractive force of a vehicle is computed at any given speed. Specifically, Equation [3-3] computes the effective tractive force as the minimum of the tractive force applied by the engine, Ft, and the maximum force that can be sustained between the vehicle tires and the pavement surface, F_{max}. The tractive force is computed using Equation [3-4], which assumes that the vehicle power does not change with speed and is equal to the maximum potential power of the vehicle. The power transmission efficiency parameter η further accounts for power loss in the transmission system as well as losses associated with engine accessories such as fan, ventilator, water pump, magneto, distributor, fuel pump and compressor. Equation [3-5], finally, determines the maximum tractive force that can be sustained between the vehicle tires and the pavement surface without the

wheels spinning. This force is a function of coefficient of friction and the mass of the vehicle applied to the tractive axle.

$$F = \min(F_t, F_{\max}) \quad [3\text{-}3]$$

$$F_t = 3600 \cdot \eta \cdot \frac{P}{v} \quad [3\text{-}4]$$

$$F_{\max} = 9.8066 \cdot p_{mta} \cdot M \cdot \mu \quad [3\text{-}5]$$

where: F_t = Tractive force applied on the vehicle (N),
F_{max} = Maximum attainable Tractive force (N),
P = Maximum *e*ngine power (kW),
η = Power transmission efficiency,
v = Vehicle speed (km/h),
p_{Mta} = Portion of vehicle mass on tractive axle,
μ = Coefficient of friction between vehicle tires and pavement, and
α = Fraction of acceleration power effectively used by driver.

Equations [3-6] through [3-9] further describe how the external resistance forces can be calculated. Equation [3-6] indicates that the total external resistance force is the sum of the aerodynamic, rolling, and grade resistance forces. In Equation [3-7], the aerodynamic resistance force is shown to be a function of the vehicle frontal area, the altitude, the vehicle's drag coefficient, and the square of the vehicle speed. The rolling resistance force is further shown in Equation [3-8] to be a function of the total mass and speed of the vehicle, while Equation [3-9] indicates that the grade resistance force is a function of the road grade and mass of the vehicle.

$$R = R_a + R_r + R_g \quad [3\text{-}6]$$

$$R_a = 0.047285 \cdot C_d \cdot C_h \cdot A \cdot v^2 \quad [3\text{-}7]$$

$$R_r = 9.8066 \cdot C_r \cdot (c_2 v + c_3) \cdot \frac{M}{1000} \quad [3\text{-}8]$$

$$R_g = 9.8066 \cdot M \cdot i \quad [3\text{-}9]$$

where: R_a = Aerodynamic resistance (N),
R_r = Rolling resistance (N),
R_g = Grade resistance (N),
A = Frontal area of vehicle (m^2),
H = Altitude (m),
C_d = Air drag coefficient,
C_h = Altitude coefficient = 1 – (0.000085 · H), and
C_r, c_1, c_2 = Rolling resistance constants
i = Grade magnitude (m/100 m)

For example, Figure 3-4 illustrates how the vehicle dynamics model compares to field data for light duty vehicles (Rakha, Snare et al. 2004). As can be observed, the model that was calibrated for the test vehicle provides a very good fit to field observations. Similar fits were also obtained for a wide range of light duty vehicles and trucks.

Cruising Mode

Between deceleration and acceleration events, it is assumed that a vehicle travels at a constant speed. As was indicated earlier, the speed at which a vehicle cruises is computed so that the total travel time along the segment under consideration is not altered. The cruising speed is determined through an iterative process that adjusts the cruising speed and corresponding deceleration and acceleration times until a match is found between the resulting travel time and the travel time determined by the average speed.

While the assumption of a constant cruising speed may not reflect typical observed speed variability, this approach represents only a first step in constructing realistic drive cycles based on a limited number of trip parameters. It should be reminded that the model is designed for use in cases in which detailed speed profiles are not available. Assumptions of constant cruising speeds are also fairly common in traffic simulation models. In this case, it would be expected that speed variability while cruising would result in additional fuel consumption and emissions. In particular, small differences at high speeds can result in large differences in emissions, depending on whether a vehicle engine goes into enrichment or enleanment mode. One way for accounting for the additional emissions that may result from speed variability would be to use microscopic fuel consumption and emission models to analyze second-by-second speed profiles with varying degrees of speed variability and use the evaluation results to determine a series of correction factors to be utilized with these models. Research in this direction is currently underway.

3.2.4 Fuel Consumption and Emission Estimates by Drive Mode

This section describes how fuel consumption and emissions of HC, CO, NOx, and CO_2 are computed for the cruising, idling, decelerating, and accelerating modes. for light-duty, gasoline engine vehicles that are operating under hot stabilized conditions.

Cruise Mode

The rates at which individual vehicles consume fuel and emit pollutants while traveling at a constant speed are obtained by applying the appropriate cruise speed and an acceleration rate of zero to the microscopic models defined by Equation [3-1]. This yields fuel consumption and emission relationships of the form given by Equation [3-10]. To obtain total fuel consumption and emissions during a cruising event, the rates given by Equation [3-10] are then multiplied by the total duration of the event.

$$MOE_e^{cruise} = \exp(k_{0,0}^e + k_{1,0}^e \cdot v + k_{2,0}^e \cdot v^2 + k_{3,0}^e \cdot v^3) \quad [3\text{-}10]$$

where: $MOE_e{}^{cruise}$ = Fuel consumption or pollutant emission rate while cruising (l/s or mg/s),
s = Vehicle cruising speed (km/h), and
$k^e_{i,0}$ = Vehicle-specific acceleration regression coefficients for MOE_e.

Figure 3-5 illustrates the rates that were obtained for a LDV-2 that was generated based on the average characteristics of 15 light-duty vehicles that were tested on a chassis dynamometers by the EPA in 1997 (Rakha, Ahn et al. 2004). This category includes vehicles of model year ranging between 1990 and 1994, with engine sizes of less than 3.2 liters, and with had less than 83,653 miles driven. The figure first demonstrates that fuel consumption and emission rates all increase

with higher cruising speed, as expected, but that these increases are not linear. It is also observed that the rates at which HC, CO and NO_X are emitted are highly dependent on the cruising speed, especially at high speeds, where small speed increases result in significantly higher emission rates. For the HC and CO emissions, these increases are again a consequence of the engine running with a higher fuel-to-air ratio at high speeds. For the NO_X, the higher emissions at high speed are mostly due to other mechanisms, as NO_X is relatively insensitive to the fuel-to-air ratio. It can also be observed that the NO_X emissions begin to ramp up at a lower speed than the HC and CO emissions, probably due to a reduction in the effectiveness of the EGR, and stay somewhat flatter at high speeds. Since NO_X is produced by high combustion temperature, the higher the engine load is, the higher the emissions are. The figure further demonstrates that the optimum distance-based efficiency occurs for cruise speeds around 80 and 90 km/h. In particular, it demonstrates that small differences in cruise speeds under typical arterial and highway driving may have only minor impacts on fuel consumption and emission rates. However, the same figure indicates that speed variations on freeways, where cruise speeds typically vary between 100 and 120 km/h, can result in much more significant impacts on fuel consumption and emission rates, as was discussed by Rakha and Ding (Rakha and Ding 2003).

Deceleration Mode

Applying the VT-Micro model that was defined in Equation [3-1] to a deceleration maneuver from a pre-defined cruising speed to a complete stop, Equation [3-11] was derived to express the relationship between the total fuel consumed and pollutants emitted by a single vehicle while decelerating from a given initial speed to a final speed of 0 km/h at a constant deceleration rate. Specifically, Equation [3-11] was obtained by integrating the instantaneous fuel consumption and emission rates provided by Equation [3-11] over the entire duration of a deceleration event at a constant deceleration rate. Because of the non-linear nature of the relationships considered, a closed analytical solution could not be found. Instead, regression relationships were fitted to the data, as demonstrated in Equation [3-11].

$$MOE_e^{decel} = \exp\left(d_0 + d_1\ v_c + d_2\ v_c^2 + d_3\ v_c^3 + d_4\ v_c^4 + d_5\ v_c^5 + d_6\ v_c^6\right) \quad [3\text{-}11]$$

where: MOE_e^{decel} = Total fuel consumed, pollutant emitted, traveled distance or travel time while decelerating (L/s, mg/s, m or sec),
v_c = Vehicle initial speed (km/h), and
$d_0,\ldots,d_6$ = Vehicle-specific regression coefficients.

While the deceleration relationships were developed to express the total fuel consumed and pollutants emitted over a full deceleration maneuver (deceleration to a speed of 0 km/h), these relationships can also be used to consider partial stops. For example, in computing the fuel consumption for a deceleration maneuver from 60 to 50 km/h, the fuel consumption for a deceleration maneuver from 50 to 0 km/h is subtracted from the fuel consumption rate for a deceleration maneuver from 60 to 0 km/h.

For example, Figure 3-6 illustrates the deceleration relationships that were developed for the light-duty composite vehicle for constant deceleration rates of -0.5, -1.0, -1.5 and -2.0 m/s^2. It is observed that the fuel consumption and emission rates do not exhibit linear relationships with respect to the starting cruise speed despite an assumed constant deceleration rate. This non-linearity is due to the non-linear instantaneous vehicle fuel consumption and emission rates.

Result from a previous research effort that was conducted by Rakha *et al.* (Rakha, Dion et al. 2001) demonstrated that predicted fuel consumption and emission rates were marginally impacted by deceleration rates. The main impact of considering varying deceleration rates is therefore not to improve the model predictions during deceleration maneuvers; instead the analysis enhances the model predictions by altering the distance traveled while cruising and accelerating.

Idling Mode

As was the case for the cruise and deceleration models, the fuel consumption and emission rates for the idling model are based on the use of the underlying VT-Micro model. In this case, idling rates are determined by using the models of Equation [3-1] with an instantaneous speed of 0 km/h and an instantaneous acceleration rate of 0 km/h/s. This yields constant rates that are then multiplied by the average stop duration to estimate the total fuel consumed and emissions during an average idling event.

Acceleration Mode

As was done for the deceleration mode, the fuel consumed and pollutants emitted by a vehicle during an acceleration event is computed by integrating the fuel consumption and emission rates estimated using Equation [3-1] over the entire acceleration event. After computing the total fuel consumption and emissions for a series of final target speeds, regression models of the form defined by Equation [3-12] were then developed for each measure of effectiveness. As was the case with the deceleration models, these relationships estimate the total distance traveled, time consumed, fuel consumed, and pollutants emitted for an acceleration maneuver from a full stop up to a final cruise speed v_C.

$$MOE_e^{accel} = \exp\left(b_0 + b_1\ v_c + b_2\ v_c^2 + b_3\ v_c^3 + b_4\ v_c^4 + b_5\ v_c^5 + b_6\ v_c^6\right) \quad [3\text{-}12]$$

where: MOE_e^{accel} = Total distance traveled, time consumed, fuel consumed or pollutants emitted while accelerating (m, s, L/s, and mg/s),
v_c = Vehicle final speed (km/h), and
$b_0,\ldots,b_6$ = Vehicle-specific regression coefficients.

As was the case with Equation [3-11], Equation [3-12] can be used to estimate the distance traveled, time consumed, fuel consumption, and emissions that are associated with partial acceleration events. For instance, to estimate the fuel consumed for an acceleration from a speed of 50 km/h to a speed of 60 km/h, the model defined by Equation [3-12] would first be applied to estimate the fuel consumed for an acceleration from 0 to 60 km/h, and then to estimate the fuel consumed for an acceleration from 0 to 50 km/h. The difference between the two estimates would then be the fuel consumed to accelerate from 50 to 60 km/h.

Figure 3-7 illustrates the acceleration relationships that were developed for the LDV-2 vehicle that was described earlier for various levels of driver acceleration (α = 0.33, 0.50, 0.60, 0.66 and 0.75). As can be observed, the fuel consumed to reach a given speed increases with every reduction in the level of acceleration. In this case, while accelerating at a lesser rate puts a lesser load on the engine and a lesser requirement in fuel consumption, the total quantity of fuel consumed to reach the target speed increases as the vehicle spends more time accelerating. However, the above observation does not necessarily hold for CO and NO_x emissions. As can be

observed, the total vehicle emissions to reach speeds of up to 90 to 110 km/h typically decrease when the acceleration level is reduced from 75% to 50% before starting to increases again. This behavior is due to the non-linearity of vehicle emissions with respect to speed increases, as was observed in Figure 3-2. When comparing Figure 3-6 to Figure 3-7 it is observed that significantly higher fuel consumption and emission are associated with acceleration event in comparison with a deceleration event because of the higher engine load that is associated with acceleration event.

3.3 VALIDATION OF MESOSCOPIC MODEL

This section validates the mesoscopic model by comparing the model outputs to outputs from the underlying microscopic model and the EPA data. Specifically, two comparisons are made. First, the mesoscopic and microscopic fuel consumption and emission estimates are compared for the EPA drive cycles. Second, the estimates from mesoscopic model are compared against EPA field data for the 14 EPA drive cycles are compared. The objective of the exercise was to investigate the ability of the VT-Meso model to correctly predict changes in vehicle fuel consumption and emission rates across different drive cycles.

3.3.1 Construction of Test Scenario

In order to compare the results of the mesoscopic and microscopic models it was essential that the number of vehicle stops be estimated for both the urban and highway drive cycles using Equation [3-13]. This equation estimates the total partial stops incurred during a trip, as described by Rakha *et al.* (Rakha, Kang et al. 2001). The equation defines a full stop as a deceleration from the facility free-flow speed to a speed of zero. Half a stop would then be a deceleration from the free-flow speed to half the free-flow speed. The free-speeds utilized with Equation [3-13] are superimposed on the drive cycles. Figure 3-8 illustrates how the free-speed is superimposed on the EPA drive cycles. These free-flow speeds were determined based on facility type and were generally set to correspond to speed limits along each section.

$$N_{stops} = \sum_{t=1}^{T} \frac{\left(v_{t+1} - v_t\right)}{v_{cruise}} \quad for\ all\ v_{t+1} \le v_t \qquad [3\text{-}13]$$

where: N_{stops} = Estimated number of full stops,
v_t = Vehicle instantaneous speed in time interval t (km/h),
T = Number of time intervals t in speed profile.

The EPA developed new facility-specific and area-wide drive cycles based on real-world driving studies. Table 3-2 summarizes the characteristics of the 14 EPA drive cycles and corresponding synthetic drive cycles. In each drive cycle, the estimation of the number of vehicle stops is computed using Equation [3-13], which sums up all partial stops along the trip. After computing the average speed, the stopped delay is computed as the total time that a vehicle travels at a speed of 0 km/h. Finally, the average stopped delay is computed by dividing the total stopped delay by the number of vehicle stops.

3.3.2 Comparison of Mesoscopic and Microscopic Estimates for EPA Drive Cycle

To validate the mesoscopic model, the first step was to compare the mesoscopic energy and emission models to the microscopic model estimates. Figure 3-9 compares the average fuel consumption and emission rates that were estimated for the LDV-2 vehicle being considered by both the VT-Meso and VT-Micro models for the fifteen drive cycles described in Table 3-2 using the numbers of equivalent stops provided by Equation [3-13] and various assumed acceleration rates within the VT-Meso model (α = 0.25 to 1.00). For this comparison, a constant deceleration rate of 1.25m/s^2 was used. While it is not surprising that the absolute emission values are not identical, given the differences between the actual and constructed drive cycles, the figure generally indicates that the mesoscopic model estimates appear to be consistent with the microscopic estimates. In this case, the variability of results between the microscopic and mesoscopic estimates can be attributed to differences between the actual and constructed drive cycles. Other parameters that could affect the mesoscopic model estimates include the various assumptions made by the mesoscopic model when generating synthetic drive scenarios, particularly regarding the assumed deceleration and acceleration rates. In general the mesoscopic model appears to estimate fuel consumption, HC emission, and CO_2 emissions consistent with the microscopic estimates; however, the model tends to overestimate the CO and NO_x emissions.

Result from a previous research conducted by Rakha and Ding (Rakha and Ding 2003) further help in assessing the importance of correctly estimating the three trip parameters used by the mesoscopic model, and more particularly, in determining their individual impacts on the evaluation results. The study indicates that fuel consumption is relatively insensitive to the level of aggressiveness of accelerating drivers. This is in agreement with the results of Figure 3-9, which illustrate very little variations in fuel consumption as a function of acceleration level. In terms of vehicle emissions, the study indicates that HC and CO emission rates are typically more sensitive to the level of acceleration than to the cruise speed for speeds ranging between 0 and 120 km/h. This sensitivity is apparent in Figure 3-9, where significant variations in predicted rates are observed for the both HC and CO when considering various acceleration levels. Also, the current research indicates that NO_x emissions are relatively sensitive to both the level of acceleration and the cruise speed. This is clearly apparent when analyzing and comparing the results of Figure 3-9. However, while increases in acceleration level typically result in higher emission rates for HC and CO, this is not always the case for NO_x.

As indicated earlier, VT-Mesoscopic model can choose different deceleration rates to estimate fuel consumption and emission. Figure 3-10 illustrates the fuel consumption and emission rates associated with a LDV-2 vehicle accelerating at 60 percent the maximum acceleration rate (α = 0.60) and decelerating at different deceleration rates. The deceleration rates range from -0.75 to -2.00 m/s^2. This figure clearly shows that the mesoscopic model gives similar fuel consumption and emission estimates for different deceleration rates. Fuel consumption and emission rates are more sensitive to acceleration and cruising maneuvers; the impact of different deceleration rates is not significant.

3.3.3 Comparison of Mesoscopic Model Estimates and EPA Data

To validate the model using real-world data, the EPA data was utilized for validation purpose because other independent data were not available at the time of this study. The use of the EPA data offers a number of benefits. First, the EPA data includes off-cycle (non-FTP) emission results over different facility types and therefore provides a good assessment of model estimates over different roadway types and different levels of congestion. Second, the EPA data was utilized to develop EPA's MOBILE6 model, this comparison ensures that the VT-Meso model are consistent with MOBILE6 estimates across different facility types and different levels of congestion.

Figure 3-11 and Figure 3-12 compare the VT-Meso model emission estimates against laboratory measurements for 14 drive cycles. The 5th‰ and 95th‰ emission rates are computes based on difference in vehicle emissions within a vehicle category. LDT1 category includes 11 vehicles while LDV2 category includes 15 vehicles. The vertical line and horizontal bar represent the 95th‰, 5th‰, and mean value of measured EPA emission data, while the horizontal lines represent VT-Meso emission estimates associated with different acceleration levels. Figure 3-11 and Figure 3-12 illustrate a good fit between the model estimates and the laboratory measurements. Specifically, all predictions lie within the 5th‰ and 95th‰ limits. Furthermore, the model estimates generally follow the mean laboratory measurements.

3.4 CONCLUSION

This paper describes the development of a set of mesoscopic relationships that predict vehicle fuel consumption and emission rates for steady state, hot stabilized, light duty vehicles based on a vehicle's average speed, an average number of stops per unit distance, and an average stop duration. These relationships are intended for use as post-processors of traffic simulation models that estimate average traffic speed and average number of stops on a link but do not provide detailed speed profiles.

To evaluate the proposed model, mesoscopic fuel consumption and emission rates were compared against microscopic and EPA data. These evaluations indicate that the mesoscopic model produces fuel consumption and emission rates that are consistent with those produced by the underlying microscopic model for both the EPA drive cycles. In particular, it is demonstrated that the simple consideration of average speed, number of stops and stop duration leads to relatively strong correlations between the predicted changes in fuel consumption, HC emissions, and CO2 emissions against microscopic model prediction and EPA data. On the other hand, some difficulties were observed in correctly predicting changes in CO and NO_x emissions. For NO_x emissions, the difficultly was partly attributed to difficulties associated with the procedure used to convert speed variations into equivalent numbers of stops.

An analysis of predicted fuel consumption and emission rates for various deceleration rates indicated very little sensitivity to changes in this parameters. The main impact of considering varying deceleration rates is therefore not to improve predicted rates, but to determine the feasibility of a given scenario as changes in deceleration rates affect the deceleration distance and the distance that can be used to accelerate.

Based on the above results, further research appears to be required to improve the accuracy of the mesoscopic model. Further research should be conducted to determine how speed variability can be accounted for in the fuel consumption and emission estimation processes without requiring second-by-second analysis of speed and acceleration profiles. Further research can also be conducted to characterize typical speed variability for different facility types (collectors, arterials and freeways) and different levels of congestion. Such research would in turn allow the development of improved factors or equations for converting speed variations, stop-and-go patterns, and partial stops into equivalent number of stops for the purpose of estimating vehicle fuel consumption and emissions. The existing model also requires further enhancement to include diesel and high-emitting vehicles, and to consider the impact of cold-starts on fuel consumption and emissions.

Table 3-1: Impact of Vehicle Stops on Fuel Consumption and Emissions

	Scenario 1	Scenario 2	Scenario 3
Trip length (km)	2.0	2.0	2.0
Average seed (km/h)	50.0	50.0	50.0
Number of stops	0	1	2
Cruise speed (km/h)	50.0	55.3	63.3
Fuel consumed (L)	0.175	0.204	0.250
HC emissions (mg)	163.2	202.7	290.3
CO emissions (mg)	2778.0	3638.7	5775.5
NOx emissions (mg)	215	415.1	745.6

Table 3-2: EPA's new facility-specific drive cycle characteristics

Cycle	Avg. speed (km/h)	Max. speed (km/h)	Duration (s)	Length (km)	Time Stopped (s)	Equivalent Stop (stops)	Average stop duration (s)
FWHS	101.12	119.52	610	17.15	0	1.72	0
FWAC	95.52	116.96	516	13.68	0	1.53	0
FWYD	84.64	112.96	406	9.54	0	1.89	0
FWYE	48.8	100.8	456	6.18	4	3.31	1.2
FWYF	29.76	79.84	442	3.66	7	3.04	2.3
FWYG	20.96	57.12	390	2.27	10	2.02	4.9
RAMP	55.36	96.32	266	4.10	15	2.10	7.2
ARTA	39.68	96.24	737	8.11	103	9.27	11.1
ARTC	30.72	79.2	629	5.38	122	8.67	14.1
ARTE	18.56	63.84	504	2.59	148	5.66	26.2
LOCL	20.64	61.28	525	2.99	125	6.34	19.7
AREA	31.04	83.68	1348	11.60	294	14.48	20.3
LA92	39.36	107.52	1435	15.70	204	11.49	17.8
FNYC	11.36	44.32	600	1.89	215	8.86	24.3

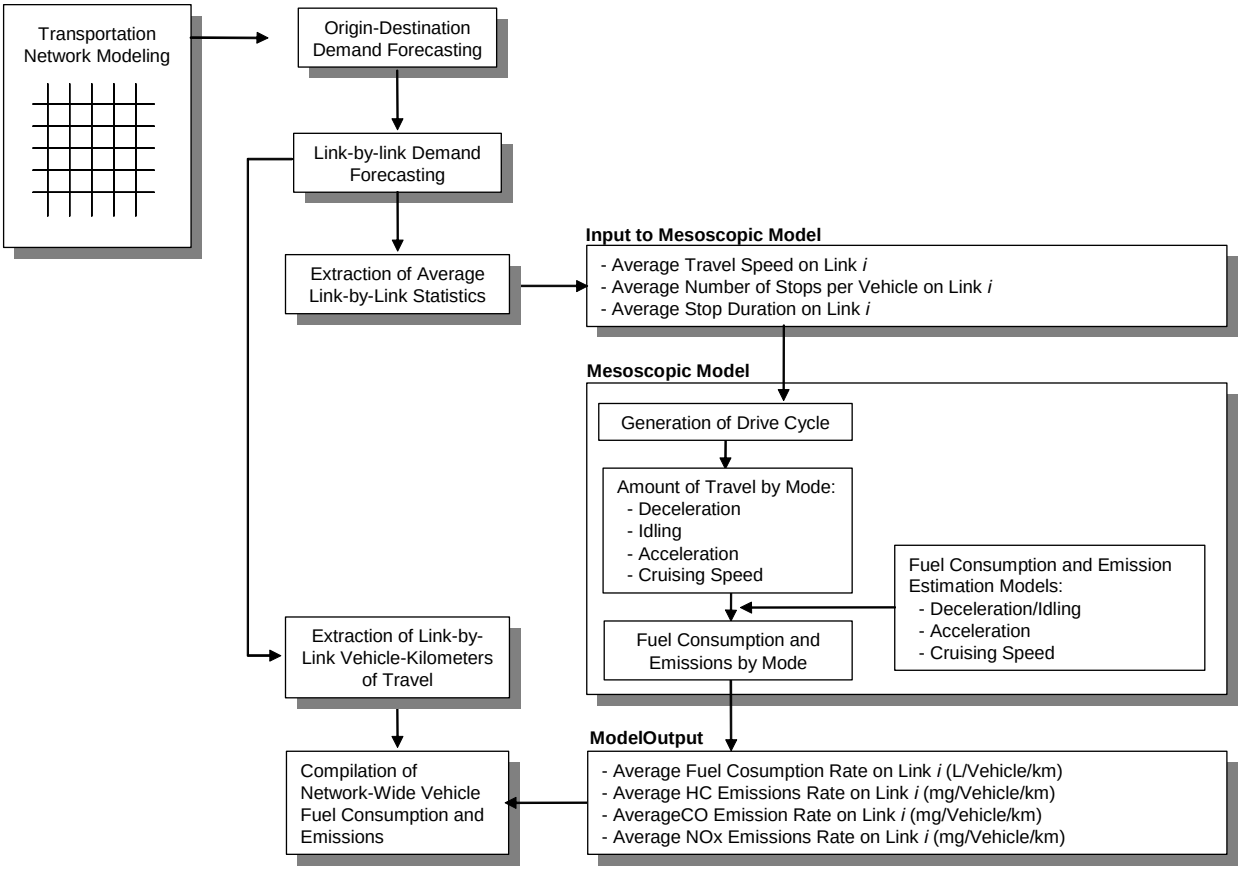

Figure 3-1: Application Framework of Proposed Mesoscopic Fuel Consumption and Emission Estimation Model

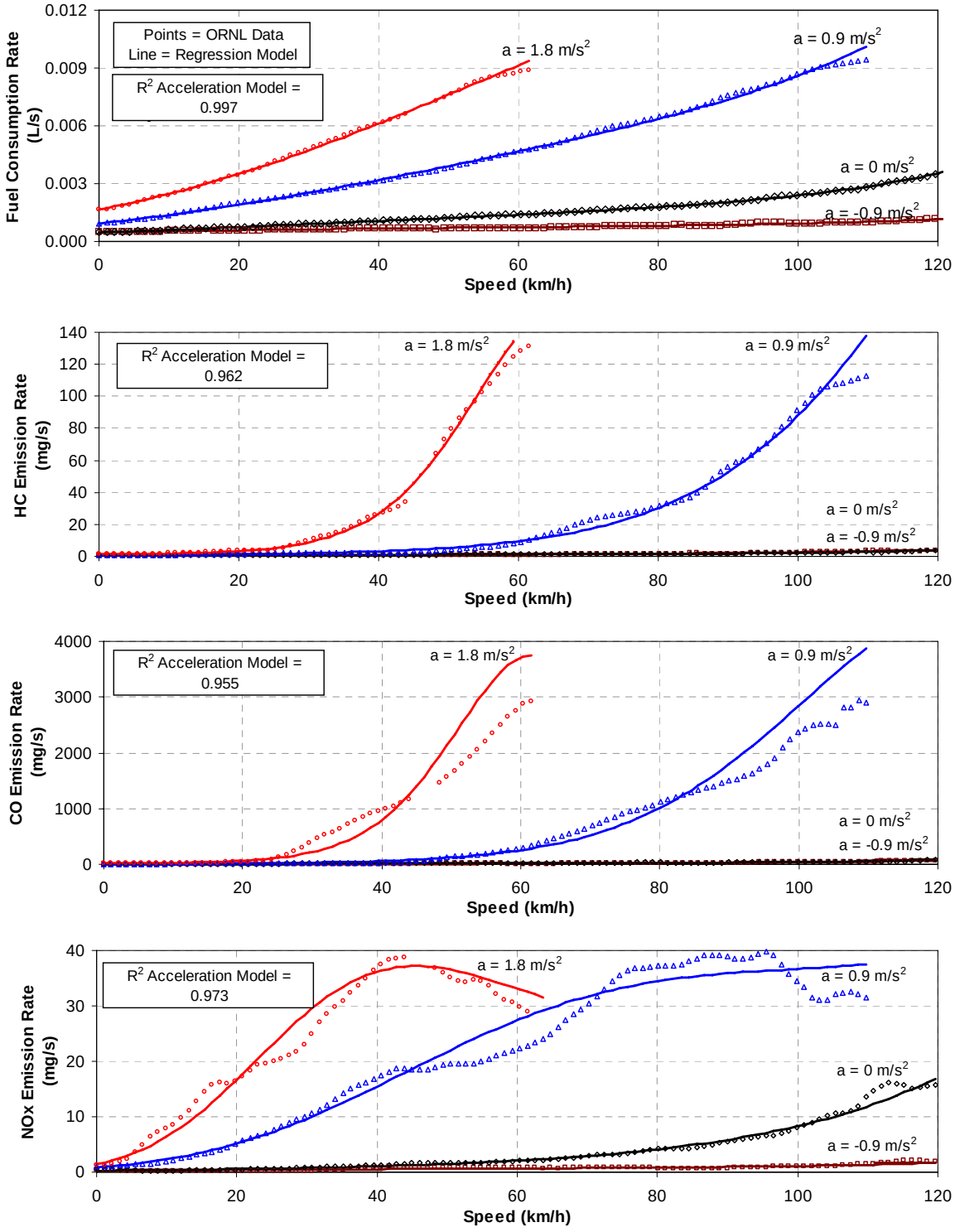

Figure 3-2: Validation of Underlying Microscopic Models (ORLN Composite Vehicle)

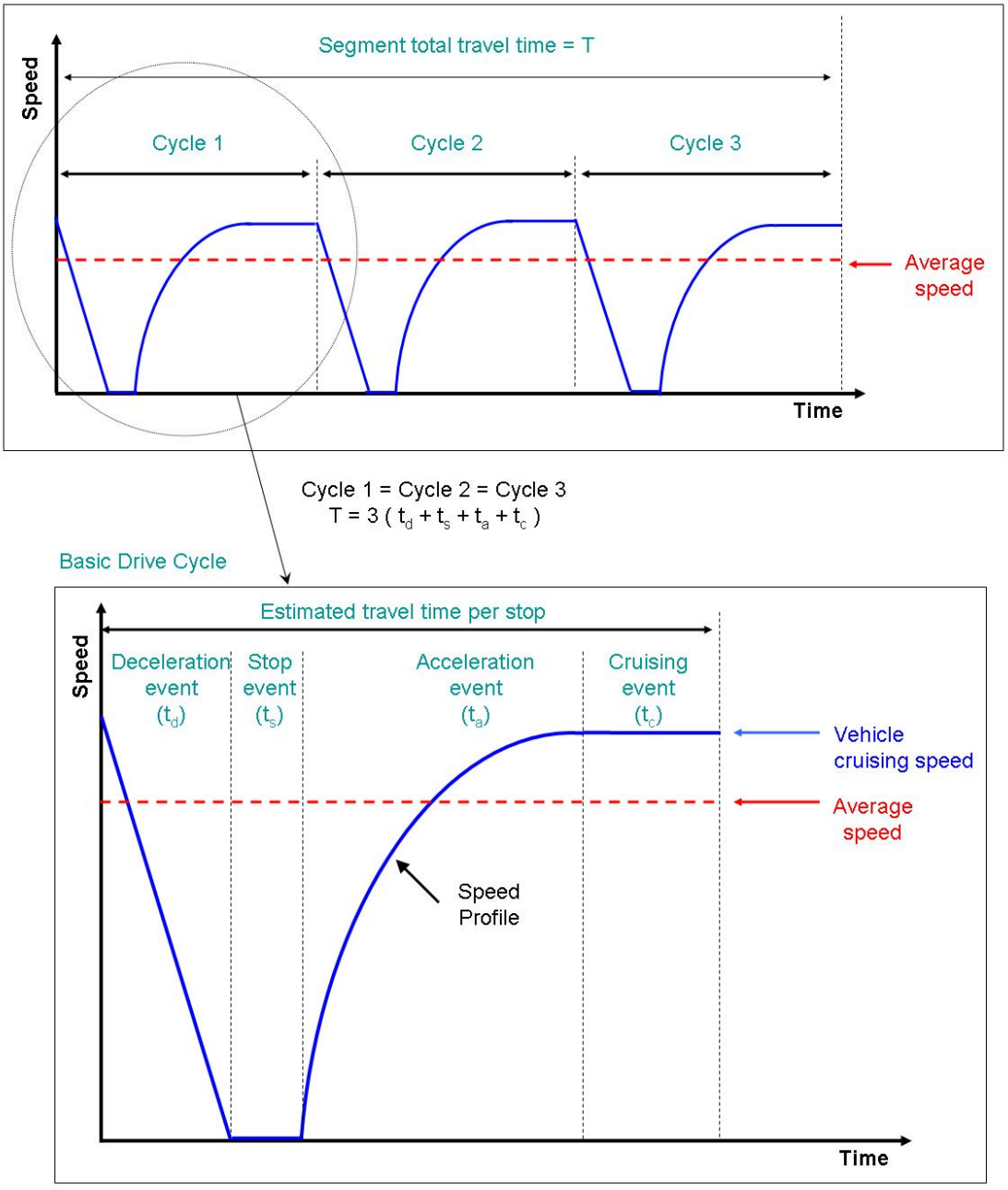

Figure 3-3: Example of Synthetic Speed Profile

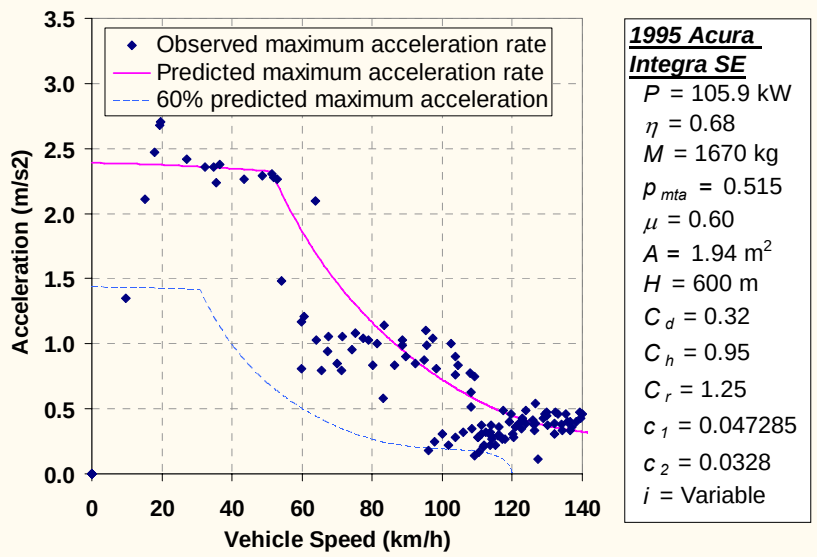

Figure 3-4: Example of Speed-Acceleration Relationship

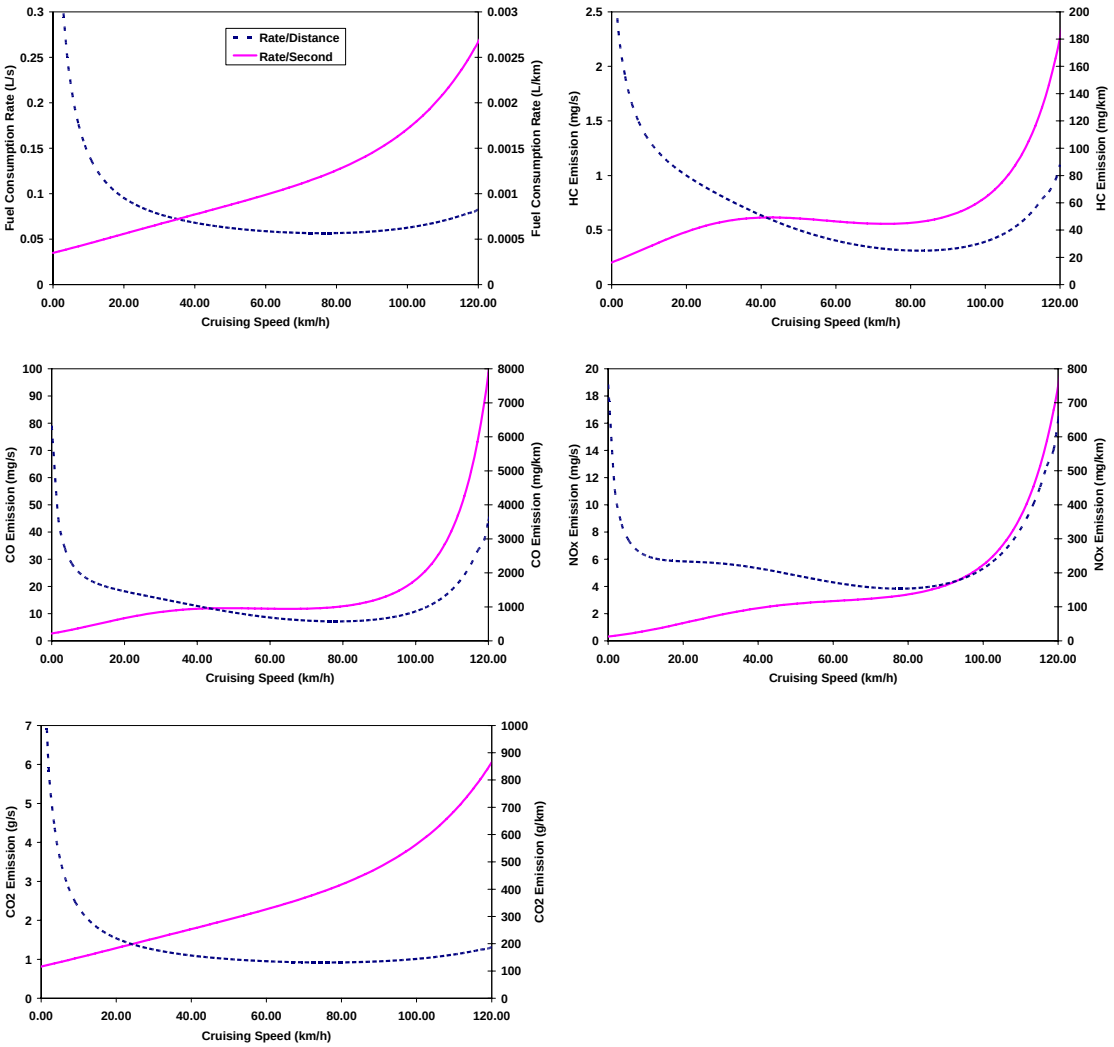

Figure 3-5: Fuel Consumption and Emission Rates for Cruising Mode (LDV-2)

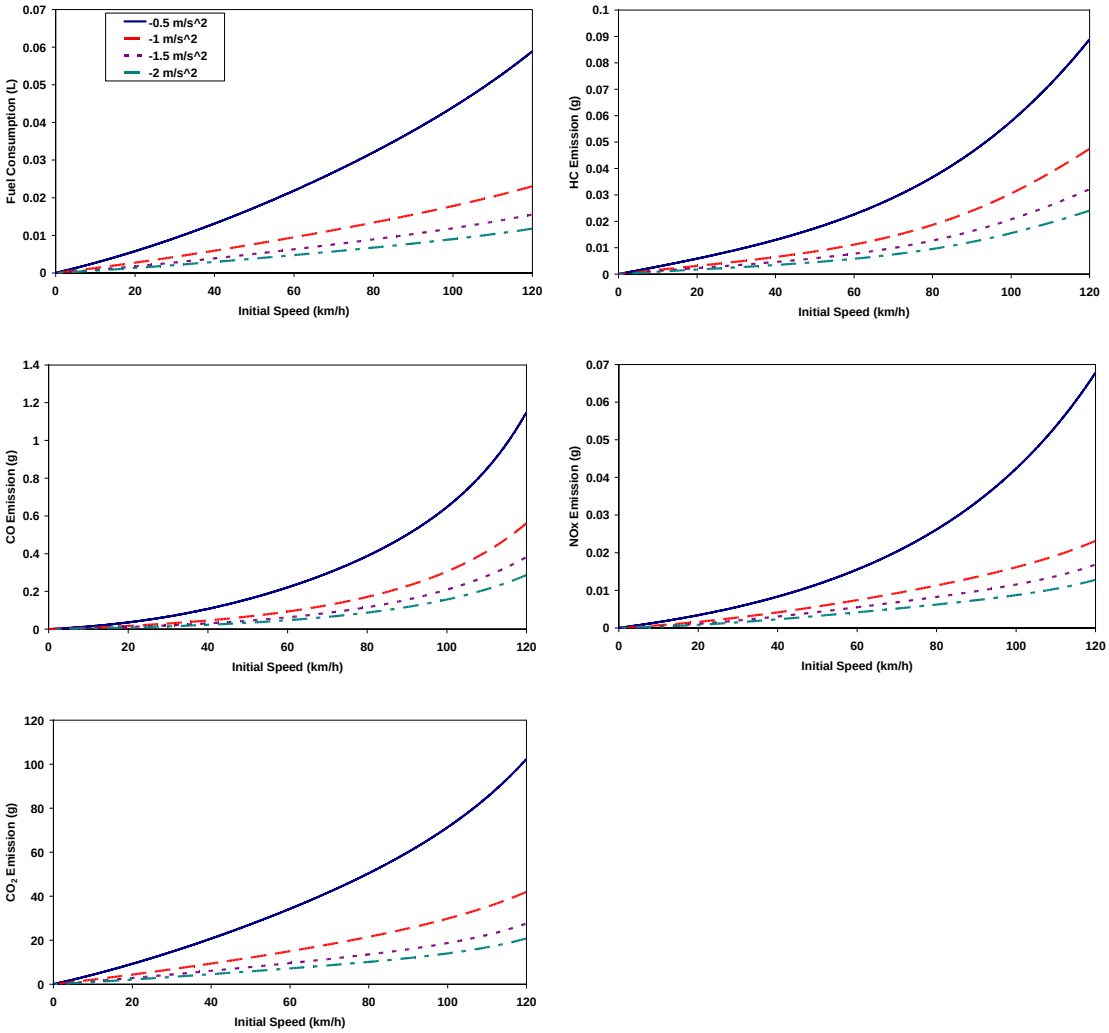

Figure 3-6: Total Fuel Consumption and Emission for Different Deceleration Rates (Light-Duty Composite Vehicle)

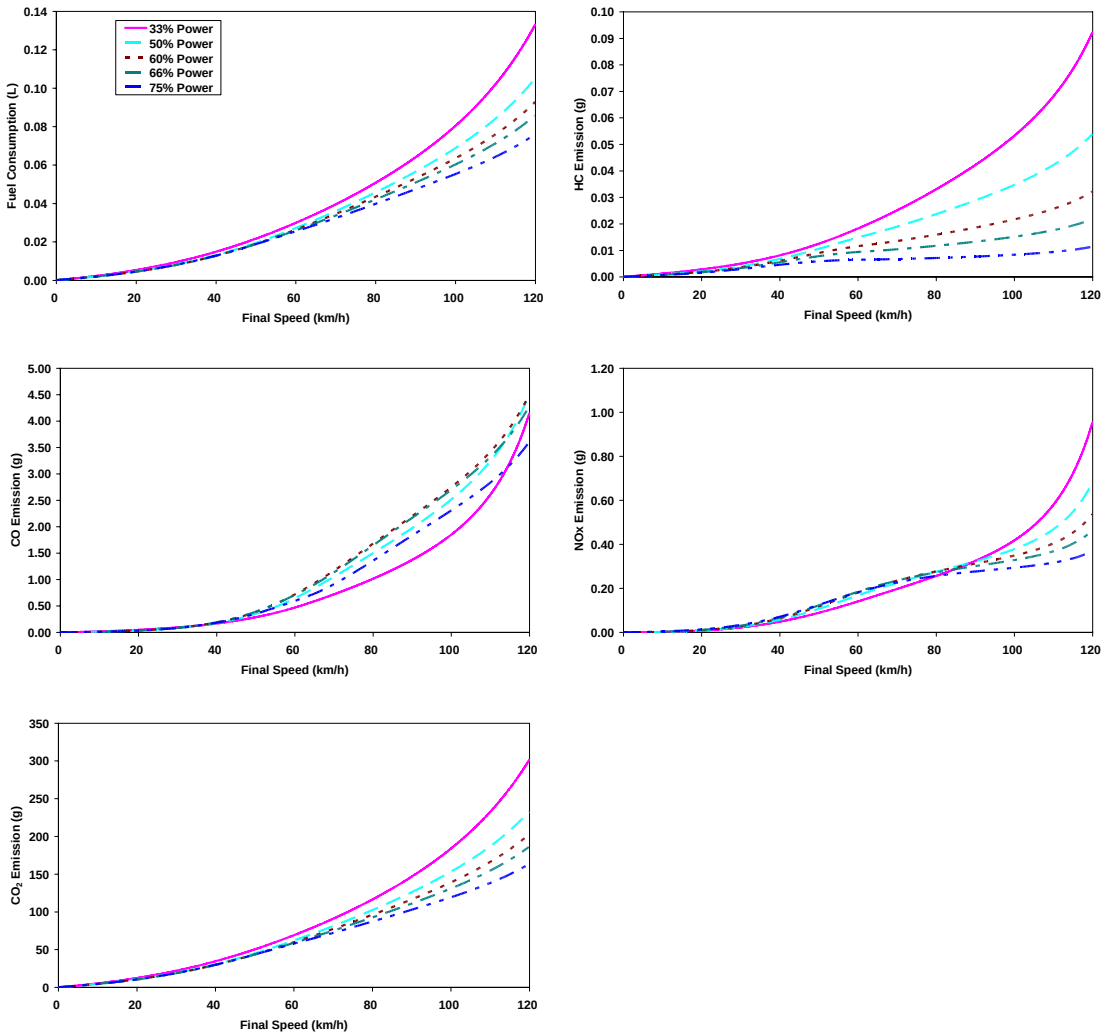

Figure 3-7: Total Fuel Consumption and Emission for Different Acceleration Power (LDV-2)

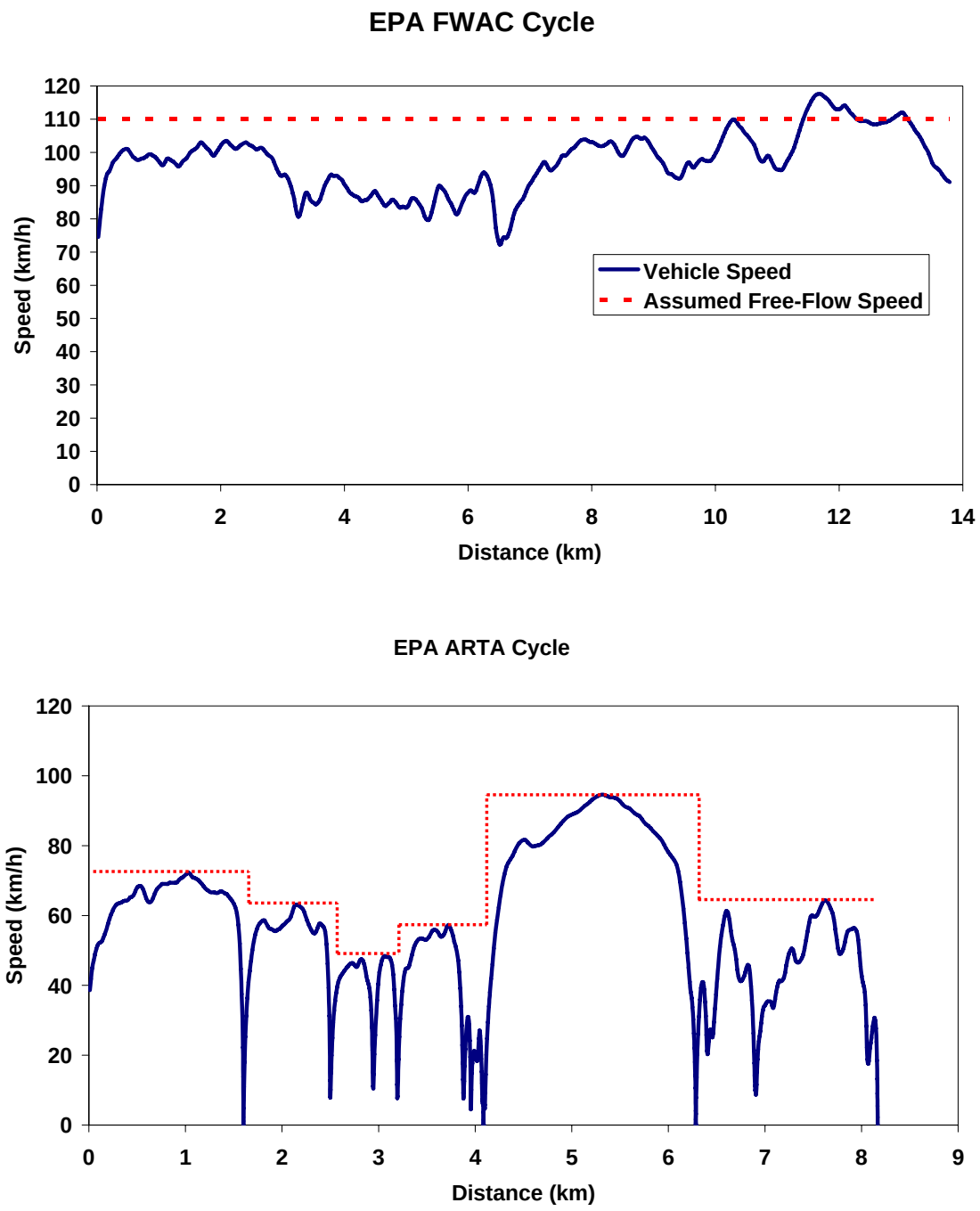

Figure 3-8: Test Drive Cycles

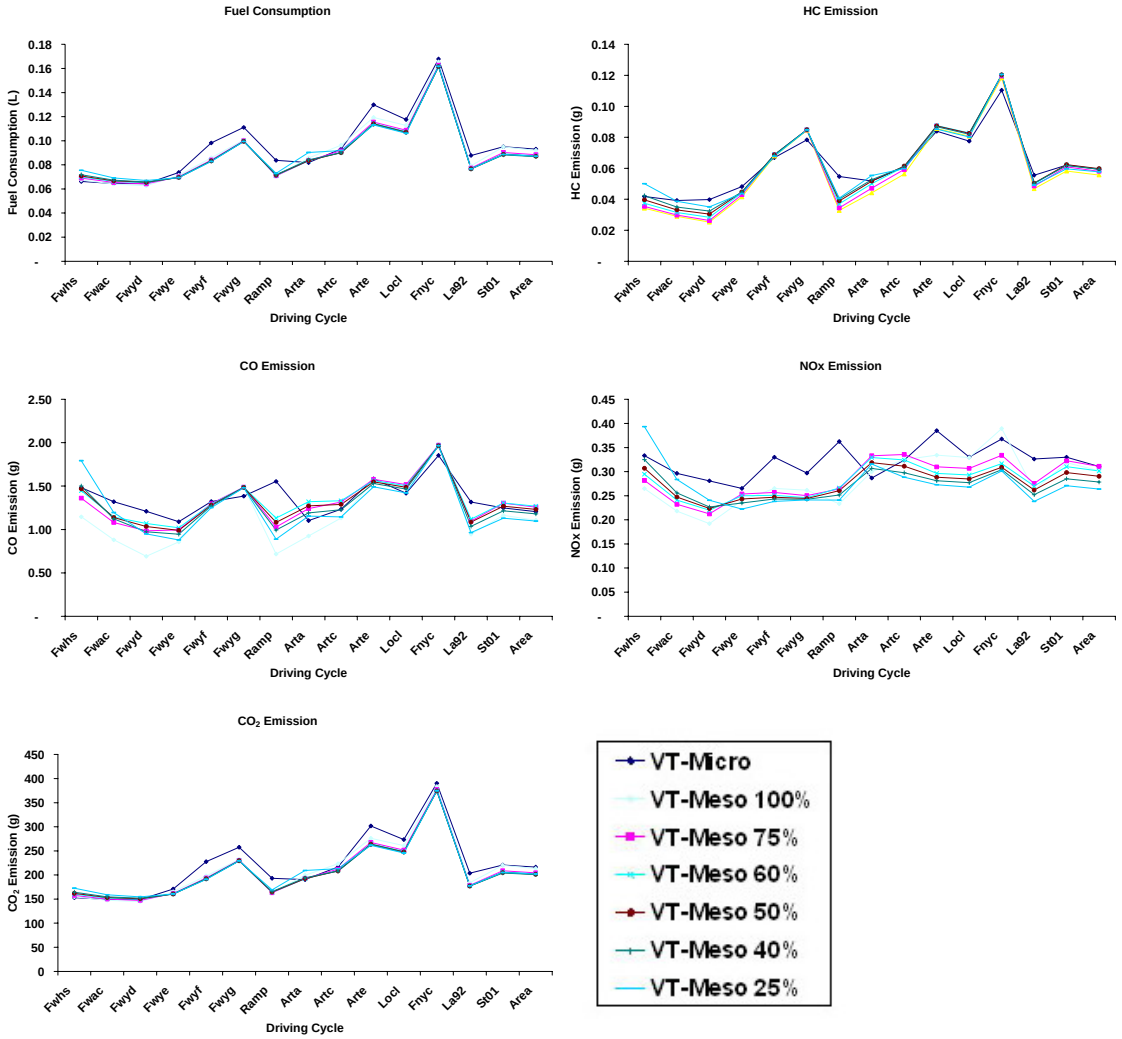

Figure 3-9: Comparison of Mesoscopic and Microscopic Fuel Consumption and Emission Estimates (LDV-2)

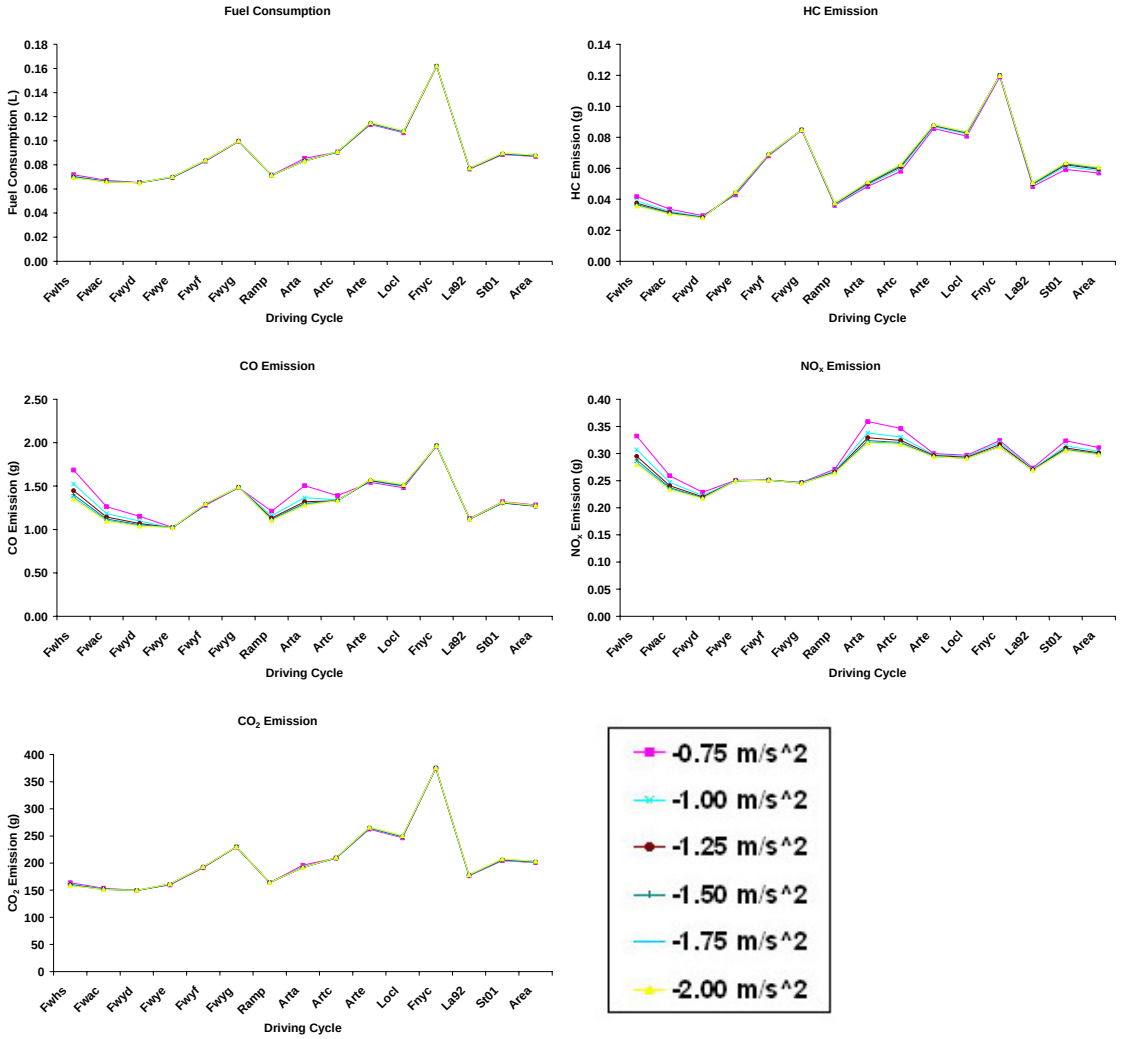

Figure 3-10: Mesoscopic Fuel Consumption and Emission Estimates at Different Deceleration Rates (LDV-2)

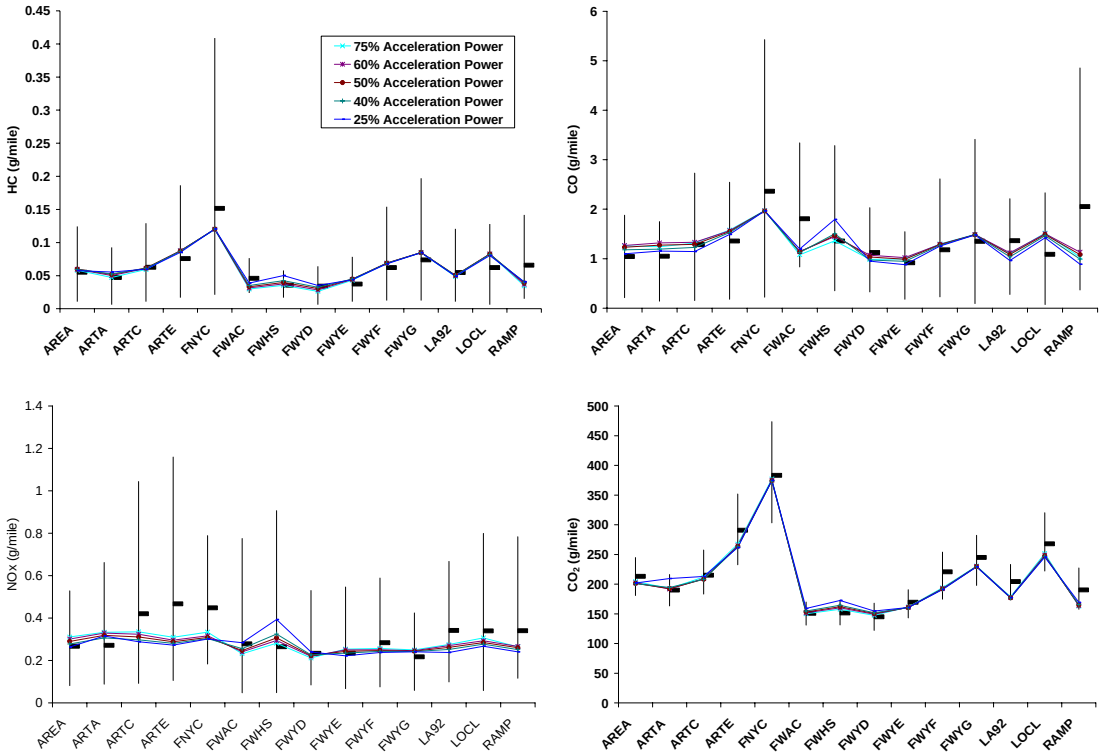

Figure 3-11: Comparison of Mesoscopic Estimates and the EPA data (LDV-2)

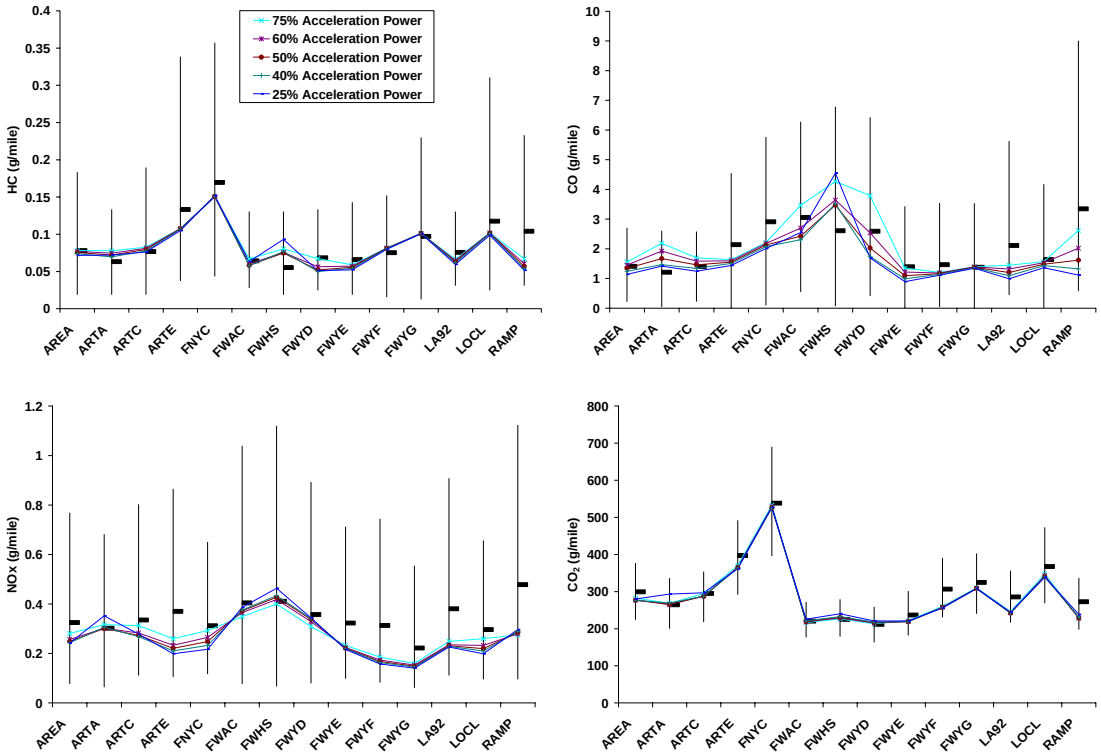

Figure 3-12: Comparison of Mesoscopic Estimates and the EPA data (LDT-1)

Chapter 4 : CHARACTERIZATION OF TYPICAL DRIVER DECELERATION BEHAVIOR FOR ENVIRONMENTAL MODELING

Huanyu Yue[1] and Hesham Rakha[2]

Abstract

The current state-of-practice in the U.S. for estimating vehicle emissions involves estimating the average vehicle speed and total vehicle miles of travel using a macroscopic transportation-planning model. Vehicle emissions are then computed based on the average speed using a macroscopic emission model. Network-wide emissions are finally computed as the product of the estimated vehicle emissions and vehicle miles of travel. This state-of-practice methodology would produce identical emission estimates for all drive cycles exhibiting identical average speeds, regardless of the specific speed profile associated with each drive cycle. In an attempt to overcome this limitation of current state-of-the-art procedures Chapter 3 developed a mesoscopic model that estimates average light-duty vehicle fuel consumption and emission rates on a link-by-link basis based on up to three independent variables, namely: average travel speed, average number of stops per unit distance, and average stop duration. The model performs these estimations by separately analyzing the fuel consumption and emissions during each mode of operation of a vehicle (decelerating, idling, accelerating, and cruising) using relationships derived from instantaneous microscopic fuel consumption and emission models. Consequently, an accurate characterization of typical vehicle deceleration behavior is critical to the accurate modeling of vehicle emissions. The scope of this research effort is to characterize vehicle deceleration behavior for environmental modeling. The study demonstrates that while the deceleration rate typically increases as the vehicle approaches its desired final speed, the use of a constant deceleration rate over the entire deceleration maneuver is adequate for environmental modeling purposes. Finally, the study demonstrates that the application of the mesoscopic model is both feasible and practical and that it produces results that are reasonable in terms of both their absolute magnitudes and their relative trends for the decelerating mode.

1 Graduate Student Assistant, Charles Via Department of Civil and Environmental Engineering, 3500 Transportation Research Plaza (0536), Blacksburg, VA 24061. E-mail: yue@vt.edu

2 Professor of Civil and Environmental Engineering and Leader of the Transportation Systems and Operations Group, Virginia Tech Transportation Institute, 3500 Transportation Research Plaza (0536), Blacksburg, VA 24061. Tel.: (540) 231-1505, Fax: (540) 231-1555, E-mail: hrakha@vt.edu.

4.1. Introduction

4.1.1 Problem Definition

Current state-of-the-art models estimate vehicle emissions based on typical urban driving cycles. Most of these models offer simplified mathematical expressions to compute fuel and emission rates based on average link speeds without regarding transient changes in a vehicle's speed and acceleration as it travels on a highway network (EPA 1993). This presents a problem when the drive cycles encountered in the field differ from those assumed within the models because estimated emission rates may not correspond to actual emissions. A particular problem occurs when comparing drive cycles with identical average speeds, as identical emission rates are then estimated for all cycles despite differences in the second-by-second speed profiles. Significant differences exist in fuel consumption and emission rates despite the identical average speeds, thus indicating a need to look beyond the average speed as a single explanatory variable. Unfortunately, the application of microscopic models may be costly and time consuming for some applications. Also, these tools may require a level of data resolution that is not available. In response to the need to develop vehicle fuel consumption and emissions models that are more accurate than current macroscopic models but also less data intensive than microscopic models, this mesoscopic model was applied in an attempt to make predictions using a limited number of easily measurable input parameters. The scope of this paper is to validate if the mesoscopic model can give reasonable results in terms of both their absolute magnitudes and their relative trends for the decelerating mode only.

4.1.2 Mesoscopic Model

The mesoscopic model relies on three input variables, namely the average trip speed, the number of vehicle stops, and the stopped delay, to construct a representative drive cycle along a given roadway segment. Currently, the model does not distinguish between freeway and arterial facilities in constructing a drive cycle. However, further enhancements to the model will investigate the potential of considering different facility types in constructing drive cycles. Figure 4-1 details the process used to estimate average vehicle fuel consumption and emission rates for a given roadway segment.

The first step involves the construction of a synthetic drive cycle based on the trip parameters of average speed, average number of stops, and average delay per stop on the segment under consideration. As an example, Figure 4-2 demonstrates how a drive cycle can be constructed using the three mentioned input parameters. In this case, it is assumed that the vehicle makes, on average, three stops of a given duration over the segment considered. To account for those three stops, the trip speed profile is constructed by fitting three identical stop-and-go cycles over the entire segment considered. Within each cycle, the cruise speed is computed to maintain the same trip time (identical average speed). (While the above drive cycle generation does not obviously model the actual driving profile—actual profiles would not show such perfect repetition—it should be kept in mind that the objective of the VT-Meso model is not to produce precise estimates of vehicle fuel consumption and emissions, but rather to provide quick, reasonable estimates for cases in which actual drive cycles are not available. If drive cycles were available, then a microscopic model would be more suitable for such an application.) After constructing the

drive cycle, the model estimates the proportion of time that a vehicle typically spends cruising, decelerating, idling, and accelerating while traveling on the link. A series of fuel consumption and emission estimation models are then used to determine the amount of fuel consumed and emissions of HC, CO, CO_2 and NO_X emitted by a vehicle during each mode of operation. Subsequently, the total fuel consumed and pollutants emitted by the vehicle while traveling along the segment considered are estimated by summing the corresponding estimates across the different modes of operation and dividing the results by the distance traveled to obtain distance-based average vehicle fuel consumption and emission rates.

This section presents the general approach behind the synthetic drive cycle construction. A more detailed description of the model's assumptions regarding the characterization of the deceleration, idling, acceleration, and cruising modes of a vehicle will be addressed in the next section.

4.1.3 Paper Layout

This paper is organized into five sections. The first section describes the microscopic and mesoscopic fuel consumption and emission models. The second section describes the procedures of data collection. The third section describes the characterization of typical driver deceleration rates. The fourth section describes comparisons of field emissions measurements, emissions estimates from the VT-Micro model, and emissions estimates from the VT-Meso model. Finally, the paper provides a summary of the findings and recommendations for future work.

4.2. Fuel Consumption and Emission Models

The mesoscopic model utilizes a microscopic vehicle fuel consumption and emission model that was developed at Virginia Tech to compute mode-specific fuel consumption and emission rates. This section describes the microscopic fuel consumption and emission models that were used to develop the mesoscopic model. Also, this section describes how typical drive cycles are constructed using selected trip information in the mesoscopic model.

4.2.1 Microscopic Model

The microscopic vehicle fuel consumption and emission model that was developed at Virginia Tech to compute mode-specific fuel consumption and emission rates (Rakha, Van Aerde et al. 2000; Ahn, Rakha et al. 2002, Rakha, Ahn et al. 2004) was used for this research. This model, known as VT-Micro, predicts the instantaneous fuel consumption and emission rates of HC, CO, CO_2, and NO_X of individual vehicles based on their instantaneous speed and acceleration levels. It was developed to bridge the gap between traffic model simulator outputs, transportation planning models, and environmental impact models. The initial intent behind the development of this model was not to capture all the elements that affect vehicle fuel consumption and emission rates, but simply to develop a model in which vehicle dynamics are explicit enough to account for speed and acceleration variations, two elements that have been shown to have significant impacts on vehicle fuel consumption and emission rates.

$$MOE_e = \begin{cases} \sum_{i=0}^{3}\sum_{j=0}^{3} \exp\left(k_{i,j}^{e} \times v^i \times a^j\right) & for\ a \geq 0 \\ \sum_{i=0}^{3}\sum_{j=0}^{3} \exp\left(l_{i,j}^{e} \times v^i \times a^j\right) & for\ a < 0 \end{cases} \quad [4\text{-}1]$$

where: MOE_e = Instantaneous fuel consumption or emission rate (L/s or mg/s),
a = Instantaneous acceleration of vehicle (km/h/s),
v = Instantaneous speed of vehicle (km/h),
$k^e_{i,j}$ = Vehicle-specific acceleration regression coefficients for MOE_e,
$l^e_{i,j}$ = Vehicle-specific deceleration regression coefficients for MOE_e.

Equation [4-1] indicates the generic form of the microscopic model that was used in this study. This model was developed using fuel consumption and emission data that were collected by the Oak Ridge National Laboratory (ORNL) and which provided steady-state fuel consumption and emission rates of hydrocarbon (HC), carbon monoxide (CO), carbon dioxide (CO_2), and oxides of nitrogen (NO_X) for eight light-duty vehicles that were deemed representative of a 1995 U.S. vehicle fleet.

For each vehicle, fuel consumption and emission rates for hot-stabilized, steady-state operation were obtained through both field measurements and dynamometer testing. Vehicles were first tested on-road to obtain realistic road loads and determine engine conditions as a function of vehicle speed and acceleration. The engine conditions were then duplicated on a chassis dynamometer while making fuel consumption and emission measurements. The regression models that were developed based on the ORNL data resulted in very good fits. As an example, Figure 4-3 illustrates the evaluation results for a composite vehicle having the average characteristics of the eight ORNL test vehicles. As can be observed, the figure indicates an ability to follow very closely the trends in increasing fuel consumption with higher speeds and sharper acceleration, as well as relatively good agreements between the predicted and observed emission trends for the pollutant considered.

Further refinement and validation of the microscopic models were more recently made using data that had been collected by the EPA in 1997. This second dataset included dynamometer fuel consumption and emission measurements under ambient conditions for 43 normal-emission, light-duty vehicles and 17 normal-emission, light-duty trucks. A comparison of the fuel consumption and emission rates produced by the microscopic models against in-laboratory measurements made on a dynamometer using the ARTA drive cycle for various groups of vehicles within the EPA database further confirmed the validity of the microscopic model, as described in Rakha et al., (Rakha, Ahn et al. 2003) and Rakha et al., (Rakha, Ahn et al. 2004).

Since the above datasets considered only normal light-duty vehicles operated under hot stabilized conditions and ignored the effects of additional engine loads on vehicle fuel consumption and emission rates, such as the effect of vehicle start and air conditioning usage, these limitations are thus reflected not only in the resulting microscopic models, but also the proposed mesoscopic models that are based on them. Further research is however currently underway to expand the microscopic models to include high-emitting vehicles, capture vehicle start effects, and model diesel engine vehicle emissions. Once these developments are completed, adjustments could then be made to the proposed mesoscopic model to expand its prediction capabilities.

4.2.2 Mesoscopic Model

First, this section gives the detailed description of the model assumptions that characterize the deceleration, idling, acceleration, and cruising modes of operation of a vehicle. Second, this section describes how fuel consumption and emissions of HC, CO, CO_2, and NO_X are computed for the four modes of operation for light-duty, gasoline engine vehicles that are operating under hot stabilized conditions.

4.2.2.1 Synthetic Drive Cycle Construction

Vehicle Deceleration

The model currently assumes that drivers decelerate at a constant rate that can be set by the user. Specifically, the model allows the user to specify the deceleration rate in the range of -2.00 m/s^2 to -0.25 m/s^2 in increments of 0.25 m/s^2.

The assumption that drivers decelerate at a constant rate was made to simplify the development of the initial model. In reality, different drivers are likely to decelerate at different rates. Individual drivers are also likely to apply rates that vary with speed and the distance from the obstacle ahead. For example, it is often observed that drivers increase their braking level as they come closer to an obstacle ahead. However, while the model currently assumes constant deceleration rates, variable rates could be considered. Once determined, typical variable deceleration rates could be implemented by simply using the appropriate rates when using the underlying microscopic models to calculate the total fuel consumed and pollutants emitted during a given deceleration prior to generating the model's prediction equations.

Vehicle Idling

A vehicle is assumed to be idling when it reaches a speed of 0 km/h. This mode of operation is only considered when the input parameters to the model specify that at least one full stop occurs within the segment being analyzed. If the user specifies a number of stops that is less than one, the model will then assume that only a partial stop occurs and thus that a vehicle decelerates only to a given speed before starting to accelerate again.

Vehicle Acceleration

In the modeling of vehicle acceleration, the model considers a vehicle dynamics model that was initially developed by Rakha et al. Rakha, Lucic et al. 2001 and Rakha and Lucic Rakha and Lucic 2002 for modeling truck acceleration behavior and that was later applied to the modeling of light-duty passenger cars by Snare Snare 2002 and Rakha et al. (Rakha, Snare et al. 2004). As indicated by Equation [4-2], the model is based on the principle that the acceleration of a vehicle is proportional to the resulting force applied to it. The model predicts acceleration rates that decrease with increasing speeds. The decreased acceleration rates are a result of two factors. First, the vehicle tractive effort (F) decreases with vehicle speed. Second, the aerodynamic and rolling resistance forces increase with vehicle speeds. It should be noted that the acceleration factor (α) is used to reduce the vehicle acceleration level to reflect the fact that drivers do not typically use the full power of a vehicle while accelerating, as is discussed by Rakha and Snare (Rakha, Snare et al. 2004). The acceleration factor (α) accounts for the fact that drivers do not utilize the full power of the vehicle while accelerating, as derived by Rakha and Snare (Rakha, Snare et al.

2004). Specifically, Snare and Rakha indicate that drivers accelerate at 62.5% of the maximum acceleration on average, with aggressive drivers accelerating at 85% of the available power and passive drivers accelerating at only 40 percent. Since the intent of the model is to evaluate typical driving behavior, it was thus determined that typical accelerations should be considered by the model instead of maximum feasible accelerations. In particular, assuming that vehicles accelerate at their maximum potential can lead to gross overestimation of vehicle fuel consumption and emission rates.

$$a = \alpha\left(\frac{F - R}{M}\right) \quad [4\text{-}2]$$

where: a = Vehicle instantaneous acceleration (m/s^2)
F = Residual force (N),
R = Total resistance force (N), and
M = Vehicle mass (kg).
α = Fraction of the maximum acceleration that is utilized by the driver.

Equations [4-3], [4-4], and [4-5] further indicate how the effective tractive force of a vehicle is computed at any given speed. Specifically, Equation [4-3] computes the effective tractive force as the minimum of the tractive force applied by the engine, Ft, and the maximum force that can be sustained between the vehicle tires and the pavement surface, F_{max}. The tractive force is computed using Equation [4-4], which assumes that the vehicle power does not change with speed and is equal to the maximum potential power of the vehicle. The power transmission efficiency parameter further accounts for power loss in the transmission system as well as losses associated with engine accessories such as fan, ventilator, water pump, magneto, distributor, fuel pump, and compressor. Equation [4-5], finally, determines the maximum tractive force that can be sustained between the vehicle tires and the pavement surface without the wheels spinning. This force is a function of coefficient of friction and the mass of the vehicle applied to the tractive axle.

$$F = \min(F_t, F_{\max}) \quad [4\text{-}3]$$

$$F_t = 3600 \cdot \eta \cdot \frac{P}{v} \quad [4\text{-}4]$$

$$F_{\max} = 9.8066 \cdot p_{mta} \cdot M \cdot \mu \quad [4\text{-}5]$$

where: F_t = Tractive force applied on the vehicle (N),
F_{max} = Maximum attainable Tractive force (N),
P = Maximum engine power (kW),
η = Power transmission efficiency,
v = Vehicle speed (km/h),
p_{Mta} = Portion of vehicle mass on tractive axle,
μ = Coefficient of friction between vehicle tires and pavement, and
α = Fraction of acceleration power effectively used by driver.

Equations [4-6] through [4-9] further describe how the external resistance forces can be calculated. Equation [4-6] indicates that the total external resistance force is the sum of the aerodynamic, rolling, and grade resistance forces. In Equation [4-7], the aerodynamic resistance force is shown to be a function of the vehicle frontal area, the altitude, the vehicle's drag coefficient, and the square of the vehicle speed. The rolling resistance force is further shown in Equation [4-8] to be a function of the total mass and speed of the vehicle, while Equation [4-9] indicates that the grade resistance force is a function of the road grade and mass of the vehicle.

$$R = R_a + R_r + R_g \quad [4\text{-}6]$$

$$R_a = 0.047285 \cdot C_d \cdot C_h \cdot A \cdot v^2 \quad [4\text{-}7]$$

$$R_r = 9.8066 \cdot C_r \cdot (c_2 v + c_3) \cdot \frac{M}{1000} \quad [4\text{-}8]$$

$$R_g = 9.8066 \cdot M \cdot i \quad [4\text{-}9]$$

where: R_a = Aerodynamic resistance (N),
R_r = Rolling resistance (N),
R_g = Grade resistance (N),
A = Frontal area of vehicle (m^2),
H = Altitude (m),
C_d = Air drag coefficient,
C_h = Altitude coefficient = 1 – (0.000085 · H), and
C_r, c_1, c_2 = Rolling resistance constants
i = Grade magnitude (m/100 m)

Cruising Mode

Between deceleration and acceleration events, it is assumed that a vehicle travels at a constant speed. As was indicated earlier, the speed at which a vehicle cruises is computed so that the total travel time along the segment under consideration is not altered. The cruising speed is determined through an iterative process that adjusts the cruising speed and corresponding deceleration and acceleration times until a match is found between the resulting travel time and the travel time determined by the average speed.

While the assumption of a constant cruising speed may not reflect typical observed speed variability, this approach represents only a first step in constructing realistic drive cycles based on a limited number of trip parameters. Again, the model is designed for use in cases in which detailed speed profiles are not available. Assumptions of constant cruising speeds are also fairly common in traffic simulation models. In this case, it would be expected that speed variability while cruising would result in additional fuel consumption and emissions. In particular, small differences at high speeds can result in large differences in emissions, depending on whether a vehicle engine goes into enrichment or enleanment mode. One way of accounting for the additional emissions that may result from speed variability would be to use microscopic fuel consumption and emission models to analyze second-by-second speed profiles with varying

degrees of speed variability and to use the evaluation results to determine a series of correction factors to be utilized with these models. Research in this direction is currently underway.

4.2.2.2 Fuel Consumption and Emission Estimates by Drive Mode

Cruise Mode

The rates at which individual vehicles consume fuel and emit pollutants while traveling at a constant speed are obtained by applying the appropriate cruise speed and an acceleration rate of zero to the microscopic models defined by Equation [4-1]. This yields fuel consumption and emission relationships of the form given by Equation [4-10]. To obtain total fuel consumption and emissions during a cruising event, the rates given by Equation [4-10] are then multiplied by the total duration of the event.

$$MOE_e^{cruise} = \exp(k_{0,0}^e + k_{1,0}^e \cdot v + k_{2,0}^e \cdot v^2 + k_{3,0}^e \cdot v^3) \quad [4\text{-}10]$$

where: MOE_e^{cruise} = Fuel consumption or pollutant emission rate while cruising (l/s or mg/s),
s = Vehicle cruising speed (km/h), and
$k^e_{i,0}$ = Vehicle-specific acceleration regression coefficients for MOE_e, which are shown in Table 4-2.

Deceleration Mode

Applying the VT-Micro model that was defined in Equation [4-1] to a deceleration maneuver from a pre-defined cruising speed to a complete stop, Equation [4-11] was derived to express the relationship between the total fuel consumed and pollutants emitted by a single vehicle while decelerating from a given initial speed to a final speed of 0 km/h at a constant deceleration rate. Specifically, Equation [4-11] was obtained by integrating the instantaneous fuel consumption and emission rates provided by Equation [4-1] over the entire duration of a deceleration event at a constant deceleration rate. Because of the non-linear nature of the relationships considered, a closed analytical solution could not be found. Instead, regression relationships were fitted to the data, as demonstrated in Equation [4-11].

$$MOE_e^{decel} = d_0 + d_1 v_c + d_2 v_c^2 + d_3 v_c^3 + d_4 v_c^4 + d_5 v_c^5 + d_6 v_c^6 \quad [4\text{-}11]$$

where: MOE_e^{decel} = Total fuel consumed, pollutant emitted, traveled distance or travel time while decelerating (L/s, mg/s, m or sec),
v_c = Vehicle initial speed (km/h), and
$d_0,\ldots,d_6$ = Vehicle-specific regression coefficients, which are shown in Table 4-3.

While the deceleration relationships were developed to express the total fuel consumed and pollutants emitted over a full deceleration maneuver (deceleration to a speed of 0 km/h), these relationships can also be used to consider partial stops. For example, in computing the fuel consumption for a deceleration maneuver from 60 to 50 km/h, the fuel consumption for a deceleration maneuver from 50 to 0 km/h is subtracted from the fuel consumption rate for a deceleration maneuver from 60 to 0 km/h.

For example, Figure 4-4 illustrates the deceleration relationships that were developed for the 1999 Crown Victoria for constant deceleration rates of -0.5, -1.0, -1.5 and -2.0 m/s^2. It is observed that the fuel consumption and emission rates do not exhibit linear relationships with respect to the starting cruise speed despite an assumed constant deceleration rate. This non-linearity is due to the non-linear instantaneous vehicle fuel consumption and emission rates.

Result from a previous research effort that was conducted by Rakha *et al.* (Rakha, Dion et al. 2001) demonstrated that predicted fuel consumption and emission rates were marginally impacted by deceleration rates. The main impact of considering varying deceleration rates is therefore not to improve the model predictions during deceleration maneuvers; instead the analysis enhances the model predictions by altering the distance traveled while cruising and accelerating.

Idling Mode

As was the case for the cruise and deceleration models, the fuel consumption and emission rates for the idling model are based on the use of the underlying VT-Micro model. In this case, idling rates are determined by using the models of Equation [4-1] with an instantaneous speed of 0 km/h and an instantaneous acceleration rate of 0 km/h/s. This yields constant rates that are then multiplied by the average stop duration to estimate the total fuel consumed and emissions during an average idling event.

Acceleration Mode

As was done for the deceleration mode, the fuel consumed and pollutants emitted by a vehicle during an acceleration event is computed by integrating the fuel consumption and emission rates estimated using Equation [4-1] over the entire acceleration event. After computing the total fuel consumption and emissions for a series of final target speeds, regression models of the form defined by Equation [4-12] were then developed for each measure of effectiveness. As was the case with the deceleration models, these relationships estimate the total distance traveled, time consumed, fuel consumed, and pollutants emitted for an acceleration maneuver from a full stop up to a final cruise speed vc.

$$MOE_e^{accel} = d_0 + d_1 v_c + d_2 v_c^2 + d_3 v_c^3 + d_4 v_c^4 + d_5 v_c^5 + d_6 v_c^6 \quad [4\text{-}12]$$

where: $MOE_e{}^{accel}$ = Total distance traveled, time consumed, fuel consumed or pollutants emitted while accelerating (m, s, L/s, and mg/s),
v_c = Vehicle final speed (km/h), and
$b_0,\ldots,b_6$ = Vehicle-specific regression coefficients, which are shown in Table 4-4.

As was the case with Equation [4-12], Equation [4-12] can be used to estimate the distance traveled, time consumed, fuel consumption, and emissions that are associated with partial acceleration events. For instance, to estimate the fuel consumed for an acceleration from a speed of 50 km/h to a speed of 60 km/h, the model defined by Equation [4-12] would first be applied to estimate the fuel consumed for an acceleration from 0 to 60 km/h, and then to estimate the fuel consumed for an acceleration from 0 to 50 km/h. The difference between the two estimates would then be the fuel consumed to accelerate from 50 to 60 km/h.

4.3. Data Collection

The first task in this research effort was to establish a database of vehicle deceleration data. The data are designed to represent the typical deceleration of a vehicle decelerating to a complete stop. Two data sets are included in this study: one data set was collected during the spring and summer of 2003 on the 460 Bypass in Virginia, and the other one was collected during the autumn and winter of 1998 in Michigan by the Ford Motor Company. The present section describes the procedures applied for collecting the data.

4.3.1 Drivers

Participants were licensed drivers and were selected from four age groups, 20 to 29 years, 30 to 39 years, 40 to 49 years, and 50 years or older. Several drivers were chosen from each age group. For the data collected in Virginia, 24 participants were included in the study, which includes 7 female drivers. For the data collected in Michigan, 24 participants were included in the study, which included 12 male drivers and 12 female drivers. Table 4-1 shows a breakdown of licensed drivers on the road for the test drives, listed by age and gender.

4.3.2 Test Vehicle

The test vehicles were equipped with a Global Positioning System (GPS) unit that measured the vehicle speed to an accuracy of 0.1 m/s (0.305 ft/sec). Drivers were instructed to come to a complete stop at the stop sign or traffic lights. The vehicle was equipped with radar detectors in the front and the back of the vehicle. These radar detectors measure the distance headway and speed of seven vehicles in front and rear of the test vehicle. A four-door 1999 Ford Crown Victoria was used in Virginia for the data collection; a four-door 1994 Ford Taurus SHO was used for the data collection in Michigan.

The test vehicles record data at 10 Hz. Recorded vehicle parameters include longitudinal acceleration, velocity, range, range rate, throttle position, and brake cylinder pressure. A laptop computer connected to the vehicles was used to collect driving data.

4.3.3 Drive Cycles

4.3.3.1 Drive Cycle in Virginia

The test drives were performed during the spring and summer of 2003 on the 460 Bypass in Virginia. The lengths of the test drive on the 460 Bypass East and West were 3.9 km (2.44 miles) and 4.5 km (2.8 miles), respectively. Posted speed limit on the routes is 55 mph, and the posted speed limit of the off-ramps is 45 mph. The horizontal layouts of the test sections are fairly straight with some minor horizontal curvature that does not impact vehicle speeds. 460 Bypass East has a downgrade followed by an upgrade portion in the section where deceleration is being studied, which is illustrated in Figure 4-5, whereas 460 Bypass West has a predominant upgrade portion in the same deceleration zone, which is illustrated in Figure 4-6. The vertical profiles of the test sections were then generated by interpolating between elevation data from GPS using a cubic spline interpolating procedure. The cubic spline interpolation ensured that the elevations, the slopes, and the rate of change of slopes were identical at the boundary conditions. A polynomial regression relationship was fit to the grade data (R^2 of 0.951) for two reasons. First,

this ensured a smooth transition in the roadway grade while maintaining the same vertical profile. Second, it also facilitated the solution of the ODE because it ensured that the grade function was continuous. The modified grade and vertical elevation, which are illustrated in Figure 4-6 (b) (thick line), demonstrate an almost identical vertical profile with much smoother grade transitions when compared to the direct interpolation. The data of deceleration driving mode were extracted. In order to get a more representative estimate, each test driver was requested to make five or ten runs.

4.3.3.2 Drive Cycle in Michigan

The study was conducted on a pre-selected 20-mile route on surface streets in Dearborn Michigan, which is shown in Figure 4-7. The route and time of the test drives were selected so as to generate a large amount of driving in traffic at slower speeds as well as slowing and stopping behind other vehicles. Posted speeds on the route ranged primarily from 35 mph to 45 mph with a brief section posted at 55 mph. The route included 49 traffic lights.

4.3.4 Data

Typical output data from GPS receivers include latitude, longitude, attitude, heading, speed, and time. The GPS receiver used was able to update these parameters once every second. The instantaneous deceleration level of a vehicle at each recording point can be determined using the forward difference formulation that is presented in Equation [4-13].

$$a_t = \frac{u_{t+\Delta t} - u_t}{\Delta t} \qquad [4\text{-}13]$$

where: a_t = Instantaneous deceleration of vehicle at time t (m/s^2)
u_t = Instantaneous speed of vehicle at time t (km/h)
Δ_t = Interval between observations at times t and t – Δt (s)

Using the GPS-measured instantaneous speeds and the corresponding calculated instantaneous accelerations, the fuel consumed and pollutants emitted by a vehicle during a given trip can be estimated using microscopic energy and emission models.

The field emission data were also collected for some test drives. The data include the fuel consumption and emission rates of hydrocarbon (HC), carbon monoxide (CO), carbon-dioxide (CO_2) and oxides of nitrogen (NO_X).

4.4. Characterization of Typical Deceleration Rates

For each test drive, the time headway was investigated to identify if the vehicle was following other vehicles. If the time headway was within the range of 0 to 4 seconds, the vehicle was considered to be following the other vehicle. There are three types of deceleration maneuvers from the test drive data: first, deceleration to a complete stop in front of a traffic light with a lead vehicle; second, deceleration to a complete stop in front of a traffic light without a lead vehicle; and third, deceleration to a complete stop in front of a stop sign without a lead vehicle.

It is clear that the deceleration rates applied by drivers will be some fraction of the maximum deceleration capability. However, it is unclear whether the percentage of deceleration power used varies as a function of speed. It is also unclear how much variability there is between different drivers. Therefore, the following procedure was developed for this task:

1. First, analyze the average deceleration rates of the entire deceleration maneuver. The average deceleration rates distribution are compared with normal distribution.
2. Second, the deceleration rates for different speed intervals are calculated. Then these rates are analyzed to discover the trend.
3. Third, compare the three different types of deceleration maneuvers.

The statistics results are shown in Table 4-5. For the deceleration in front of a stop sign without a lead vehicle, the results show that the drivers break harder when the speed is lower, which means the deceleration rate is speed dependent. Figure 4-8 demonstrates that the deceleration rate typically increases as the vehicle approaches its desired final speed. Figure 4-9 through Figure 4-13 illustrate the comparisons between the deceleration rate frequency distribution and the normal distribution for different scenarios. The deceleration rates' frequency distributions do not follow the normal distribution. It is clear from these figures that the deceleration rates of most drivers are greater than the mean values of the decelerating rates.

Brackstone et al. (Brackstone, Sultan et al. 2000) investigated the approach process between vehicles. In this research, the drivers were instructed to drive at a cruising speed of the driver's choice and that if their path were to become blocked by a slower vehicle, they were to decelerate as they saw fit and follow it. In total, 70 approach processes were observed in their study, and for each approach process the speed and spacing were recorded. As shown in Figure 4-13, the relationship between relative speed (a negative value indicating closing) and spacing can be described by a linear relationship. In the current study, a similar investigation was conducted to examine the relationship between the distance from the stop sign and the relative speed when the vehicles start to decelerate. In total, 279 approach processes were observed in this study. The relationship between spacing and approaching speed is shown in Figure 4-14. The relationship between relative speed and spacing can be described by a linear relationship. A linear relationship can be seen from Figure 4-15; the high speeds correspond to the longer stopping distance. Most drivers decelerate 100 to 250 m from the stop sign.

Figure 4-15 illustrates that the slope of the trend line is 0.019, and the slope of the trend line in Figure 4-14 is 0.06. The range of relative speed in Figure 4-14 is between 0 and 15 m/s, while the range of relative speed in Figure 4-15 is between 15 and 27m/s. The observed approaching processes in Figure 4-15 have higher speeds than the approaching process in Figure 4-14. As discussed before, the deceleration rate typically increases as the vehicle approaches its desired final speed. In other words, the deceleration rate increases as the speed decreases. Since the observations in Figure 4-14 have higher speeds, it is reasonable that the slope in Figure 4-15 is greater than the slope in Figure 4-14.

4.5. Emission Estimate Comparison

4.5.1. Speed Profile

Figure 4-16 illustrates the speed profile of a typical drive cycle. For each profile, speeds were measured by driving probe vehicles equipped with Global Positioning System (GPS) equipment. The red point in this figure represents the start point of the deceleration section.

4.5.2. Emission Comparison

A direct comparison of the VT-Micro model fuel consumption and emission estimates and field data for the deceleration maneuvers was conducted for the test drives. The constant deceleration rate was used for this comparison. In these comparisons, the VT-Meso model was not expected to produce identical estimates. Instead, the objective of the exercise was to investigate the ability of the VT-Meso model to correctly predict changes in vehicle fuel consumption and emission rates.

Equation [4-11] was applied to get the fuel consumption and emission estimations for the deceleration maneuver. The regression coefficients, shown in Table 4-3, were developed by using curve-fitting technology.

Figure 4-17 and Figure 4-18 compare the average fuel consumption and emission rates that were estimated for the light-duty composite vehicle being considered by both the VT-Meso and VT-Micro models with the filed data. The figures show that the VT-Meso model generally overestimates fuel consumption and emissions. The figures clearly demonstrate that the VT-Meso model correctly predicts trends of increasing or decreasing fuel consumption and HC emissions. Specifically, the model produces the highest and lowest estimates for the same cycles for which the highest and lowest VT-Micro model estimates are obtained.

4.6. Conclusions

This research effort includes characterization of typical driver deceleration behavior. It illustrates that the application of the VT-Mesoscopic model is both feasible and practical and that it produces results that are reasonable in terms of both their absolute magnitude and their relative trends for the decelerating mode.

The deceleration rate increases when the speed decreases; drivers tend to decelerate harder at the end of the deceleration trips, which means the deceleration rate is speed-dependent. However, the use of a constant deceleration rate over the entire deceleration maneuver is adequate for environmental modeling purposes. Future study should be conducted to investigate the relationship between speed and deceleration rate. Meantime, data collection is underway to collect more female driver data, which will give us a normally distributed database.

Comparisons of fuel consumption and emission rates predicted by the proposed VT-Meso model against microscopic estimates demonstrated the ability of the VT-Meso model's proposed approach to predicting changes in vehicle fuel consumption and emission rates. The estimates from the VT-Meso model would not always match estimates from microscopic models because

of differences in the underlying drive cycles (VT-Meso model constructs simplistic drive cycles). The model, however, constitutes an interesting alternative to existing models because it is more accurate than current macroscopic models but also less data intensive than microscopic models. Further enhancements may be considered in constructing drive cycles to reflect typical speed variations as a function of the facility type. It should also be noted that the consideration of these parameters removes any dependency on pre-set drive cycles and allows the model to distinguish between drive cycles with identical average speeds. It further allows use of the model to perform quick evaluations of alternative scenarios without requiring detailed data or modeling, as is demanded by microscopic models.

Table 4-1: Test Drivers Characteristics

(a) Data Collected in Virginia

	Male	Female	
20–29	11	5	16
30–39	3	2	5
40–49	2	0	2
> 50	1	0	1
	17	7	Total

(b) Data Collected in Michigan

	Male	Female	
20–29	4	4	8
40–49	4	4	8
> 50	4	4	8
	12	12	Total

Table 4-2: Regression Coefficients for Cruise Mode

HC (g)	-6.565E+00	3.884E-02	-8.547E-04	5.620E-06
CO (g)	-4.744E+00	3.677E-02	-9.238E-04	7.000E-06
NO_x (g)	-7.412E+00	3.596E-02	-1.123E-04	-3.806E-07
CO_2 (g)	1.214E-01	9.530E-03	1.189E-04	-7.158E-07
Fuel(liters)	-1.443E-03	1.732E-05	6.040E-08	-2.832E-10

Table 4-3: Regression Coefficients for Deceleration Maneuver

	Constant	S	S^2	S^3	S^4	S^5	S^6	R^2
-0.50 m/s²								
HC	6.876E-01	3.547E-01	1.966E-02	-6.324E-04	1.133E-05	-9.852E-08	3.482E-10	0.99999
CO	1.541E+01	-8.753E-01	5.115E-01	-1.978E-02	3.647E-04	-3.170E-06	1.074E-08	0.99989
NO_x	1.671E-01	1.560E-01	3.948E-03	-4.084E-05	1.131E-06	-5.912E-10	-2.998E-11	1.00000
CO_2	3.132E-01	5.313E-01	6.195E-04	5.706E-05	-4.017E-07	6.647E-09	-3.025E-11	1.00000
Fuel	1.404E-04	2.440E-04	3.011E-07	2.700E-08	-2.140E-10	3.039E-12	-1.179E-14	1.00000
-0.75 m/s²								
HC	7.147E-01	2.110E-01	1.212E-02	-4.375E-04	8.197E-06	-7.233E-08	2.568E-10	0.99999
CO	1.019E+01	5.234E-01	2.333E-01	-9.635E-03	1.842E-04	-1.635E-06	5.683E-09	0.99995
NO_x	1.738E-01	1.003E-01	1.172E-03	5.120E-06	4.051E-08	4.598E-09	-2.999E-11	1.00000
CO_2	5.161E-01	3.465E-01	-5.232E-05	3.900E-05	-2.950E-07	4.413E-09	-1.963E-11	1.00000
Fuel	2.347E-04	1.596E-04	-7.486E-08	1.971E-08	-1.736E-10	2.253E-12	-8.721E-15	1.00000
-1.00 m/s²								
HC	7.690E-01	1.432E-01	1.000E-02	-3.937E-04	7.523E-06	-6.683E-08	2.362E-10	0.99998
CO	8.579E+00	1.272E+00	9.578E-02	-4.500E-03	9.130E-05	-8.374E-07	3.039E-09	0.99998
NO_x	1.868E-01	7.749E-02	1.496E-04	1.789E-05	-2.450E-07	4.670E-09	-2.210E-11	1.00000
CO_2	6.253E-01	2.604E-01	-3.325E-04	2.897E-05	-2.166E-07	2.976E-09	-1.310E-11	1.00000
Fuel	2.866E-04	1.204E-04	-2.220E-07	1.526E-08	-1.363E-10	1.650E-12	-6.371E-15	1.00000
-1.25 m/s²								
HC	6.864E-01	6.587E-02	1.208E-02	-4.684E-04	8.654E-06	-7.506E-08	2.576E-10	0.99997
CO	5.459E+00	1.477E+00	3.337E-02	-1.982E-03	4.339E-05	-4.112E-07	1.585E-09	1.00000
NO_x	9.290E-02	6.586E-02	-2.475E-04	1.894E-05	-2.679E-07	3.548E-09	-1.447E-11	1.00000
CO_2	3.183E-01	2.115E-01	-4.339E-04	2.217E-05	-1.558E-07	1.955E-09	-8.528E-12	1.00000
Fuel	1.457E-04	9.819E-05	-2.772E-07	1.216E-08	-1.051E-10	1.175E-12	-4.474E-15	1.00000
-1.50 m/s²								
HC	9.528E-01	7.662E-02	1.035E-02	-4.407E-04	8.488E-06	-7.549E-08	2.619E-10	0.99995
CO	9.866E+00	1.852E+00	-1.715E-02	-1.398E-04	1.050E-05	-1.299E-07	6.430E-10	1.00000
NO_x	2.434E-01	5.840E-02	-3.547E-04	1.540E-05	-2.044E-07	2.330E-09	-8.688E-12	1.00000
CO_2	7.626E-01	1.794E-01	-4.161E-04	1.676E-05	-1.080E-07	1.219E-09	-5.208E-12	1.00000
Fuel	3.540E-04	8.343E-05	-2.531E-07	9.095E-09	-7.152E-11	7.532E-13	-2.822E-15	1.00000
-1.75 m/s²								
HC	1.031E+00	7.876E-02	8.375E-03	-3.733E-04	7.363E-06	-6.645E-08	2.328E-10	0.99995
CO	1.222E+01	1.623E+00	-1.810E-02	3.251E-06	6.926E-06	-9.447E-08	5.007E-10	1.00000
NO_x	3.041E-01	5.009E-02	-2.935E-04	1.268E-05	-1.665E-07	1.906E-09	-7.122E-12	1.00000
CO_2	9.382E-01	1.538E-01	-3.377E-04	1.397E-05	-8.754E-08	9.899E-10	-4.263E-12	1.00000
Fuel	4.363E-04	7.142E-05	-2.061E-07	7.549E-09	-5.803E-11	6.152E-13	-2.320E-15	1.00000
-2.00 m/s²								
HC	8.585E-01	-2.116E-02	1.294E-02	-4.837E-04	8.640E-06	-7.318E-08	2.441E-10	0.99996
CO	4.552E+00	1.270E+00	-7.491E-03	-2.150E-04	8.988E-06	-1.021E-07	4.907E-10	1.00000
NO_x	9.998E-02	4.433E-02	-2.876E-04	1.208E-05	-1.588E-07	1.763E-09	-6.514E-12	1.00000
CO_2	3.245E-01	1.342E-01	-2.726E-04	1.191E-05	-7.215E-08	8.392E-10	-3.685E-12	1.00000
Fuel	1.497E-04	6.247E-05	-1.791E-07	6.725E-09	-5.245E-11	-5.519E-13	-2.078E-15	1.00000

Table 4-4: Regression Coefficients for Acceleration Maneuver

	Constant	S	S^2	S^3	S^4	S^5	S^6	R^2
α = 25%								
HC	1.930E+00	2.774E-01	5.709E-02	-1.175E-03	1.707E-05	-1.662E-07	7.158E-10	0.99997
CO	5.071E+00	5.668E+00	2.062E-01	-1.231E-02	3.942E-04	-5.156E-06	2.370E-08	0.99970
NO_x	-1.115E+00	2.364E+00	-1.560E-01	7.342E-03	-1.086E-04	7.759E-07	-2.205E-09	0.99997
CO_2	5.928E-01	1.085E+00	-4.324E-02	2.941E-03	-5.219E-05	4.028E-07	-1.120E-09	0.99998
Fuel	1.376E-04	5.560E-04	-2.591E-05	1.588E-06	-2.820E-08	2.175E-10	-5.998E-13	0.99997
α = 33%								
HC	1.779E+00	4.390E-01	2.478E-02	-5.338E-05	-1.672E-06	-9.473E-09	1.924E-10	1.00000
CO	-1.428E+00	1.204E+01	-7.296E-01	2.876E-02	-4.059E-04	2.094E-06	-9.365E-10	0.99994
NO_x	1.165E+00	1.298E+00	-6.061E-02	3.773E-03	-4.950E-05	3.482E-07	-1.107E-09	0.99999
CO_2	1.103E+00	8.330E-01	3.058E-02	2.395E-03	-4.287E-05	3.352E-07	-9.588E-10	1.00000
Fuel	3.895E-04	4.440E-04	-2.100E-05	1.381E-06	-2.470E-08	1.939E-10	-5.538E-13	0.99999
α = 40%								
HC	2.006E+00	4.013E-01	2.134E-02	-1.049E-04	1.518E-06	-4.124E-08	2.727E-10	0.99999
CO	8.508E+00	6.377E+00	-2.348E-01	9.811E-03	-7.172E-05	-3.679E-07	5.031E-09	0.99998
NO_x	3.245E+00	-1.555E-01	9.013E-02	-2.305E-03	5.563E-05	-4.675E-07	1.215E-09	0.99998
CO_2	1.588E+00	5.178E-01	-3.252E-03	1.151E-03	-2.002E-05	1.517E-07	-4.294E-10	1.00000
Fuel	6.558E-04	2.790E-04	-6.303E-06	7.200E-07	-1.233E-08	9.331E-11	-2.621E-13	1.00000
α = 50%								
HC	2.188E+00	5.537E-01	-4.787E-03	7.413E-04	-1.055E-05	3.943E-08	5.514E-11	0.99999
CO	6.497E+00	1.014E+01	-7.774E-01	3.072E-02	-3.736E-04	1.557E-06	1.248E-10	0.99996
NO_x	2.992E+00	-2.150E-01	9.472E-02	-2.978E-03	6.869E-05	-5.890E-07	1.641E-09	0.99999
CO_2	1.653E+00	4.939E-01	-7.249E-03	1.027E-03	-1.592E-05	1.079E-07	-2.783E-10	1.00000
Fuel	6.895E-04	2.858E-04	-1.043E-05	7.551E-07	-1.166E-08	7.950E-11	-2.035E-13	0.99999
α = 55%								
HC	2.470E+00	4.879E-01	-3.097E-03	7.040E-04	-1.083E-05	4.810E-08	1.197E-11	0.99999
CO	1.182E+01	6.899E+00	5.523E-01	2.623E-02	-3.469E-04	1.601E-06	-5.727E-10	0.99998
NO_x	2.751E+00	-8.892E-02	7.674E-02	-2.410E-03	5.818E-05	-5.078E-07	1.425E-09	0.99999
CO_2	1.721E+00	4.659E-01	-8.204E-03	9.901E-04	-1.533E-05	1.037E-07	-2.661E-10	1.00000
Fuel	7.522E-04	2.569E-04	-9.570E-06	7.089E-07	-1.112E-08	7.658E-11	-1.971E-13	1.00000
α = 60%								
HC	2.691E+00	4.407E-01	-1.360E-03	6.283E-04	-1.017E-05	4.867E-08	-6.994E-12	0.99999
CO	1.420E+01	4.660E+00	-3.510E-01	2.076E-02	-2.920E-04	1.411E-06	-6.314E-10	0.99998
NO_x	2.603E+00	-1.408E-02	6.308E-02	-1.933E-03	4.886E-05	-4.336E-07	1.223E-09	0.99999
CO_2	1.768E+00	4.516E-01	1.044E-02	1.023E-03	-1.604E-05	1.104E-07	-2.872E-10	1.00000
Fuel	7.926E-04	2.386E-04	-9.380E-06	6.864E-07	-1.096E-08	7.670E-11	-2.002E-13	1.00000
α = 66%								
HC	2.890E+00	4.141E-01	-1.009E-03	5.713E-04	-9.459E-06	4.699E-08	-1.613E-11	0.99999
CO	1.466E+01	3.624E+00	-2.206E-01	1.611E-02	-2.328E-04	1.108E-06	-2.256E-10	0.99999
NO_x	2.448E+00	5.386E-02	5.081E-02	-1.496E-03	4.026E-05	-3.659E-07	1.042E-09	0.99999
CO_2	1.809E+00	4.321E-01	-1.206E-02	1.037E-03	-1.642E-05	1.141E-07	-2.989E-10	1.00000
Fuel	8.229E-04	2.235E-04	-9.301E-06	6.623E-07	-1.068E-08	7.538E-11	-1.981E-13	1.00000
α = 75%								
HC	3.080E+00	4.095E-01	-3.956E-03	6.243E-04	-1.057E-05	5.986E-08	-6.948E-11	0.99999
CO	1.427E+01	4.683E+00	-3.257E-01	1.942E-02	-2.993E-04	1.742E-06	-2.489E-09	0.99997
NO_x	2.296E+00	1.385E-01	3.749E-02	-1.020E-03	3.056E-05	-2.882E-07	8.323E-10	0.99999
CO_2	1.827E+00	4.098E-01	-1.330E-02	1.038E-03	-1.680E-05	1.193E-07	-3.180E-10	1.00000
Fuel	8.451E-04	2.109E-04	-9.508E-06	6.464E-07	-1.062E-08	7.625E-11	-2.035E-13	1.00000
α = 100%								
HC	3.116E+00	3.069E-01	-1.840E-03	4.666E-04	-8.508E-06	5.220E-08	-7.710E-11	0.99999

CO	1.541E+01	3.188E+00	-2.003E-01	1.374E-02	-2.209E-04	1.323E-06	-1.963E-09	0.99998
NO_x	2.185E+00	2.688E-01	1.111E-02	-2.058E-06	9.593E-06	-1.175E-07	3.608E-10	0.99999
CO_2	1.844E+00	3.444E-01	-1.292E-02	9.412E-04	-1.589E-05	1.164E-07	-3.167E-10	1.00000
Fuel	8.661E-04	1.734E-04	-8.337E-06	5.593E-07	-9.531E-09	7.033E-11	-1.913E-13	1.00000

Table 4-5: Statistics Results of Deceleration Rates for Different Scenarios

(a) Deceleration to a complete stop in front of Stop Sign without a Lead Vehicle

Deceleration Rate (m/s^2)	Whole Trip	60 km/h to 50 km/h	50 km/h to 40 km/h	40 km/h to 30 km/h	30 km/h to 0 km/h
Mean	1.51	1.49	1.47	1.81	3.24
STD	0.34	0.69	0.60	0.83	0.93
Number of Trips	278	269	277	279	279

(b) Deceleration to a complete stop in front of Stop Sign with a Lead Vehicle

Deceleration Rate (m/s^2)	Whole Trip	60 km/h to 50 km/h	50 km/h to 40 km/h	40 km/h to 30 km/h	30 km/h to 0 km/h
Mean	0.97	1.16	1.41	1.68	1.13
STD	0.32	0.59	0.61	0.60	0.30
Number of Trips	192	131	192	192	192

(c) Deceleration to a complete stop in front of Stop Sign without a Lead Vehicle

Deceleration Rate (m/s^2)	Whole Trip	60 km/h to 50 km/h	50 km/h to 40 km/h	40 km/h to 30 km/h	30 km/h to 0 km/h
Mean	1.09	1.26	1.65	1.87	1.27
STD	0.36	0.62	0.57	0.59	0.35
Number of Trips	58	50	58	58	58

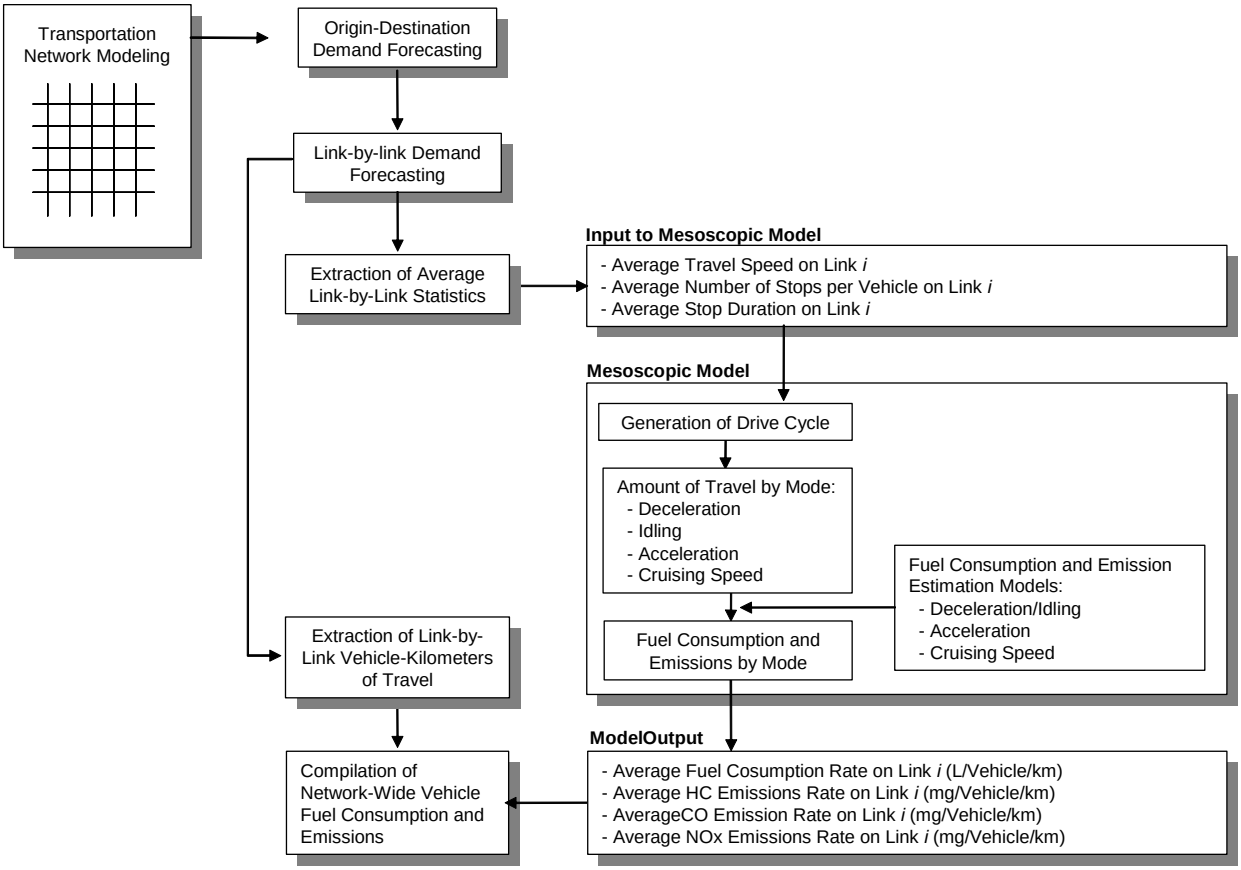

Figure 4-1: Application Framework of Proposed Mesoscopic Fuel Consumption and Emission Estimation Model

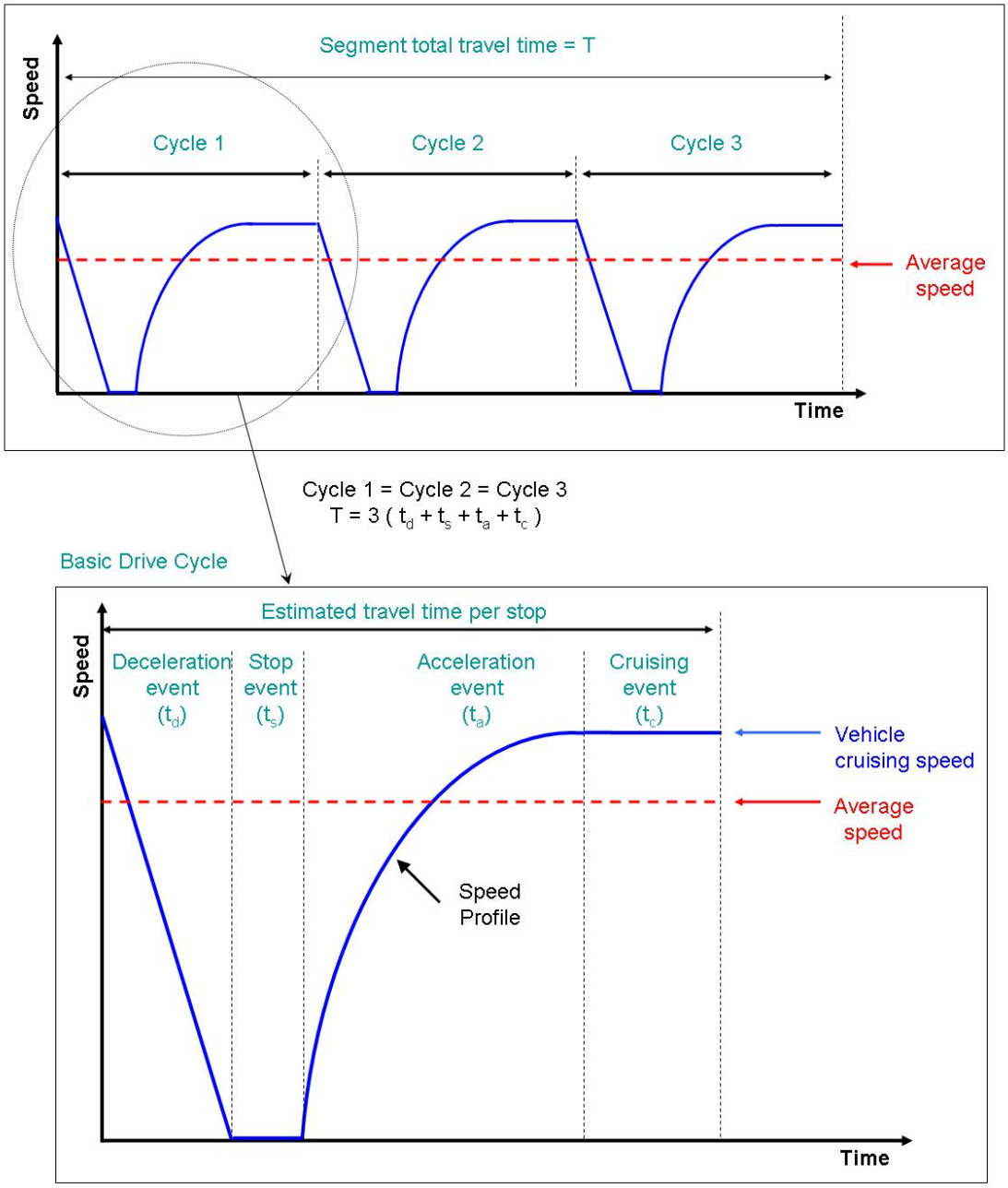

Figure 4-2: Example of Synthetic Speed Profile

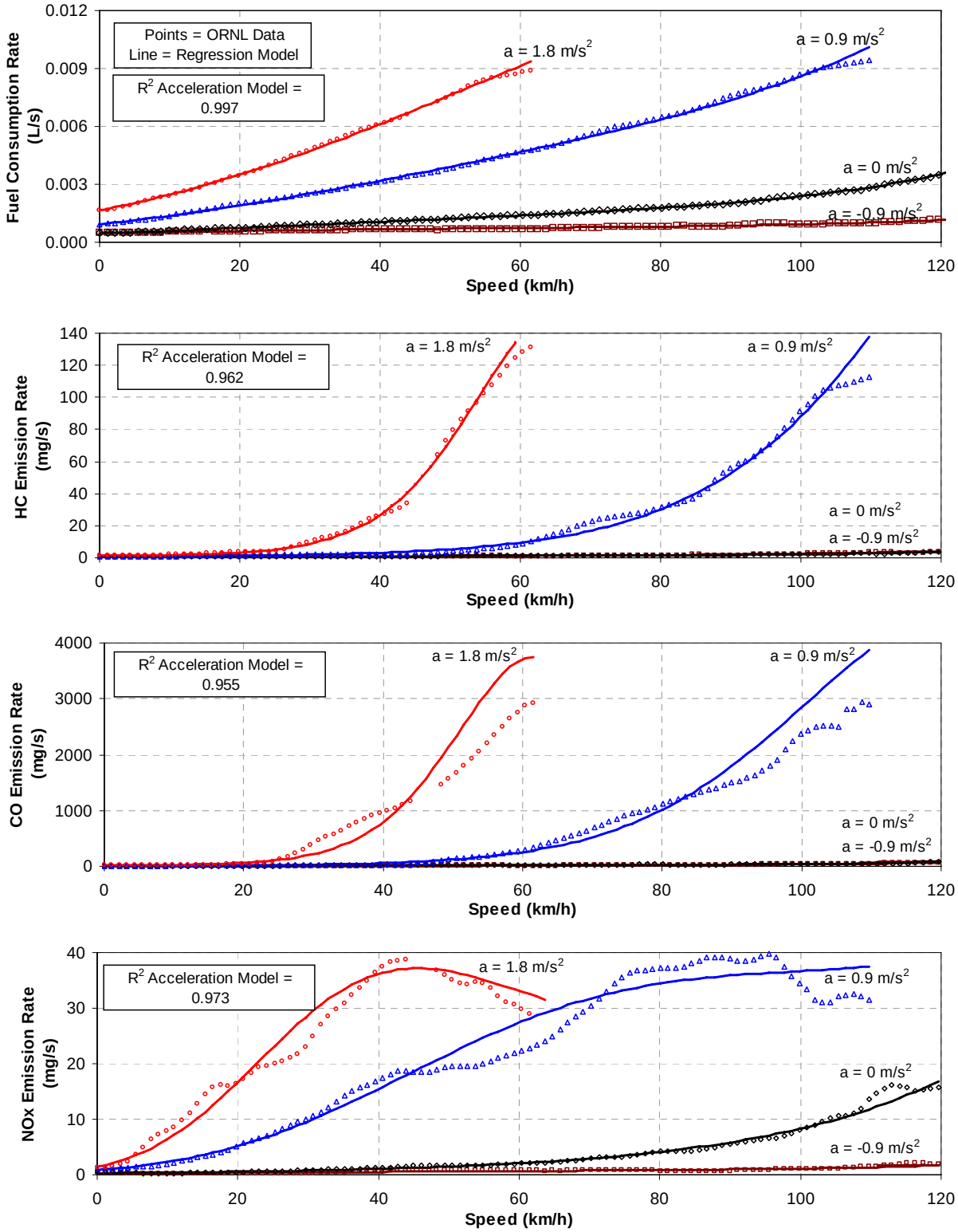

Figure 4-3: Validation of Underlying Microscopic Models for ORLN Composite Vehicle

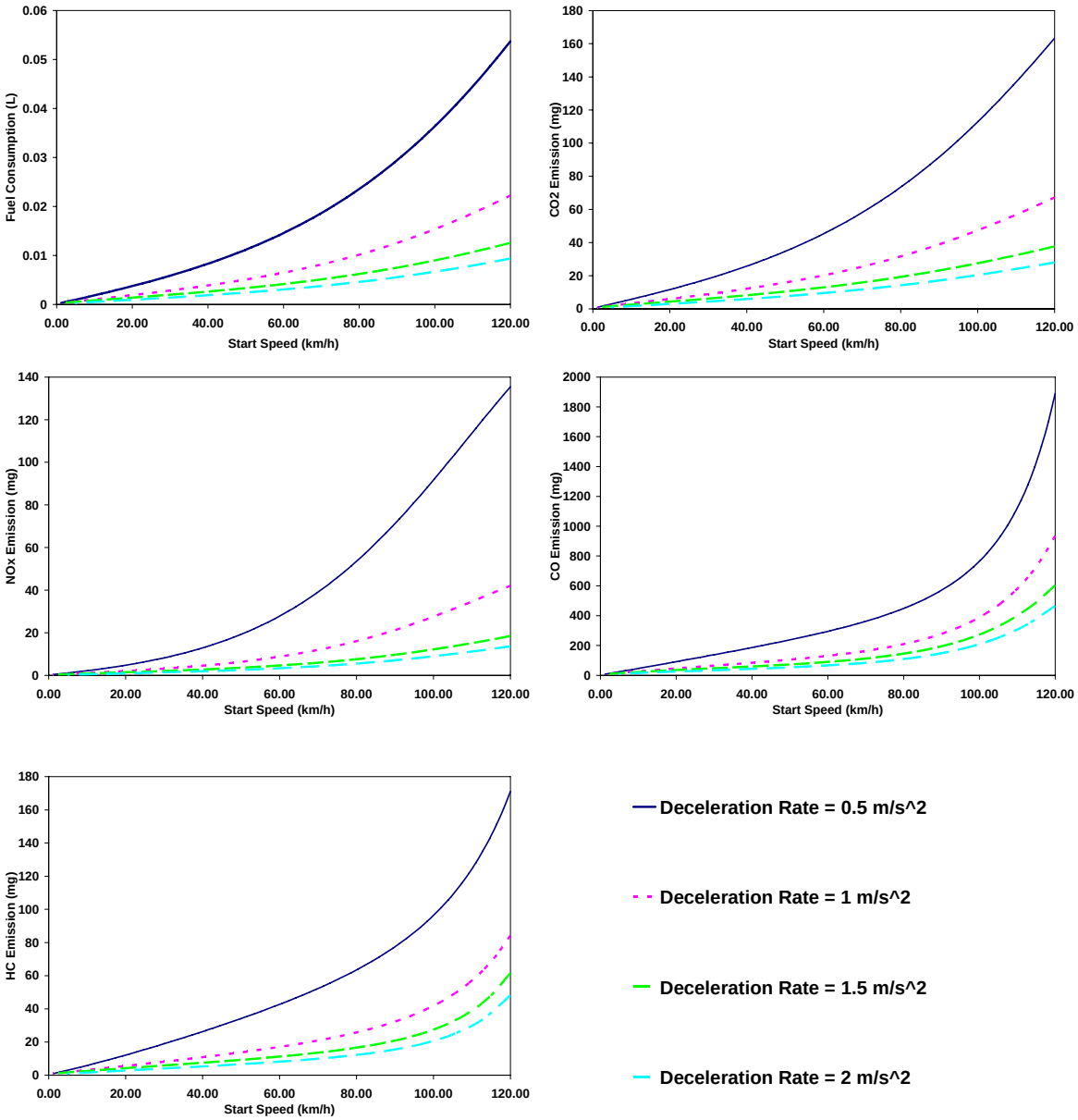

Figure 4-4: Total Fuel Consumption and Emission for Different Deceleration Rates (1999 Crown Victoria)

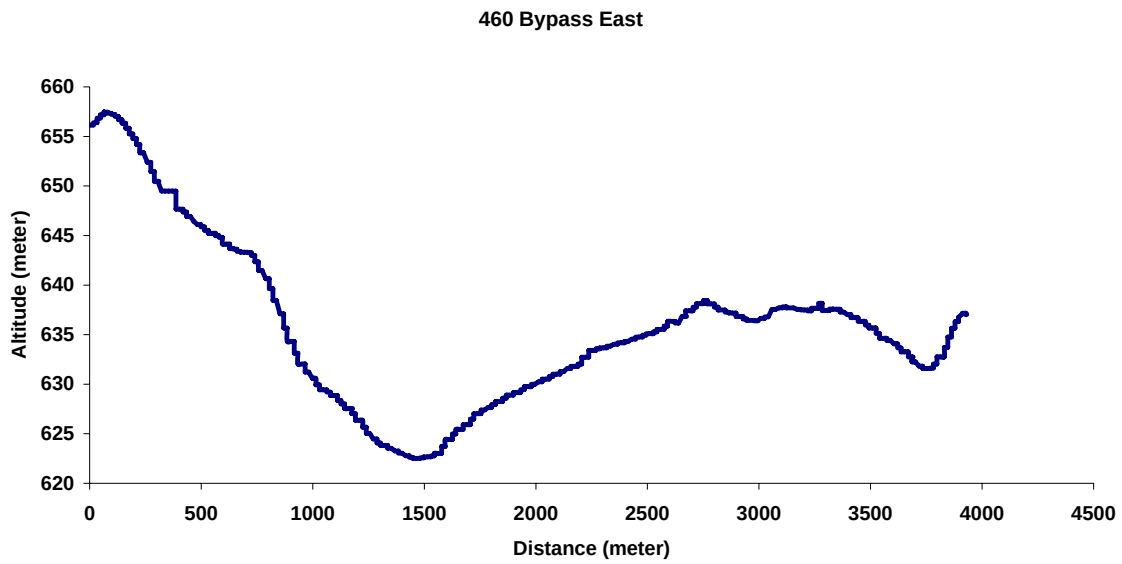

(a) 460 Bypass East

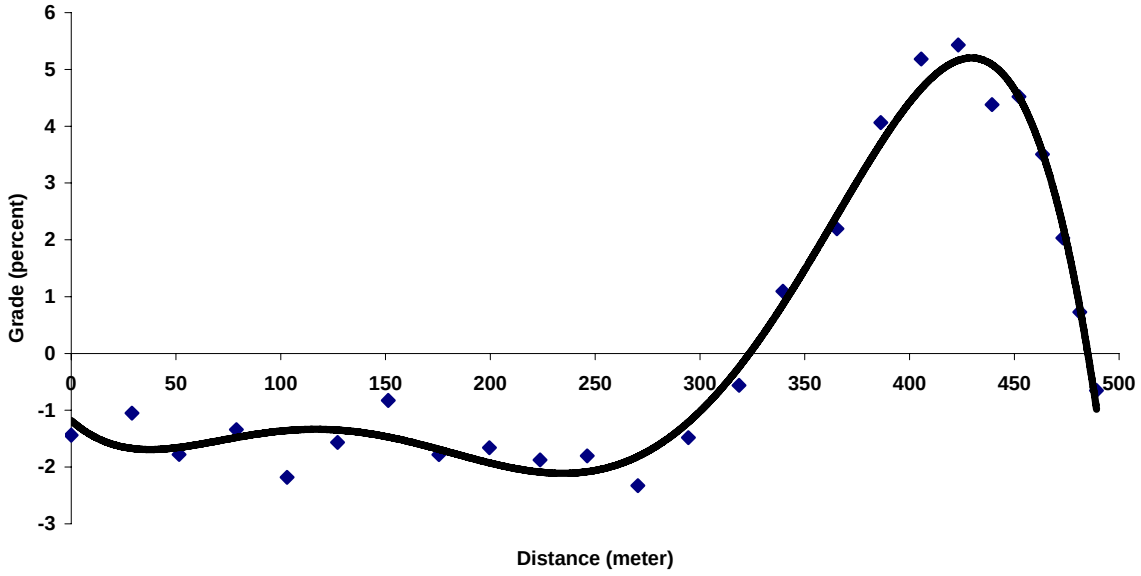

(b) 460 Bypass East Deceleration Trip Section

Figure 4-5: 460 Bypass East Vertical Profile

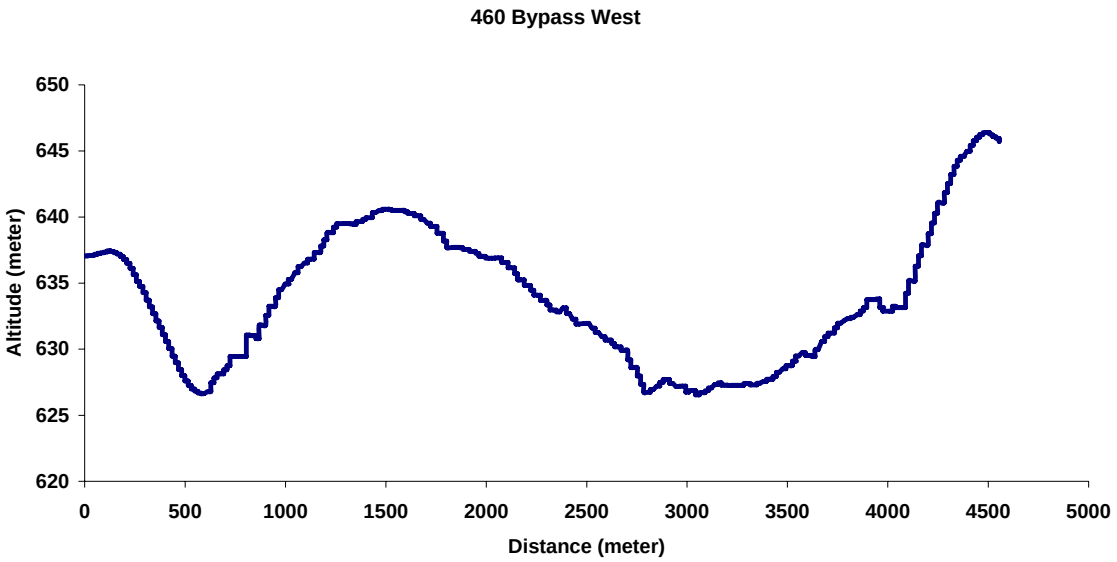

(a) 460 Bypass West

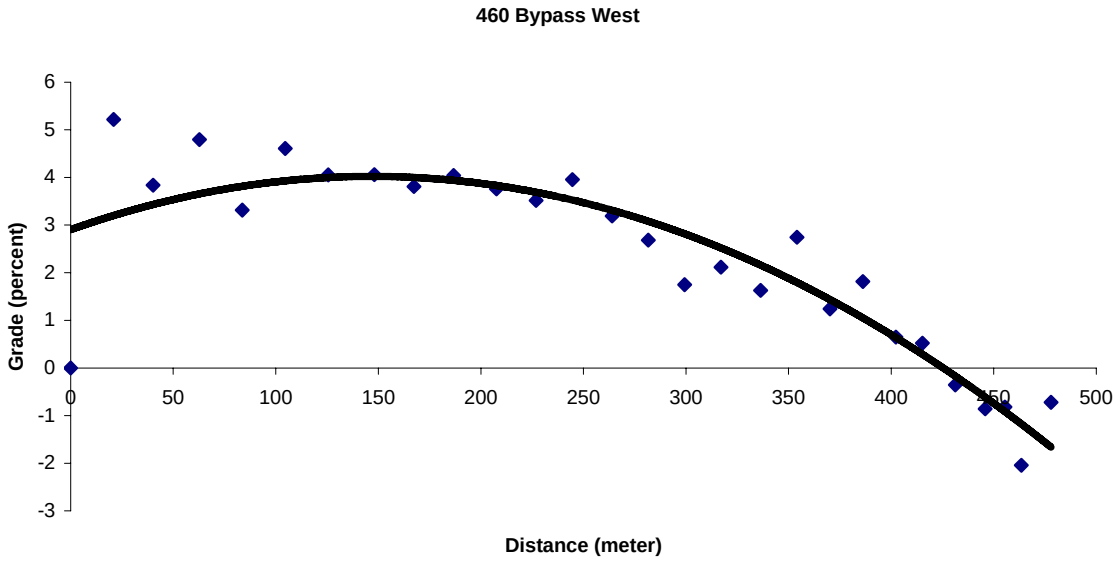

(b) 460 Bypass West Deceleration Trip Section

Figure 4-6: 460 Bypass West Vertical Profile

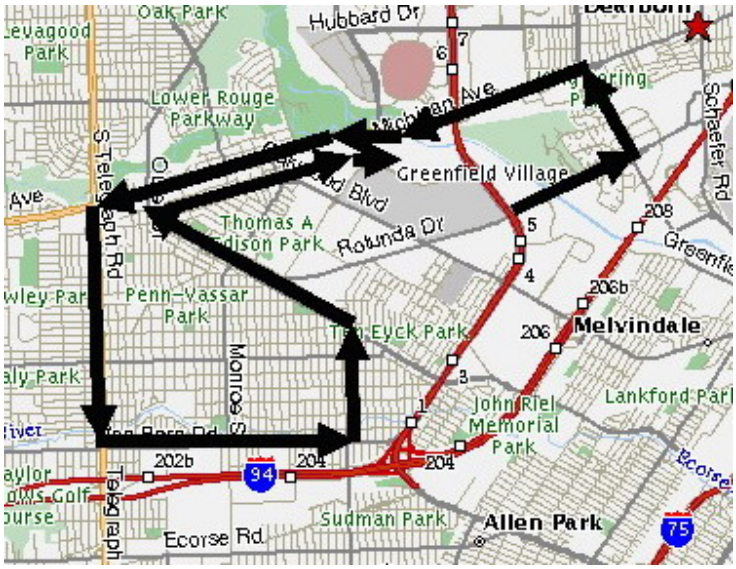

Figure 4-7: Map of Experiment Route in Michigan

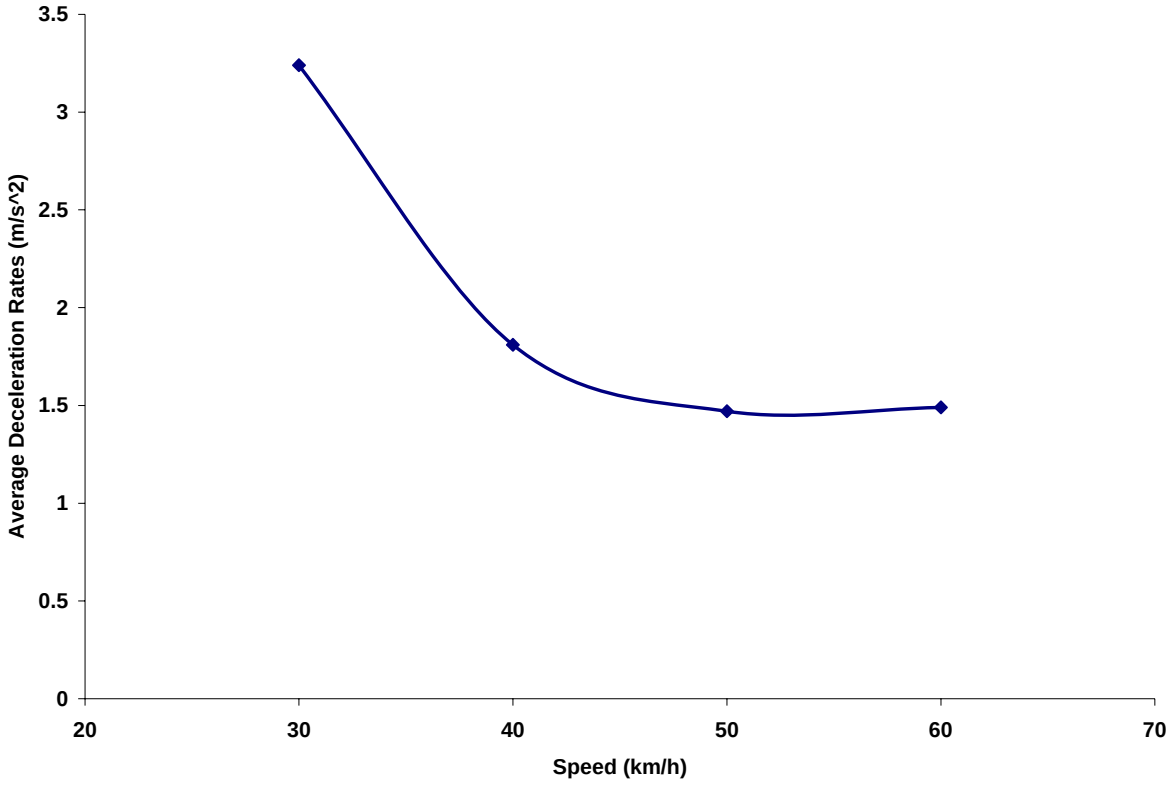

Figure 4-8: Deceleration Rates Comparison for Different Scenarios

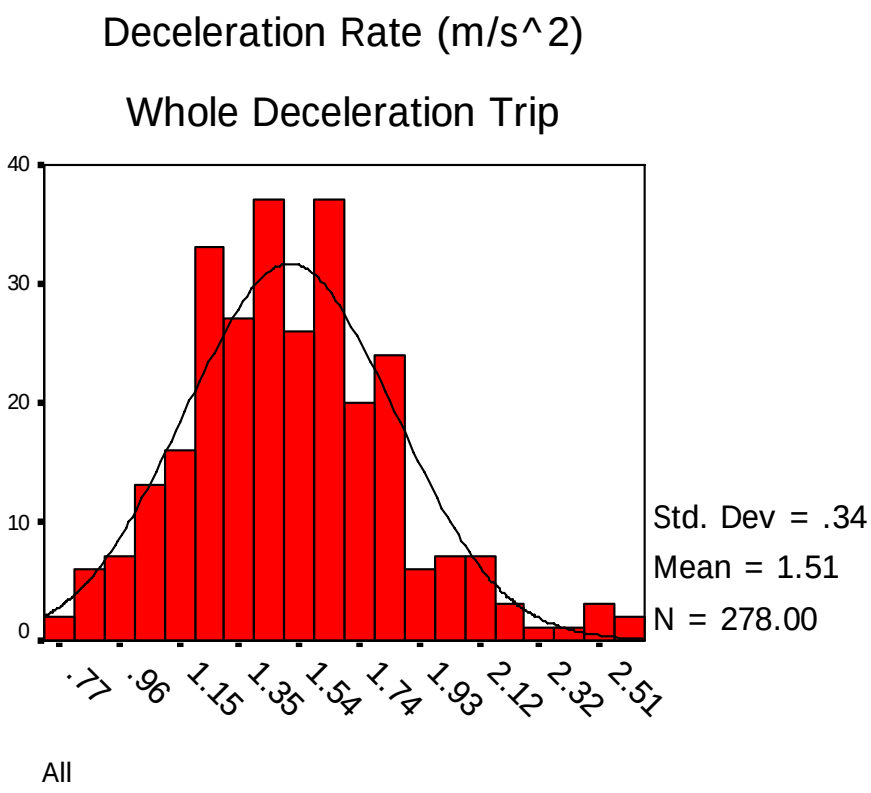

Figure 4-9: Distribution of Average Deceleration Rates (Whole Deceleration Trip)

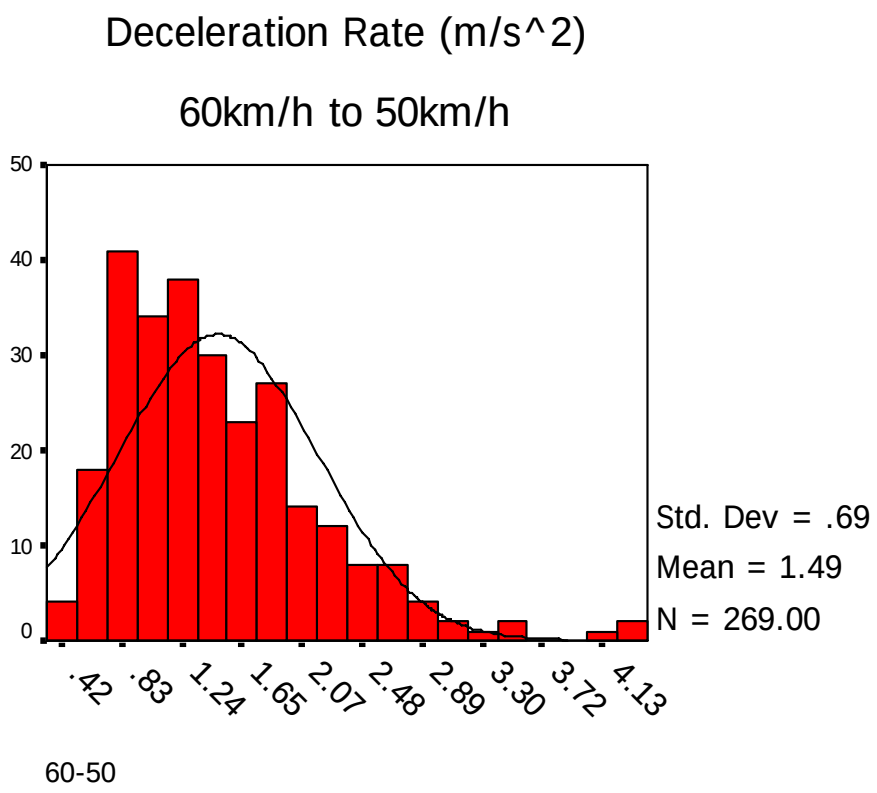

Figure 4-10: Distribution of Average Deceleration Rates (from 60 km/h to 0 km/h)

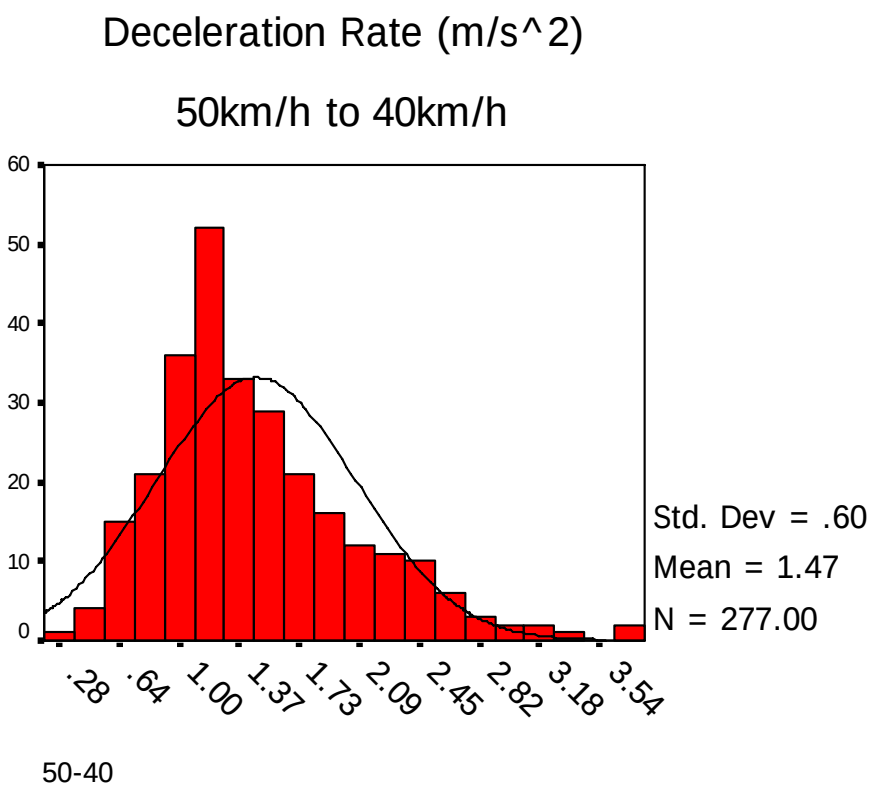

Figure 4-11: Distribution of Average Deceleration Rates (from 50 km/h to 0 km/h)

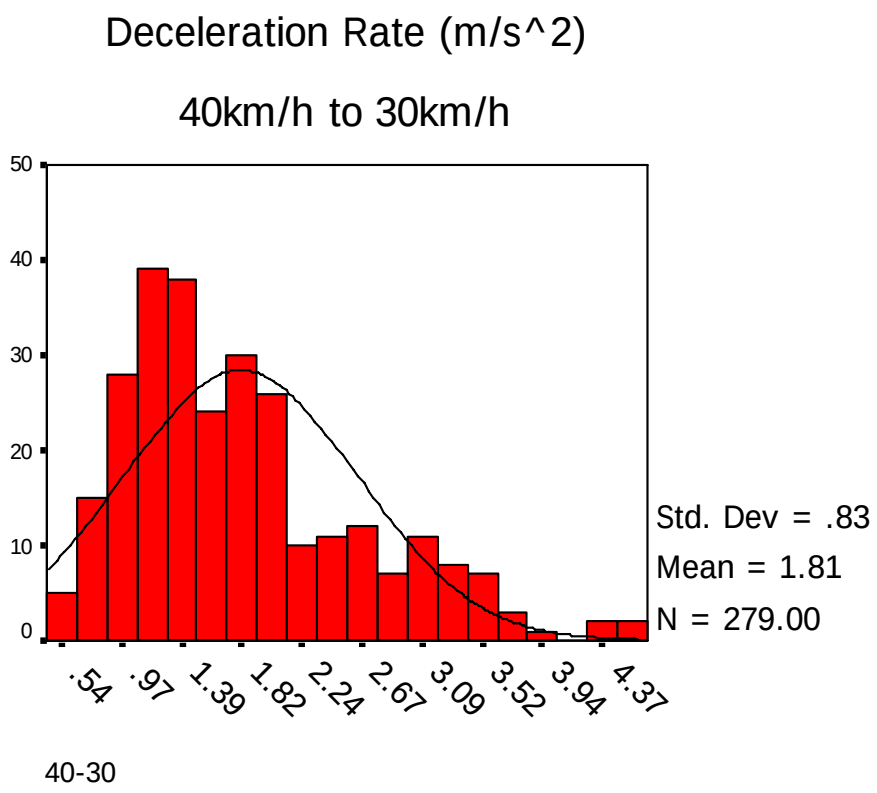

Figure 4-12: Distribution of Average Deceleration Rates (from 40 km/h to 0 km/h)

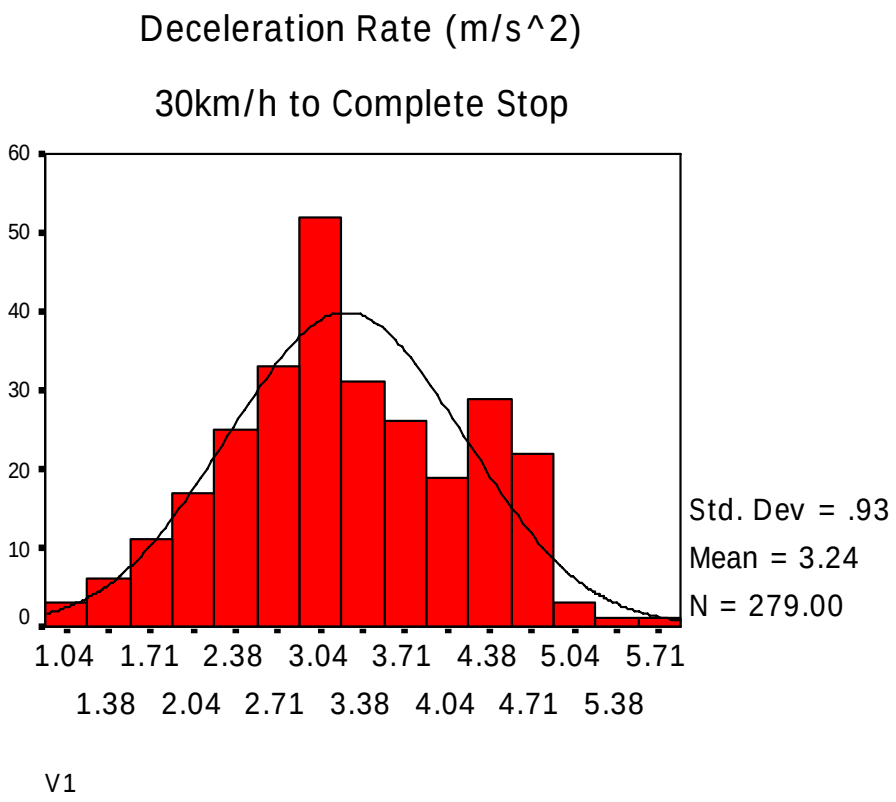

Figure 4-13: Distribution of Average Deceleration Rates (from 30 km/h to 0 km/h)

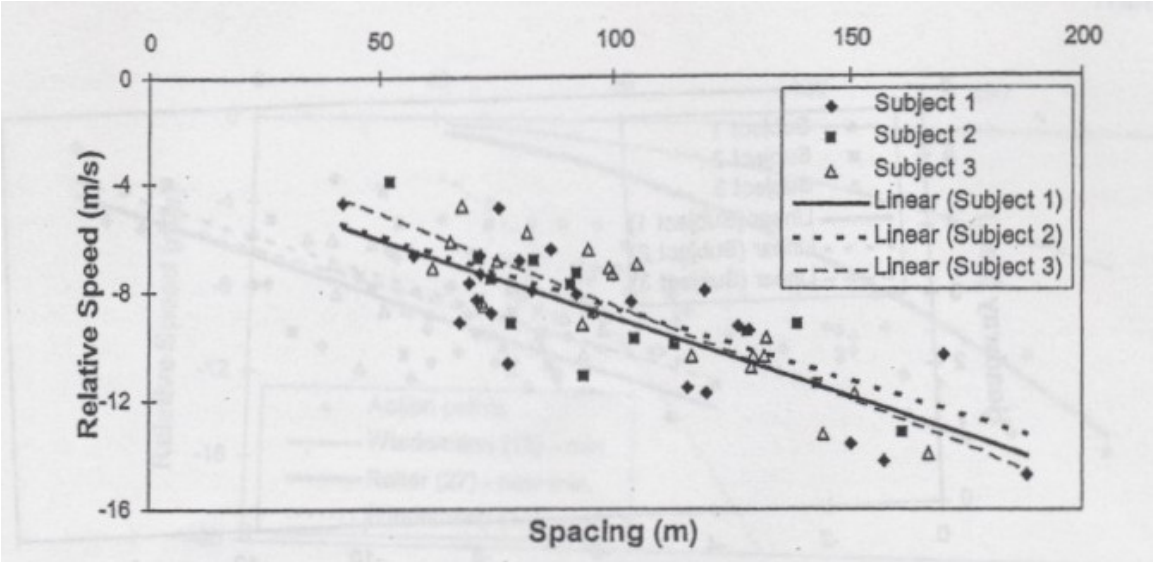

Figure 4-14: Spacing against Relative Speed for Starting Points of the Approach Process

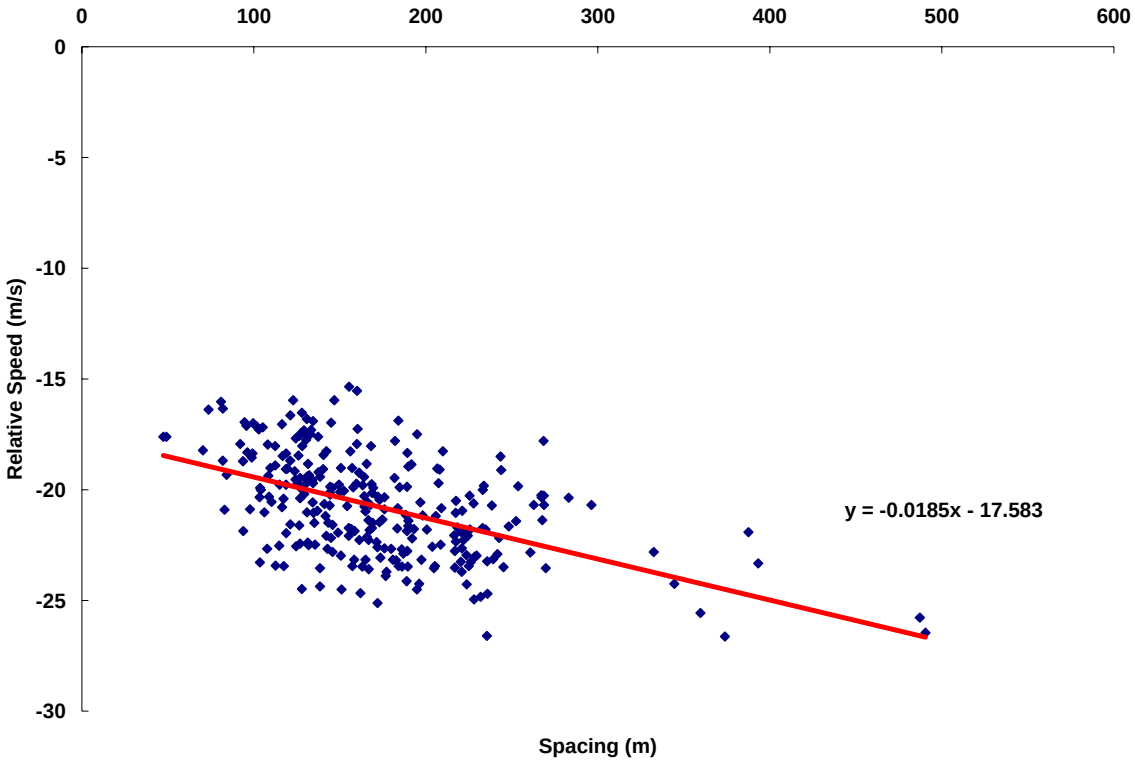

Figure 4-15: Distribution of Average Deceleration Rates (from 30 km/h to 0 km/h)

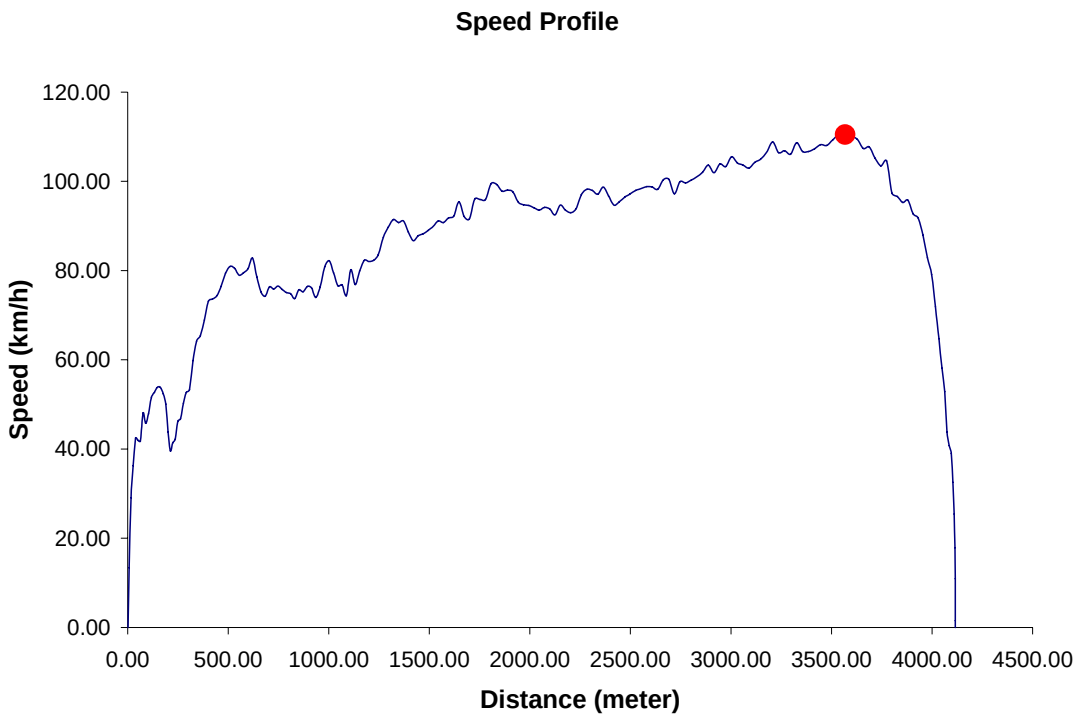

Figure 4-16: Sample Speed Profile

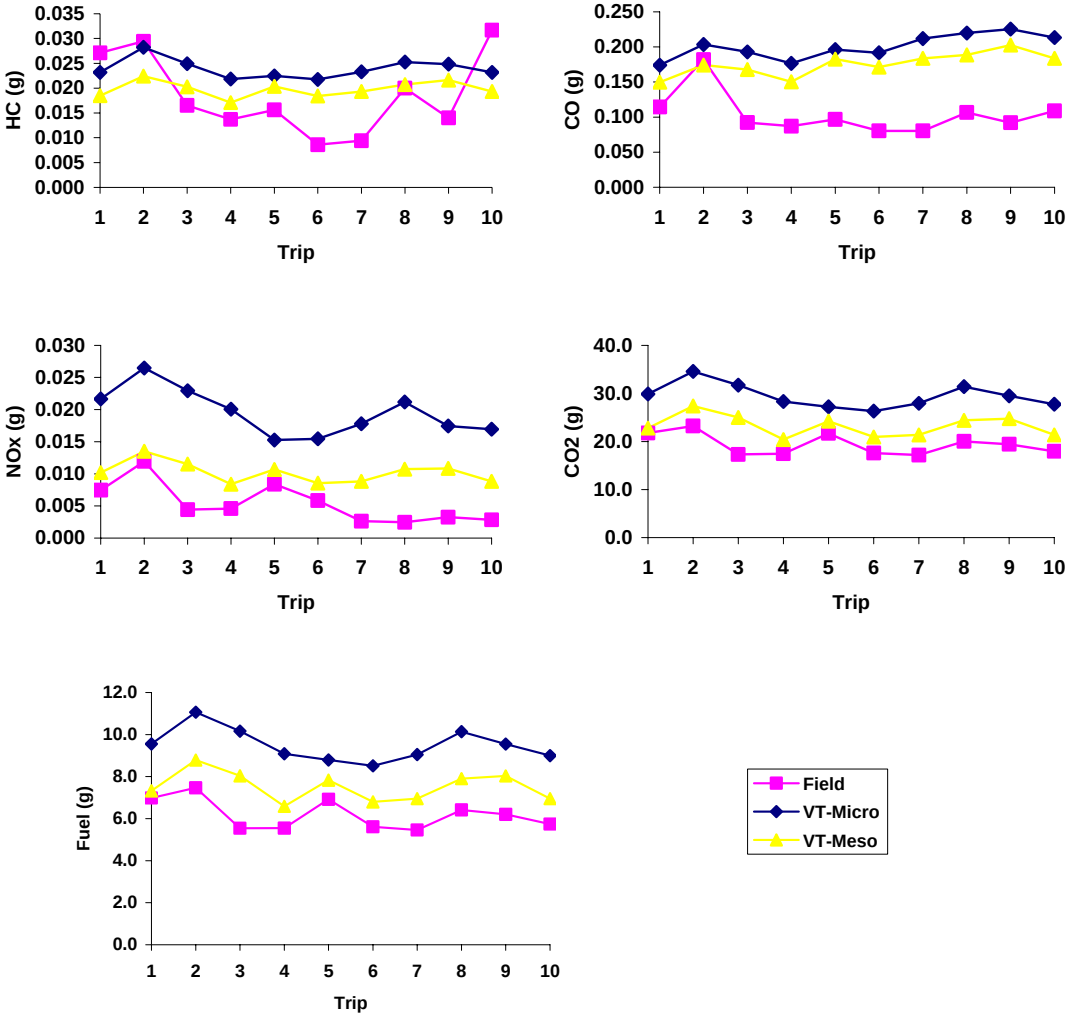

Figure 4-17: Comparisons with Field Data and VT-Micro Model (460 Bypass East)

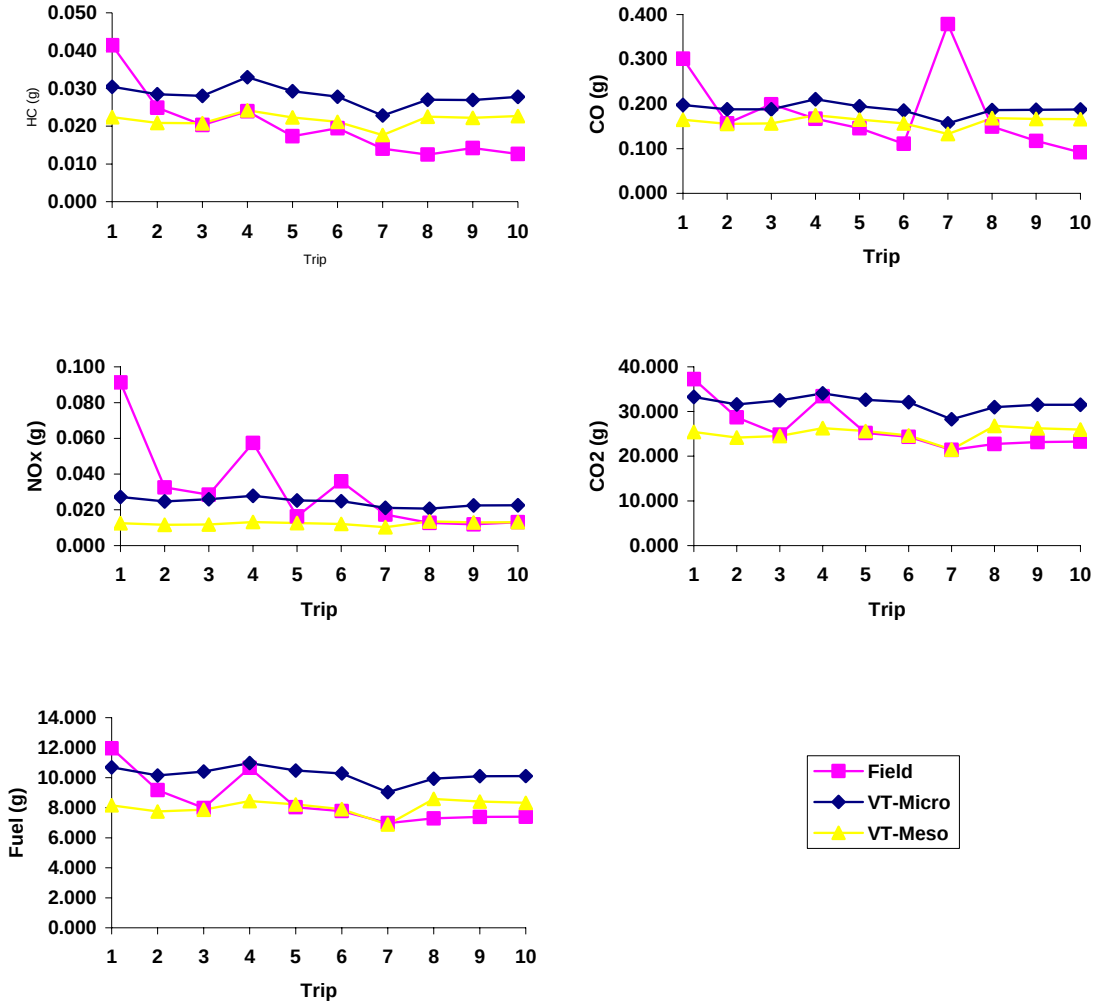

Figure 4-18: Comparisons with Field Data and VT-Micro Model (460 Bypass West)

Chapter 5 : MESOSCOPIC FUEL CONSUMPTION AND VEHICLE EMISSION MODEL FOR HOT STABILIZED HIGH-EMITTING VEHICLES

Huanyu Yue and Hesham Rakha

Abstract

This paper describes the development of a mesoscopic fuel consumption and emission model for high-emitting vehicles. The VT-Mesoscopic model estimates high-emitting vehicles fuel consumption and emission rates on a link-by-link basis based on three independent variables: average speed, number of vehicle stops per unit distance, and average stop duration. The model uses these variables to construct synthetic drive cycles for each roadway segment and then predicts average fuel consumption and emission rates for four modes: deceleration, idling, acceleration, and cruising. To validate this mesoscopic model, the VT-Meso model estimations were compared against those from the VT-Microscopic model and EPA field data. This model successfully predicts the absolute fuel consumption and vehicle emission rates and follows the trend for different simulation scenarios.

Keywords: Vehicle Emissions, Vehicle Fuel Consumption, and High Emitting Vehicle.

5.1 Introduction

High emitting vehicles (HEVs) produces higher emissions than the average emitting vehicles under normal driving conditions. Although HEVs comprise only a small fraction of the vehicle fleet, they contribute significantly to the total of mobile source emissions (Wolf, Guensler et al. 1998). Consequently, estimating accurately HEVs' emissions are critical process to determine total vehicle emissions.

Little modeling efforts related to high emitters have been done comparing to other vehicle emission studies. Most of research on high emitters focused on high emitter characterization and distribution. This research concentrates on mathematical modeling to estimate HEVs' emissions and fuel consumption. This mesoscopic model utilizes VT-Microscopic vehicle fuel consumption and emission model compute mode specific fuel consumption and emission rates (Rakha, Van Aerde et al. 2000, Ahn, Rakha et al. 2002, Rakha and Lucic 2002).

The objectives of this paper are to estimate accurate fuel consumption and emissions from HEVs, and to validate VT-Mesoscopic fuel consumption and emission models against EPA data and microscopic model.

In terms of the paper layout, the paper first presents the research efforts for high emitters. Secondly, the definition of high emitters will be discussed. The following section presents the overview of VT-Mesoscopic model framework. Subsequently, the vehicle fuel consumption and emission estimates from proposed model are compared against field data and VT-Microscopic model estimates. Finally, the conclusions of the study and recommendations for further research are presented.

5.2 Research Efforts for High Emitters

5.2.1 EPA's MOBILE6 Model

MOBILE6 was developed by the EPA's Office of Transportation and Air Quality (OTAQ). For high emitter vehicle modeling, MOBILE6 separates vehicle in two groups: a) 1981-1993 model year light-duty cars and trucks, and b) Tier 1 and later light-duty vehicles and truck. For Group A vehicles, the emissions for high emitters are calculated from the basic emission rates (BERs) by applying high emitter correction factors derived using Ohio IM240 data. Different high emitter correction factors are utilized depending on the vehicle model year and technologies. High emitter correction factors are applied as a function of vehicle mileage. For Group B vehicles, high emitter BERs are estimated using average values of sample high emitter emissions. High emitter BERs are different by vehicle model year and technologies. The high emitter BERs are multiplied by high emitter correction factors which are function of mileage. High emitter correction factors were derived using Ohio IM240 data, but adjusted for newer vehicles. In MOBILE6 one vehicle can be a high emitter in HC and NO_x and normal vehicle in CO, this is for modeling purpose only. Thus, one vehicle data could be utilized for normal and high emitter modeling in MOBILE6. Starting from the 1996 model MOBILE6 added the effects of On-Board Diagnostic (OBD) systems which are available from manufacturers. They also include Inspection and Maintenance (I/M) credits for different emission standards such as Tier1, LEV, and ULEV (Koupal and Glover 1999; Glover and Koupal 1999).

5.2.2 Comprehensive Modal Emission Model

The Comprehensive Modal Emissions Model (CMEM) is one of the most recently developed power demand-based emission models. CMEM was developed by researchers at the University of California-Riverside along with researchers from the University of Michigan and Lawrence Berkeley National Laboratory. The overall objective of CMEM model was to estimate LDV and LDT emissions as a function of the vehicle's operating mode. This model based on a simple parameterized physical approach and consists of six modules that predict engine power, engine speed, air/fuel ratio, fuel use, engine-out emissions, and catalyst pass fraction, it is capable of predicting second-by-second emissions and fuel consumption. This model was built from in-house dynamometer test on 300 real-world vehicles. Three dynamic variables, second-by-second speed, grade, and accessory use (such as air conditioning), were used as the input operating variables. The instantaneous emissions were modeled as the product of three components: fuel rate (FR), engine-out emissions indexes ($g_{emission}/g^{fuel}$), and catalyst pass fraction (CPF) (Barth, An et al. 2000).

The modal emissions model is composed of six modules: engine power demand, engine speed, air-fuel ratio, fuel rate, engine-out emissions, and catalyst pass fraction. The CMEM model utilized the following four types of high emitters that were determined based on their emission characteristics.

1. High emitter with low HC and CO and high NO_x emissions. The fuel-air ratio of this type vehicle is chronically lean or goes lean at moderate power or transient operation.
2. High emitter with normal HC and high CO emission. The fuel-air ratio of this type vehicle is chronically rich or goes rich at moderate power.

3. High emitter with moderate to slightly CO, very high HC, and moderate to low NO_x. The rngine-out hydrocarbons are high and these vehicles have mild enrichment having high engine-out CO and high CO catalyst pass fraction.
4. High emitter with high emissions for HC, CO, and NO_x. These vehicles have chronically or transiently poor catalyst performance.

5.2.3 VT-Microscopic Model

The VT-Micro vehicle fuel consumption and emission model was developed at Virginia Tech to compute mode specific fuel consumption and emission rates (Ahn, Rakha et al. 2002; Rakha, Ahn et al. 2003; Rakha, Van Aerde et al. 2000). The model predicts the instantaneous fuel consumption and emission rates of HC, CO, CO_2, and NOx of individual vehicles based on their instantaneous speed and acceleration levels. The initial intent behind the development of this model was not to capture all elements that affect vehicle fuel consumption and emission rates, but simply to develop a model in which vehicle dynamics are explicit enough to account for speed and acceleration variations, two elements that have been shown to have significant impacts on vehicle fuel consumption and emission rates.

Equation [5-1] describes the general format of the VT-Micro model that predicts instantaneous fuel consumption and emission rates of individual vehicles. The VT-Micro model framework predicts the instantaneous fuel consumption and emission rates of individual vehicles as

$$\mathrm{MOE_e} = \begin{cases} \sum_{\mathrm{i}=0}^{3}\sum_{\mathrm{j}=0}^{3} \exp\left(k_{i,j}^{e} \cdot v^{i} \cdot a^{j}\right) & \text{for a} \geq 0 \\ \sum_{\mathrm{i}=0}^{3}\sum_{\mathrm{j}=0}^{3} \exp\left(l_{i,j}^{e} \cdot v^{i} \cdot a^{j}\right) & \text{for a} < 0 \end{cases} \quad [5\text{-}1]$$

where MOE_e is the instantaneous fuel consumption or emission rate (L/s or mg/s), a is the instantaneous acceleration (km/h/s), v is the instantaneous speed (km/h), $k_{i,j}^{e}$ are vehicle-specific acceleration regression coefficients for MOE_e, and $l_{i,j}^{e}$ are the vehicle-specific deceleration regression coefficients for MOE_e. As can be observed, Equation [5-1] utilizes two sets of coefficients, one set for the acceleration mode and one set for the deceleration mode. The dual regime was introduced to account for differences in the emission rate sensitivity within the acceleration and deceleration modes of travel. Another important feature is the use of the exponent to ensure that non-negative fuel consumption and emission rates are produced by the models.

The data used to develop VT-Micro is the same as was used in the MOBILE6 modeling and validation. The general format of Equation [5-1] was first developed by testing the ability of various regression models to adequately model the observed steady-state fuel consumption and emission behaviors.

5.3 High Emitting Vehicle Definition

I/M program was recommended by EPA to develop the cutoff of the high emitters. In a I/M program, vehicles are tested on a dynamometer over a driving cycle called IM240. The IM240

cycle is designed to simulate a typical city driving cycle. In IM240 cycle, second-by-second instantaneous speed and emissions were measured. Emissions for the entire cycle were used to develop the HEV emission thresholds. The EPA recommends a cutoff that is two times the emission standard for HC and/or NO_X emissions and three times the standard for CO emissions. Figure 5-1 shows the emissions comparison between high-emitting vehicles and light-duty vehicles at constant travel speeds, this figure clearly shows that high-emitting vehicle generate much higher emissions than light-duty vehicles.

5.4 Overview of the VT-Meso Model Framework

The proposed modal model is primarily intended for use after the traffic demand has been predicted and assigned to the network to estimate link-by-link average speeds, number of vehicle stops, and stopped delay, as illustrated in Figure 5-2. The model utilizes these link-by-link input parameters to construct a synthetic drive cycle and compute average link fuel consumption and emission rates. Total link fuel consumption and emissions are then computed by multiplying the average fuel consumption and emission rates by its corresponding vehicle-kilometers of travel. Finally, system-wide parameters are estimated by summing across all links within a network. The first step involves the construction of a synthetic drive cycle that produces consistent average speed, number of vehicle stops, and stopped delay estimates. After constructing the drive cycle, the model estimates the proportion of time that a vehicle typically spends cruising, decelerating, idling and accelerating while traveling on a link. A series of fuel consumption and emission models are then used to estimate the amount of fuel consumed and emissions of HC, CO, CO_2, and NO_X emissions for each mode of operation. Subsequently, the total fuel consumed and pollutants emitted by a vehicle while traveling along a segment are estimated by summing across the different modes of operation and dividing by the distance traveled to obtain distance-based average vehicle fuel consumption and emission rates.

Because the study presented in this paper builds on (Rakha, Ahn et al. 2004) publication it only considers normal light-duty vehicles, trucks, and high-emitting vehicles operating under hot stabilized conditions and does not account for the effect of vehicle start and air conditioning usage on vehicle emissions (i.e. the models can only be applied for hot stabilized conditions).

5.4.1 Synthetic Drive Cycle Construction

This section describes how synthetic drive cycles are constructed using selected trip information. The section first presents the general approach used to construct the synthetic drive cycle and follows with a more detailed description of the model assumptions to characterize deceleration, idling, acceleration, and cruising modes of operation of a vehicle.

General Approach

As indicated in the introduction, the proposed modal model relies on three input variables, namely the average trip speed, the number of vehicle stops, and the stopped delay, to construct a synthetic drive cycle that produces equivalent vehicle fuel consumption of emission rates. Regression models were developed to estimate the time and distance traveled during each mode of operation. Using these regression models the synthetic drive cycle can be easily constructed. Currently, the model does not distinguish between freeway and arterial facilities in constructing a drive cycle; however, further research will investigate the merits of such an enhancement.

Figure 5-3 demonstrates how the synthetic drive cycle is constructed using the three input parameters. It is assumed that the vehicle makes on average three stops of a given duration over the roadway segment. To account for those three stops, the trip speed profile is constructed by fitting three identical stop-and-go cycles over the segment. Within each cycle, the cruise speed is computed to ensure that the input average speed is maintained. As a result, the cruise speed is equal to the average speed when there are no stops. In all other cases, the cruise speed is higher than the average speed, with increasing values for higher number of stops per unit distance and longer stop durations.

Figure 5-4 compares the actual FWYF drive cycle to its corresponding synthetic drive cycle. While the synthetic drive cycle generation does not obviously match the actual drive profile, as actual profiles would not show such perfect repetitiveness, it ensures that the synthetic drive cycle is consistent with the actual cycle in terms of vehicle fuel consumption of emission rates.

Deceleration, Idling, and Cruising Modes

The model currently assumes that drivers decelerate at a constant rate that can be set by the user. Specifically, the model allows the user to specify the deceleration rate in the range of -2.00 m/s^2 to -0.25 m/s^2 in increments of 0.25 m/s^2. The assumption is that drivers decelerate at a constant rate in order to simplify the development of the initial model. Research is currently underway to characterize typical driver deceleration behavior.

A vehicle is assumed to idle when it reaches a speed of 0 km/h. This mode of operation is only considered when the input parameters to the model specify that at least one full stop occurs within the segment considered. If the user specifies a number of stops that is less than one, the model assumes that a partial stop only occurs and thus the vehicle decelerates to a non-zero speed before starting to accelerate again.

Between acceleration and deceleration events, it is assumed that a vehicle travels at a constant cruise speed. As was indicated earlier, the speed at which a vehicle cruises is computed so that the total travel time along the segment under consideration is not altered. The cruising speed is determined through an iterative process that adjusts the cruising speed and corresponding deceleration and acceleration times until a match is found between the resulting travel time and the average travel time.

Acceleration Mode

In modeling vehicle acceleration, the model considers a vehicle dynamics model that was initially developed by Rakha et al. (Rakha, Lucic et al. 2001) and enhanced by Rakha and Lucic (Rakha and Lucic 2002) for modeling truck acceleration behavior and was later applied to the modeling of light-duty passenger cars by Snare (Snare 2002). As indicated by Equation [5-2], the model is based on the principle that the vehicle acceleration is proportional to the resulting force applied to it. The model predicts acceleration rates that decrease with increasing speeds. The decreased acceleration rates are a result of two factors. First, the vehicle tractive effort (F) decreases with vehicle speed. Second, the aerodynamic and rolling resistance forces increase with vehicle speeds. It should be noted that the acceleration factor (α) is used to reduce the vehicle acceleration level to reflect the fact that drivers do not typically use the full power of a vehicle while accelerating. Specifically, Rakha et al. (Rakha, Snare et al. 2004) indicate that

drivers typically accelerate at 62 percent of the maximum acceleration rate, with aggressive drivers accelerating at rates that reach 85 percent of the available power while passive drivers accelerate at only 40 percent of the maximum rate. Since the intent of the model is to evaluate typical driving behavior, it was thus determined that typical accelerations should be considered by the model instead of maximum feasible accelerations. In particular, assuming that vehicles accelerate at their maximum potential can lead to gross over-estimation of vehicle fuel consumption and emission rates.

Using the vehicle dynamics model the vehicle acceleration can be computed as

$$a = \alpha\left(\frac{F - R}{M}\right) \quad [5\text{-}2]$$

where a is the instantaneous acceleration (m/s^2), F is the residual tractive force (N), R is the total resistance force (N), M is the vehicle mass (kg), and α is the fraction of the maximum acceleration that is utilized by the driver.

Equations [5-3], [5-4], and [5-5] further demonstrate how the vehicle's effective tractive force is computed at any given speed. Specifically, Equation [5-3] computes the effective tractive force as the minimum of the tractive force applied by the engine, Ft, and the maximum force that can be sustained between the vehicle tires and the pavement surface, F_{max}. The tractive force is computed using Equation [5-4], which assumes that the vehicle power does not change with speed and is equal to the maximum potential power of the vehicle. The engine efficiency parameter η further accounts for power loss in the transmission system as well as losses associated with engine accessories such as fan, ventilator, water pump, magneto, distributor, fuel pump, and the compressor. Equation[5-5], finally, determines the maximum tractive force that can be sustained between the vehicle tires and pavement surface, which is a function of the roadway coefficient of friction and the proportion of the vehicle mass on the tractive axle.

$$F = \min(F_t, F_{\max}) \quad [5\text{-}3]$$

$$F_t = 3600 \cdot \eta \cdot \frac{P}{v} \quad [5\text{-}4]$$

$$F_{\max} = 9.8066 \cdot p_{mta} \cdot M \cdot \mu \quad [5\text{-}5]$$

It should be noted that Ft is the tractive force applied on the vehicle (N), F_{max} is the maximum attainable tractive force (N), P is the maximum engine power (kW), η is the engine efficiency, v is the vehicle speed (km/h), p_{mta} is the portion of vehicle mass on the tractive axle, μ is the coefficient of friction between the vehicle tires and roadway pavement, and α is the fraction of acceleration power effectively used by the driver.

Equations [5-6] through [5-9] further describe how the external resistance forces are calculated. Equation [5-6] indicates that the total external resistance force is the sum of the aerodynamic, rolling, and grade resistance forces. In Equation[5-7], the aerodynamic resistance force is shown to be a function of the vehicle frontal area, the altitude, the vehicle's drag coefficient, and the square of the vehicle speed. The rolling resistance force is further shown in Equation[5-8] to be a function of the total mass and speed of the vehicle, while Equation [5-9] indicates that the grade resistance force is a function of the roadway grade and vehicle mass.

$$R = R_a + R_r + R_g \quad [5\text{-}6]$$

$$R_a = 0.047285 \cdot C_d \cdot C_h \cdot A \cdot v^2 \quad [5\text{-}7]$$

$$R_r = 9.8066 \cdot C_r \cdot (c_2 v + c_3) \cdot \frac{M}{1000} \quad [5\text{-}8]$$

$$R_g = 9.8066 \cdot M \cdot i \quad [5\text{-}9]$$

It should be noted that Ra is the aerodynamic resistance (N), R_r is the rolling resistance (N), R_g is the grade resistance (N), A is the frontal area of the vehicle (m^2), H is the altitude (m), C_d is the air drag coefficient, C_h is the altitude coefficient which equals 1–0.000085H, and C_r, c_1, c_2 are the rolling resistance constants, and i is the roadway grade (m/100 m). Rakha et al. (Rakha, Snare et al. 2004) demonstrate that the model provides a very good fit to field observations for a wide range of light duty vehicles and trucks.

5.4.2 Fuel Consumption and Emission Estimates by Drive Mode

Once the drive cycles are constructed, the next step is to compute the fuel consumption and emission rates for each mode of operation. This section describes how fuel consumption and emissions of HC, CO, NO_X, and CO_2 are computed for the cruising, idling, decelerating, and accelerating modes for light-duty gasoline vehicles and trucks that operate under hot stabilized conditions.

Deceleration Mode

By applying the VT-Micro model, which was defined in Equation [5-1], to a second–by-second deceleration maneuver from a pre-defined cruising speed to a complete stop and accumulating the fuel consumption and emission rates over the entire maneuver it was possible to develop statistical models of the form

$$MOE_e^{decel} = \exp\left(d_0 + d_1\ v_c + d_2\ v_c^2 + d_3\ v_c^3 + d_4\ v_c^4 + d_5\ v_c^5 + d_6\ v_c^6\right) \quad [5\text{-}10]$$

where MOE_e^{decel} is the distance traveled, travel time, fuel consumed, or pollutants emitted while decelerating (m, s, l/s, or mg/s, respectively), v_c is the vehicle cruising speed (km/h), and $d_0,\ldots,d_6$ are vehicle-specific regression coefficients.

Equation [5-10] was obtained by integrating the instantaneous fuel consumption and emission rates provided by Equation [5-1] over the entire duration of a deceleration event at a constant deceleration rate. Because of the non-linear nature of the relationships considered, a closed analytical solution could not be found. Instead, regression relationships were fitted to the data, as demonstrated in Equation [5-10]. The statistical results indicate a good fit between VT-Meso and VT-Micro models for fuel consumption and vehicle emission estimates, the high F value shows that the dependent variable can be predicted by the independent variables and the P values for the coefficients demonstrate that all the independent variable are significant. Table 5-1 summarizes the statistical analysis result for HE-2 vehicle with 1.5m/s^2 deceleration rate, which is the average deceleration rate obtained from field test, other types of vehicles show similar result.

Table 5-2 presents sample deceleration parameters for the HE-3 vehicle. The HE-3 category was generated based on the average characteristics of 20 high-emitting vehicles that were tested on a chassis dynamometer by the EPA in 1997 (Rakha, Ahn et al. 2004). This category includes vehicles of model year ranging between 1985 and 1994, with engine sizes of less than 5.7 liters.

While the deceleration relationships were developed to express the total fuel consumed and pollutants emitted over a full deceleration maneuver (deceleration to a speed of 0 km/h), these relationships can also be used to consider partial stops. For example, in computing the fuel consumption for a deceleration maneuver from 60 to 50 km/h, the fuel consumption for a deceleration maneuver from 50 to 0 km/h is subtracted from the fuel consumption rate for a deceleration maneuver from 60 to 0 km/h.

An analysis of vehicle fuel consumption and emission rates for deceleration levels ranging from -0.5 to -2.0 m/s^2 demonstrated that the fuel consumption and emission rates do not exhibit linear relationships with respect to the starting cruise speed despite an assumed constant deceleration rate. This non-linearity is due to the non-linear instantaneous vehicle fuel consumption and emission rates.

Idling and Cruise Modes

As was the case for the deceleration mode, the fuel consumption and emission rates for the idling mode are based on the use of the underlying VT-Micro model. In this case, idling rates are determined by using the models of Equation [5-1] with an instantaneous speed of 0 km/h and an instantaneous acceleration rate of 0 km/h/s. This yields constant rates that are then multiplied by the average stop duration to estimate the total fuel consumed and emissions during an average idling event.

Alternatively, the cruise emission rates are obtained by applying the appropriate cruise speed and an acceleration rate of zero to the microscopic models defined by Equation [5-1]. This yields fuel consumption and emission relationships of the form [5-11]

$$MOE_e^{cruise} = \exp(k_{0,0}^e + k_{1,0}^e \cdot v + k_{2,0}^e \cdot v^2 + k_{3,0}^e \cdot v^3) \quad [5\text{-}11]$$

where MOE_e^{cruise} is the fuel consumption or pollutant emission rate while cruising (l/s or mg/s), v is the vehicle cruising speed (km/h), and $k^e_{i,0}$ is the vehicle-specific acceleration regression coefficients for the MOE under consideration. In computing the total fuel consumption and emissions during a cruising event, the rates given by Equation [5-11] are then multiplied by the total duration of the event.

Figure 5-5 illustrates the rates that were obtained for the HE-3 vehicle that was described earlier. The figure first demonstrates that fuel consumption and emission rates all increase with higher cruising speed, as expected, but that these increases are nonlinear. It is also observed that the rates at which HC, CO NO_X, and CO_2 are emitted are highly dependent on the cruising speed, especially at high speeds, where small speed increases result in significantly higher emission rates. For the HC, CO, and CO_2 emissions, these increases are again a consequence of the engine running with a higher fuel-to-air ratio at high speeds. In the case of NO_X, the higher emissions at high speed are mostly due to other mechanisms, as NO_X is relatively insensitive to the fuel-to-air ratio. It can also be observed that the NO_X emissions begin to ramp up at a lower

speed compared to HC, CO, and CO_2 emissions. The figure further demonstrates that the optimum distance-based efficiency occurs for cruise speeds around 80 to 90 km/h. In particular, it demonstrates that small differences in cruise speeds under typical arterial and highway driving may have only minor impacts on fuel consumption and emission rates. However, the same figure indicates that speed variations on freeways, where cruise speeds typically vary between 100 and 120 km/h, can result in more significant impacts on fuel consumption and emission rates, as was discussed by (Rakha and Ding 2003). Finally, Table 5-3 summarizes the cruise mode model coefficients for the HE-2 vehicle.

Acceleration Mode

As was done for the deceleration mode, the fuel consumed and pollutants emitted by a vehicle during an acceleration event is computed by integrating the fuel consumption and emission rates estimated using Equation [5-1] over the entire acceleration event. After computing the total fuel consumed and emissions for a series of final target speeds, regression models of the form

$$MOE_e^{accel} = \exp\left(b_0 + b_1\ v_c + b_2\ v_c^2 + b_3\ v_c^3 + b_4\ v_c^4 + b_5\ v_c^5 + b_6\ v_c^6\right) \quad [5\text{-}12]$$

were developed where MOE_e^{accel} is the total distance traveled, time consumed, fuel consumed, or pollutants emitted while accelerating (m, s, L/s, and mg/s, respectively), v_c is the vehicle cruise speed (km/h), and $b_0,\ldots,b_6$ are the vehicle-specific acceleration regression coefficients. As was the case with the deceleration models, these relationships estimate the total measures for an acceleration maneuver from a speed of zero to a final cruise speed v_c. Table 5-4 summarizes the statistical analysis result for HE-4 vehicle with 66% acceleration power, which is the average acceleration power rate obtained from field test, other types of vehicles show similar result. Table 5-2 presents the derived acceleration coefficients for an acceleration rate of 66% the maximum acceleration rate for the HE-3 vehicle. As was the case with Equation [5-10], Equation [5-12] can be used to compute the various measures associated with partial acceleration events.

An analysis of acceleration relationships for various levels of driver acceleration (α = 0.33, 0.50, 0.60, 0.66 and 0.75) demonstrate that the fuel consumed to reach a given speed increases with every reduction in the level of acceleration. In this case, while accelerating at a lesser rate puts a lesser load on the engine, the total quantity of fuel consumed to reach the target speed increases as the vehicle spends more time accelerating. However, the above observation does not necessarily hold for CO and NO_x emissions. As can be observed, the total vehicle emissions to reach speeds of up to 90 to 110 km/h typically decrease when the acceleration level is reduced from 75% to 50% before increasing. This behavior is due to the non-linearity of vehicle emissions with respect to speed increases. When comparing the deceleration and acceleration relationships it is observed that significantly higher fuel consumption and emission rates are associated with acceleration events in comparison with deceleration events because of the higher engine loads that are associated with acceleration events.

5.5 Model Validation

This section describes the validation effort of the proposed modal model. The validation effort is conducted by comparing the model output to outputs from the underlying microscopic model in addition to laboratory measurements. Two comparisons are made. First, the modal and

microscopic fuel consumption and emission estimates are compared for a number of EPA drive cycles. Second, the modal model estimates are compared against laboratory measurements using 14 EPA drive cycles. The objective of the exercise is to investigate the ability of the modal model to correctly predict changes in vehicle fuel consumption and emission rates across different drive cycles.

In order to run the modal model on various drive cycles the average speed, number of vehicle stops, and stopped delay were computed for each of the cycles. The number of vehicle stops was estimated as

$$N_{stops} = \sum_{t=1}^{T} \frac{(v_{t+1} - v_t)}{v_c} \qquad \forall \; v_{t+1} \leq v_t \qquad \text{[5-13]}$$

where N_{stops} is the estimated number of stops, v_t is the vehicle instantaneous speed in time interval t (km/h), and T is the number of time intervals t within the trip. This equation estimates the total partial stops incurred during a trip, as described by Rakha et al. 2001. The equation defines a full stop as a deceleration from the facility free-flow speed to a speed of zero. Half a stop would then be a deceleration from the free-flow speed to half the free-flow speed. Table 5-5 summarizes the modal model input parameters for the 14 EPA drive cycles. It should be noted that the average stopped delay was computed by dividing the total stopped delay by the number of vehicle stops. Further research can be conducted to characterize typical speed variability for different facility types (collectors, arterials and freeways) and different levels of congestion. Such research would in turn allow the development of improved procedures for converting speed variations, stop-and-go patterns, and partial stops into equivalent number of stops for the purpose of estimating vehicle fuel consumption and emissions. Furthermore, such research will allow for the estimation of equivalent number of stops without the need for a second-by-second speed profile.

Table 5-6 compares the average fuel consumption and emission rates for HE-4 using the proposed modal model and the VT-Micro model for the 14 drive cycles described earlier considering different acceleration levels and a constant deceleration rate of -1.50m/s^2. While it is not surprising that the absolute emission values are not identical, given the differences between the actual and constructed drive cycles, the figure generally indicates that the proposed modal model estimates are consistent with the microscopic model estimates. In this case, the difference in results between the microscopic and modal model estimates can be attributed to differences between the actual and constructed drive cycles. Other parameters that could affect the proposed modal model estimates include the various assumptions made by the modal model when generating synthetic drive cycles, particularly regarding the assumed deceleration and acceleration rates. In general the modal model appears to estimate fuel consumption, HC and CO_2 emissions consistent with the microscopic estimates; however, the model tends to underestimate the CO and NO_X emissions. Difficulty arises when applying the VT-Meso model to the FWYF, FWYG, and RAMP cycles due to the greater occurrence of stop-and-go traffic and speed variations at higher speeds. Further research should therefore be conducted to determine how speed variability can be accounted for in the fuel consumption and emission estimation processes without requiring second-by-second analysis of speed and acceleration profiles. Further research can also be conducted to characterize typical speed variability for different facility types (collectors, arterials and freeways) as a function of the congestion level. Such

research would in turn allow for the development of improved factors or equations for converting speed variations, stop-and-go patterns, and partial stops into the equivalent number of stops for the purpose of estimating vehicle fuel consumption and emissions.

Results from a previous research effort conducted by Ding and Rakha (Ding and Rakha 2002) further help in assessing the importance of correctly estimating the three trip parameters used by the modal model, and more particularly, in determining their individual impacts on the evaluation results. The study indicated that fuel consumption is relatively insensitive to the level of aggressiveness of accelerating drivers. This is in agreement with the results of Figure 5-6, which illustrate minor variations in fuel consumption rates as a function of acceleration levels. In terms of vehicle emissions, the study indicates that HC and CO emission rates are typically more sensitive to the level of acceleration than to the cruise speed for speeds ranging between 0 and 120 km/h. This sensitivity is apparent in Figure 5-7 where significant variations in predicted rates are observed for both HC and CO when considering various acceleration levels. Also, the current research indicates that NO_X emissions are relatively sensitive to both the level of acceleration and the cruise speed. This is clearly apparent when analyzing and comparing the results of Figure 5-6. However, while the model shows that increases in acceleration levels typically result in higher emission rates for HC and CO, this is not always the case for NO_X emissions.

The fuel consumption and emission estimate error associated with the proposed modal model was computed relative to the VT-Micro model estimates for each of the EPA new facility-specific drive cycles, as summarized in Table 5-6. In constructing the synthetic drive cycles an acceleration rate of 60 percent the maximum rate was assumed based on earlier research (Rakha, Snare et al. 2004) that demonstrated that the typical driver acceleration is approximately 62.5 percent the maximum acceleration rate. In addition, a constant deceleration rate of -1.50m/s^2 was utilized in the construction of the synthetic drive cycles. Comparison of vehicle fuel consumption and emission rates predicted by the proposed modal model against VT-Micro model estimates for the 15 drive cycles clearly demonstrate the ability of modal model to predict vehicle fuel consumption and emission rates across various drive cycles with an average prediction error less than 10 percent in most cases. The results clearly demonstrate strong correlations with the VT-Micro model predictions for fuel consumption, HC, CO, and CO_2 emissions. Alternatively, the model predictions are less accurate in the case of NO_X emissions with an average error in the range of 8 to 42 percent. The inaccuracy of NO_X emission estimates is partly attributed to the non-linear relationship between vehicle emissions, vehicle speed, and the vehicle acceleration/deceleration rates. Furthermore, the results demonstrate that, in general, the proposed modal model tends to underestimate vehicle fuel consumption and vehicle emission rates, which could be attributed to the fact that the synthetic drive cycles are much smoother than the actual cycles and thus involve a smaller degree of speed fluctuations. It should be noted that two of the drive cycles RAMP and LA92 involved more aggressive acceleration behavior and thus an assumption of a 60 percent acceleration rate might not be realistic. For example an increase in the acceleration rate from 60 to 75 percent resulted in a reduction in the prediction error from -25.1 to -4 percent. Consequently, the prediction errors can be reduced by calibrating the model to the typical acceleration behavior on different facility types. The impact and procedures for calibration of the acceleration behavior is a topic for further research.

It's noted that VT-Meso models has a higher prediction error for HE-2 vehicle. Based on the vehicle type classification, HE-2 type only includes one vehicle. With this small sample size, it's not surprising that the mesoscopic model estimations for HE-2 has a higher average error.

As indicated earlier, the proposed modal model provides the user with the flexibility of selecting different deceleration rates. Consequently, a sensitivity analysis of various deceleration rates in the range of -0.75 to -2.00 m/s^2 was conducted. The study demonstrated that the fuel consumption and emission rates in the model are generally insensitive to the input deceleration rate.

Having validated the proposed modal model against the underlying microscopic model, the next step was to validate the model estimates against laboratory measurements obtained from the EPA. The use of the EPA data offers a number of benefits. First, the EPA data includes off-cycle (non-FTP) emission results over different facility types and therefore provides a good assessment of model estimates over different roadway types and different levels of congestion. Second, the EPA data were utilized to develop EPA's MOBILE6 model, consequently this comparison ensures that the proposed modal model estimates are consistent with MOBILE6 estimates across different facility types and different levels of congestion.

The results demonstrate a good match between the model estimates and laboratory measurements, as demonstrated in Figure 5-7. The laboratory mean of emission rates of the vehicles in HE-4 cateogory, 5th, and 95th percentile emission rates for each drive cycle are presented together with the modal model estimates. The results demonstrate an excellent match both in terms of absolute values and cyclic trends for HC, CO, and CO_2 emissions and a good fit for NO_x emissions.

5.6 Conclusions

The paper describes a modal emission model that predicts vehicle fuel consumption and emission rates for steady state, hot stabilized, light duty vehicles based on a vehicle's average speed, average number of stops per unit distance, and average stop duration. The proposed model is intended for use as a post-processor of traffic simulation models for the estimation of energy and environmental impacts of traffic operational projects including intelligent transportation system (ITS) applications.

The proposed model was validated against the VT-Micro model and laboratory measurements. The results demonstrate that the model provides an excellent match both in terms of absolute emission rates and cyclic trends with the microscopic model estimates and laboratory measurements. The results indicate a prediction error less than 15 percent for fuel consumption, HC, CO, and CO_2 emission rates with higher prediction errors in the case of NO_x emissions (10 to 42 percent error).

An analysis of predicted fuel consumption and emission rates for various deceleration rates indicates very little sensitivity to changes in the deceleration rate. The main impact of considering varying deceleration rates is therefore not to improve predicted estimates, but to determine the feasibility of a given scenario as changes in deceleration rates affect the deceleration distance and the distance that can be used to accelerate. Variable deceleration rates

don't have a significant impact on fuel consumption and emissions, the major impact of variable deceleration rate is on synthetic drive cycle construction, which will change the overall fuel consumption and emissions with different travel times and travel distance for acceleration, deceleration, cruising, and idling modes. The results indicate that the model is sensitive to the vehicle acceleration rate that is assumed and thus should be calibrated to driver and facility specific conditions.

Based on the above results, further research appears to be required to improve the accuracy of the modal model. Further research should be conducted to determine how speed variability can be accounted for in the fuel consumption and emission estimation processes without requiring second-by-second analysis of speed and acceleration profiles. Further research can also be conducted to characterize typical speed variability for different facility types (collectors, arterials and freeways) and different levels of congestion. Such research would in turn allow the development of improved factors or equations for converting speed variations, stop-and-go patterns, and partial stops into equivalent number of stops for the purpose of estimating vehicle fuel consumption and emissions. The existing model also requires further enhancement to include diesel vehicles, and to consider the impact of cold-starts on fuel consumption and emissions.

Table 5-1 Statistical Analysis Results for Deceleration Mode of HE-2

	Fuel		HC		CO		NO_x		CO_2	
	t Stat	P-Value	t Stat	P-Value	t Stat	P-Value	t Stat	P-Value	t Stat	P-Value
Constant	-233.13	0.00	-227.50	0.00	-199.67	0.00	-239.32	0.00	-32.32	0.00
X Variable 1	39.23	0.00	41.72	0.00	56.18	0.00	45.61	0.00	39.05	0.00
X Variable 2	-24.04	0.00	-24.11	0.00	-34.95	0.00	-23.83	0.00	-24.00	0.00
X Variable 3	18.57	0.00	17.55	0.00	28.03	0.00	16.98	0.00	18.56	0.00
X Variable 4	-15.59	0.00	-13.97	0.00	-24.77	0.00	-13.65	0.00	-15.60	0.00
X Variable 5	13.68	0.00	11.51	0.00	22.46	0.00	11.55	0.00	13.68	0.00
X Variable 6	-12.33	0.00	-9.45	0.00	-19.81	0.00	-9.93	0.00	-12.33	0.00
R2		0.994		0.996		0.999		0.997		0.994
F		6560.95		9529.05		48585.55		14957.74		6330.66
Significance F		0		0		0		0		0

Table 5-2: Deceleration and Acceleration Mode Model Coefficients (HE-3)

Deceleration		d_0	d_1	d_2	d_3	d_4	d_5	d_6	R^2
	Fuel	-9.123	0.322	-0.013	0.000	0.000	0.000	0.000	0.994
	HC	-5.811	0.311	-0.013	0.000	0.000	0.000	0.000	0.992
	CO	-3.582	0.319	-0.013	0.000	0.000	0.000	0.000	0.993
-1.50 m/s^2	NO_x	-9.166	0.365	-0.013	0.000	0.000	0.000	0.000	0.997
	CO_2	-1.688	0.326	-0.013	0.000	0.000	0.000	0.000	0.994
	Time	0.000	0.031	0.003	0.000	0.000	0.000	0.000	0.991
	Distance	0.000	-0.003	0.011	0.000	0.000	0.000	0.000	0.983
Acceleration		d_0	d_1	d_2	d_3	d_4	d_5	d_6	R^2
	Fuel	-8.894	0.299	-0.010	0.000	0.000	0.000	0.000	0.998
	HC	-6.056	0.291	-0.011	0.000	0.000	0.000	0.000	0.997
	CO	-3.663	0.297	-0.010	0.000	0.000	0.000	0.000	0.998
66% max. accel.	NO_x	-9.032	0.329	-0.010	0.000	0.000	0.000	0.000	0.999
	CO_2	-1.109	0.296	-0.010	0.000	0.000	0.000	0.000	0.997
	Time	0.000	0.135	0.001	0.000	0.000	0.000	0.000	1.000
	Distance	0.000	-0.220	0.042	-0.001	0.000	0.000	0.000	1.000

Table 5-3: Cruise Mode Model Coefficients (HE-2)

	Constant	$K^e_{0.0}$	$K^e_{1.0}$	$K^e_{2.0}$
Fuel (g)	-7.48128	0.01914	-0.00014	0.0000008
HC (g)	-0.52048	0.07312	-0.00150	0.0000090
CO (g)	1.76155	0.10516	-0.00193	0.0000111
NO_x (g)	-0.41408	0.08510	-0.00092	0.0000043
CO_2 (g)	7.19167	0.01595	-0.00007	0.0000004

Table 5-4: Statistical Analysis Results for Acceleration Mode of HE-4

	Fuel		HC		CO		NO_x		CO_2	
	t Stat	P-Value	t Stat	P-Value	t Stat	P-Value	t Stat	P-Value	t Stat	P-Value
Constant	-297.49	0.00	-186.58	0.00	-102.48	0.00	-268.91	0.00	-52.22	0.00
X Variable 1	47.83	0.00	45.99	0.00	44.51	0.00	53.02	0.00	48.55	0.00
X Variable 2	-26.19	0.00	-26.36	0.00	-25.67	0.00	-24.41	0.00	-26.26	0.00
X Variable 3	19.50	0.00	19.82	0.00	19.51	0.00	17.16	0.00	19.42	0.00
X Variable 4	-16.18	0.00	-16.43	0.00	-16.32	0.00	-13.98	0.00	-16.06	0.00
X Variable 5	14.18	0.00	14.33	0.00	14.37	0.00	12.11	0.00	14.04	0.00
X Variable 6	-12.79	0.00	-12.84	0.00	-12.99	0.00	-10.80	0.00	-12.64	0.00
R2		0.998		0.997		0.997		0.999		0.998
F		21762.47		15955.34		19121.10		45136.02		22547.07
Significance F		0		0		0		0		0

Table 5-5: EPA's new Facility-Specific Drive Cycle Characteristics

Cycle	Avg. speed (km/h)	Max. speed (km/h)	Duration (s)	Length (km)	Time Stopped (s)	Equivalent Stop (stops)	Average stop duration (s)
FWHS	101.12	119.52	610	17.15	0	1.72	0
FWAC	95.52	116.96	516	13.68	0	1.53	0
FWYD	84.64	112.96	406	9.54	0	1.89	0
FWYE	48.8	100.8	456	6.18	4	3.31	1.2
FWYF	29.76	79.84	442	3.66	7	3.04	2.3
FWYG	20.96	57.12	390	2.27	10	2.02	4.9
RAMP	55.36	96.32	266	4.10	15	2.10	7.2
ARTA	39.68	96.24	737	8.11	103	9.27	11.1
ARTC	30.72	79.2	629	5.38	122	8.67	14.1
ARTE	18.56	63.84	504	2.59	148	5.66	26.2
LOCL	20.64	61.28	525	2.99	125	6.34	19.7
AREA	31.04	83.68	1348	11.60	294	14.48	20.3
LA92	39.36	107.52	1435	15.70	204	11.49	17.8
FNYC	11.36	44.32	600	1.89	215	8.86	24.3

Table 5-6: VT-Meso and VT-Micro Estimations Difference for EPA's New Facility-Specific Drive Cycles

Category	Measure	Fuel	HC	CO	NO_x	CO_2
HE1	Minimum	-21.2%	-12.9%	-19.8%	-21.7%	-22.1%
	Maximum	5.7%	6.3%	20.6%	4.3%	6.0%
	Mean	-9.0%	-4.9%	-2.5%	-8.4%	-9.6%
HE2	Minimum	-25.6%	-32.7%	-79.6%	-95.8%	-25.2%
	Maximum	-1.4%	13.8%	17.3%	5.9%	1.9%
	Mean	-14.3%	-3.5%	-6.3%	-41.6%	-14.4%
HE3	Minimum	-25.2%	-16.2%	-31.5%	-46.1%	-23.9%
	Maximum	-1.8%	-2.6%	2.4%	-6.6%	-0.7%
	Mean	-12.8%	-8.1%	-15.9%	-29.2%	-14.1%
HE4	Minimum	-24.2%	-20.7%	-33.5%	-21.2%	-21.9%
	Maximum	1.4%	-3.3%	-3.6%	2.4%	4.3%
	Mean	-12.7%	-8.0%	-14.0%	-12.0%	-12.7%

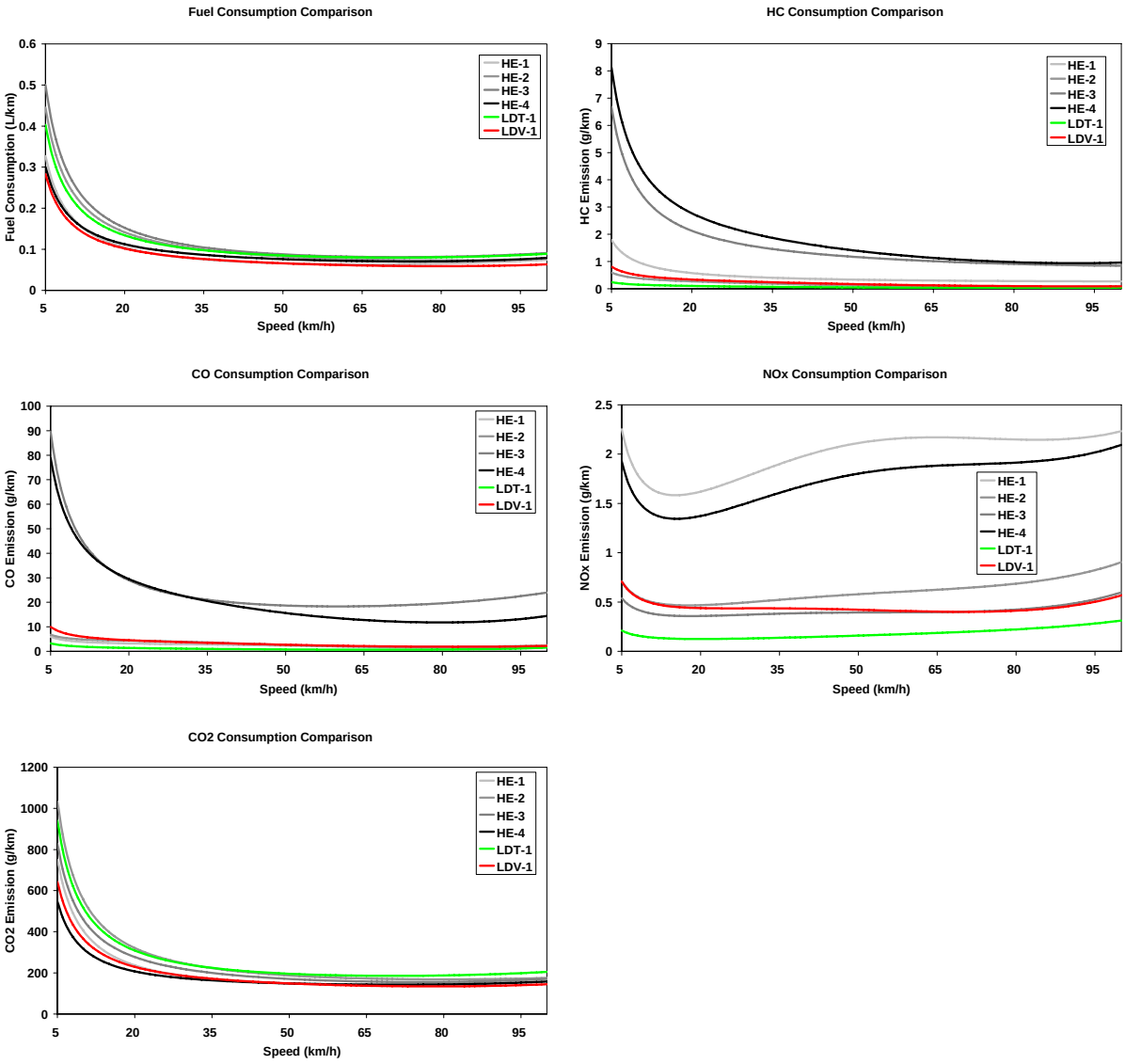

Figure 5-1: High-Emitter, LDV-1, and LDT-1 Emissions Comparison for Constant Speed

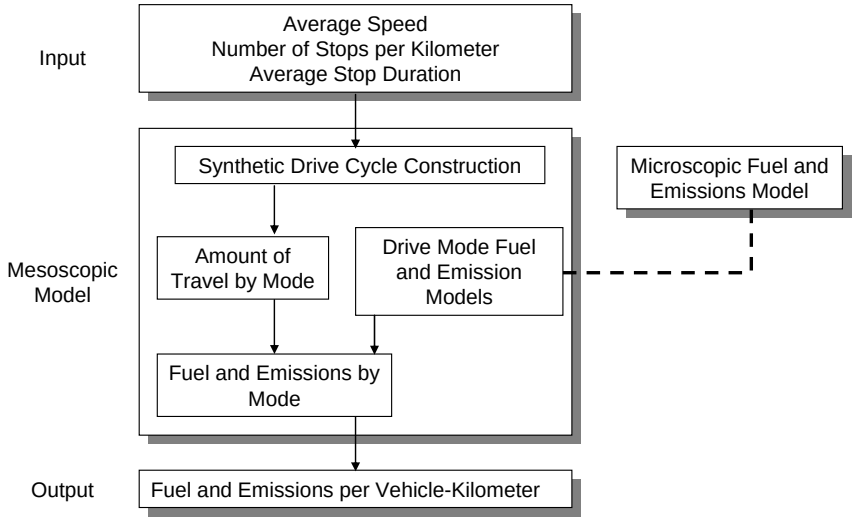

Figure 5-2: Schematic of Proposed Procedure

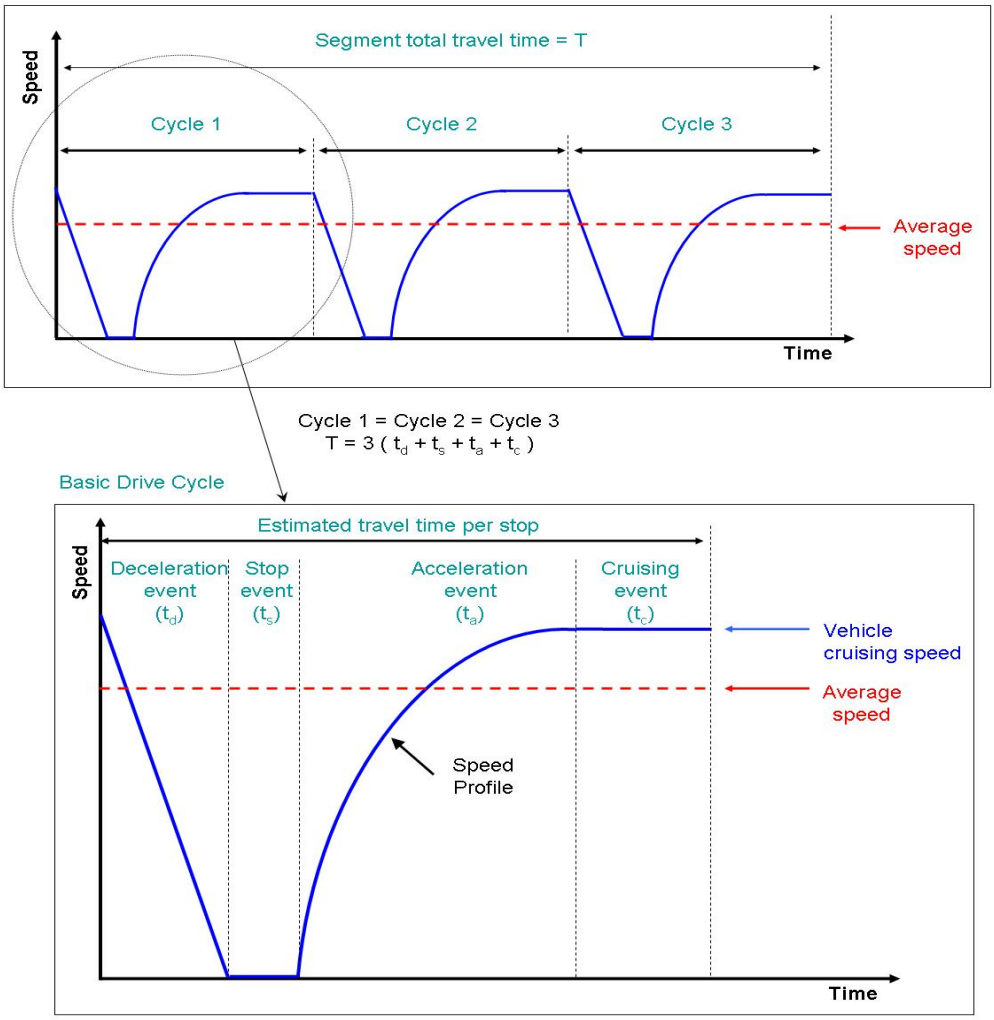

Figure 5-3: Example Synthetic Speed Profile

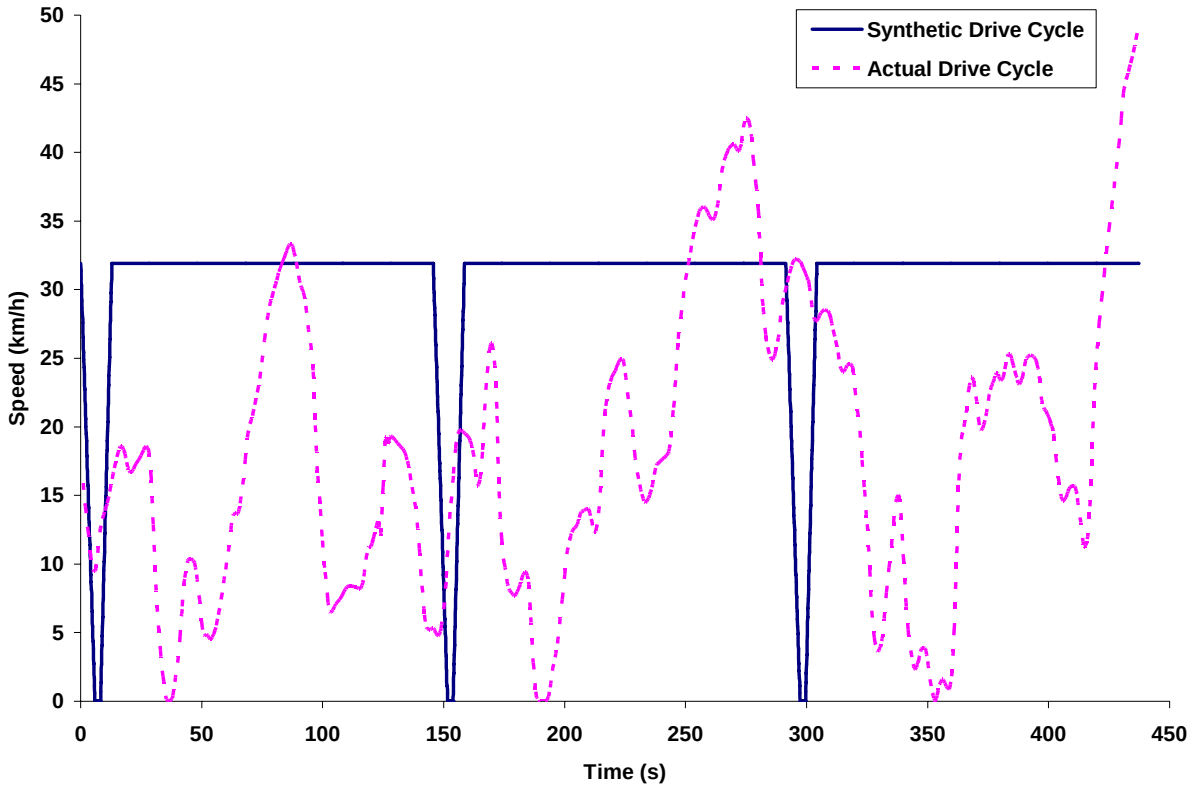

Figure 5-4: Synthetic Drive Cycle versus Actual Drive Cycle (FWYF Drive Cycle)

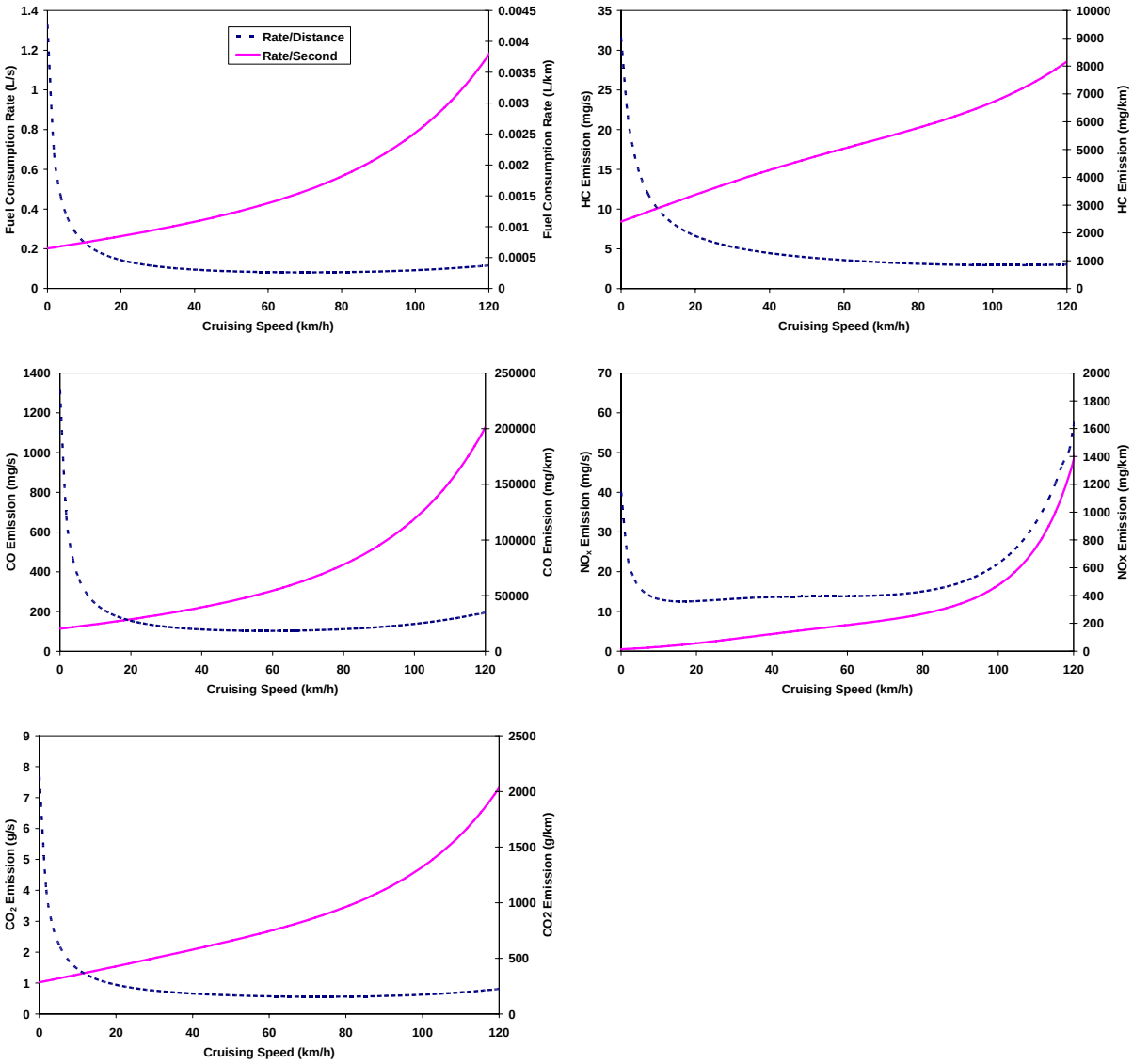

Figure 5-5: Fuel Consumption and Emission Rates for Cruising Mode (HE-3)

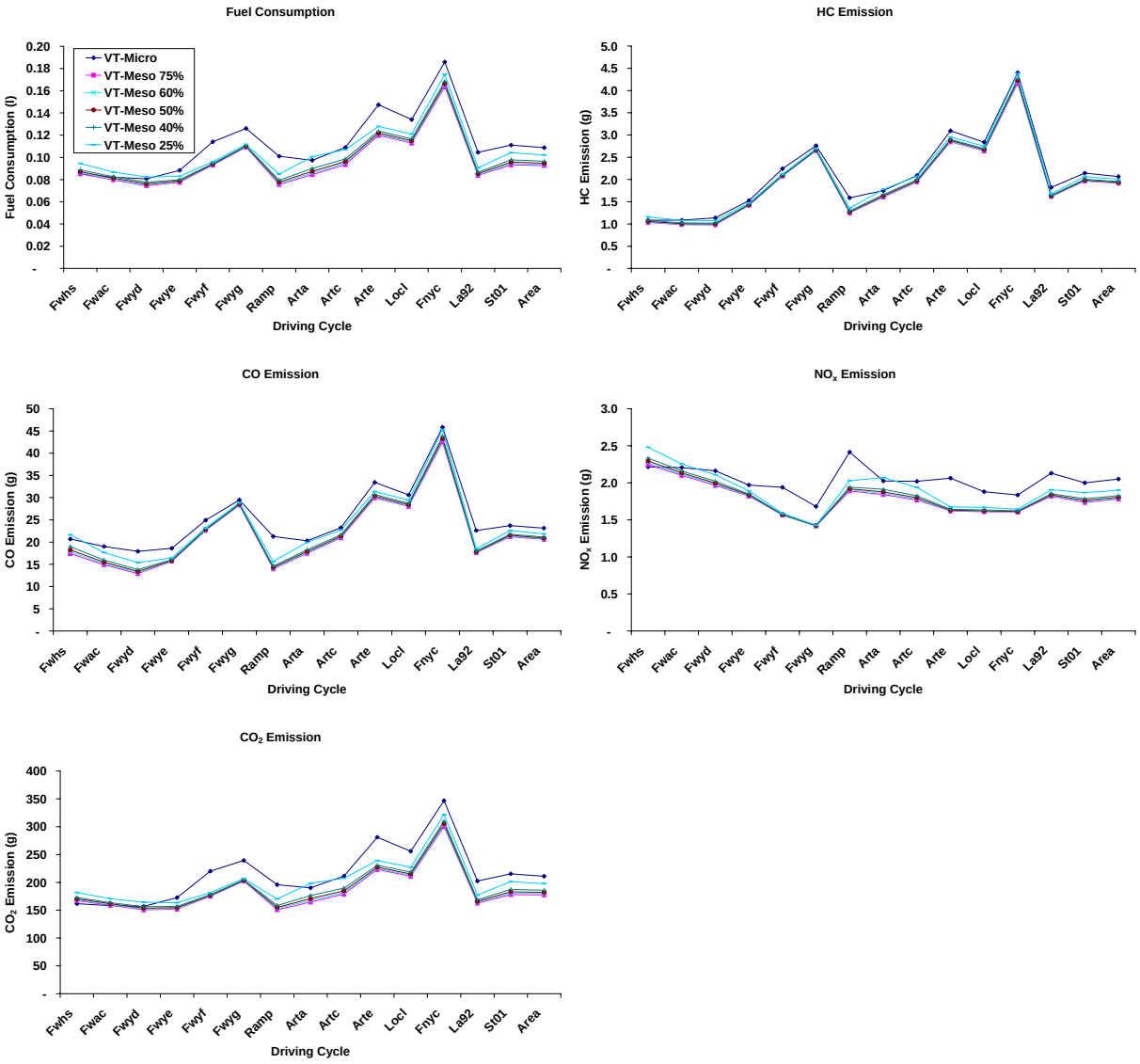

Figure 5-6: Comparison of Modal and Microscopic Fuel Consumption and Emission Estimates (HE-4)

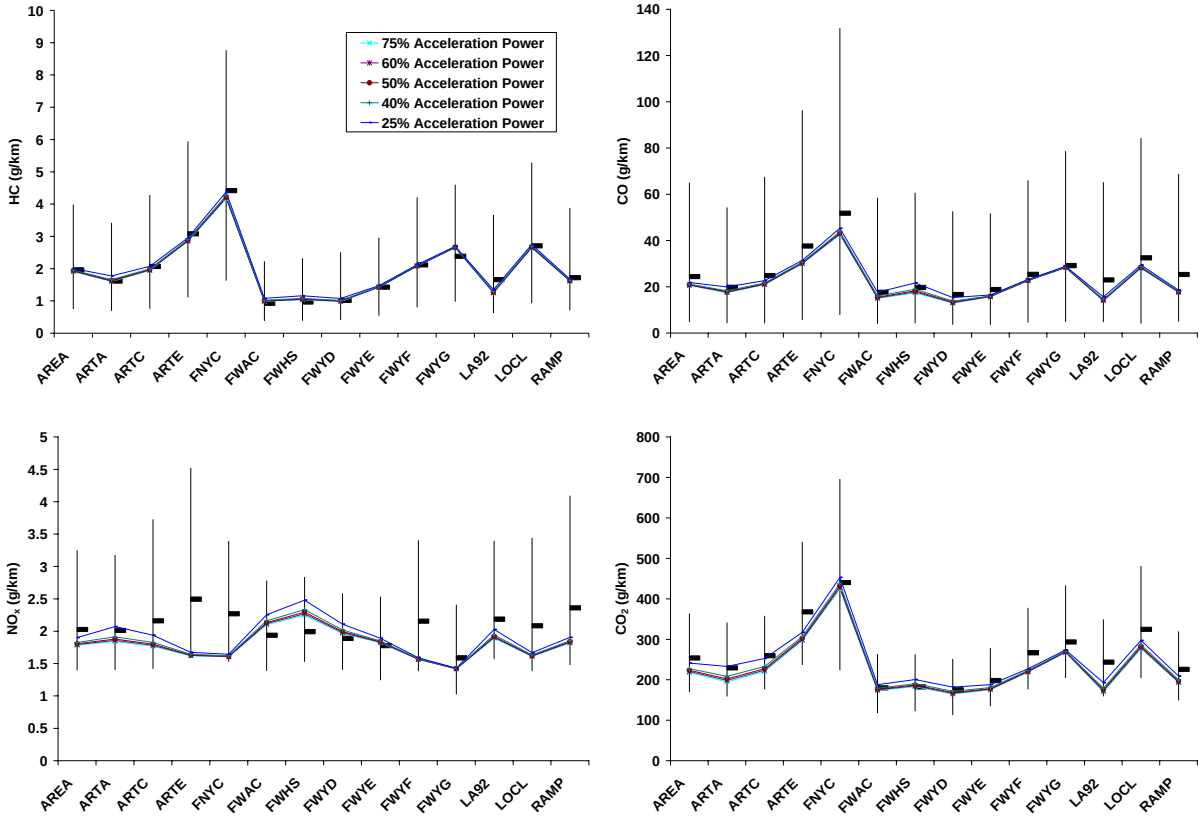

Figure 5-7: Comparison of Modal Estimates and Laboratory Measurements (HE-4)

Chapter 6 : VT-MESOSCOPIC MODEL VALIDATION

Huanyu Yue and Hesham Rakha

Abstract

The VT-Mesoscopic model estimates light-duty vehicle fuel consumption and emission rates on a link-by-link basis based on three independent variables: average speed, number of vehicle stops per unit distance, and average stop duration. The model uses these variables to construct synthetic drive cycles for each roadway segment and then predicts average fuel consumption and emission rates for four modes: decelerating, idling, accelerating, and cruising. This paper validates the VT-Meso model estimations against EPA MOBILE6 estimations and microscopic second-by-second energy and emission estimates using the INTEGRATION software. The INTEGRATION microscopic simulation software was used to estimate the vehicle fuel consumption and emission rates for different simulation scenarios. In addition, the INTEGRATION software generated link-by-link parameters for input to the VT-Meso model which in turn estimated the vehicle fuel consumption and emission rates. The exercise demonstrates that the VT-Meso model successfully predicts fuel consumption rates both in terms of absolute and relative values. Alternatively, the vehicle emission rates were consistent in terms of trends across the various simulation scenarios. The results demonstrate that such a modeling approach may be sufficient for the environmental evaluation of alternative traffic operational projects.

Keywords: Vehicle Emissions, Vehicle Fuel Consumption, Traffic Simulation, and Intelligent Transportation Systems.

6.1 Introduction

Macroscopic vehicle fuel consumption and emission models are currently the primary tools for evaluating the regional environmental impacts of transportation projects. In typical applications, a transportation planning model is first used to determine the average speed and total vehicle-miles of travel for the network or facility being considered. Then, an emission model such as MOBILE6 (EPA 2002) or EMFAC (CARB 1991) is used to compute the average fuel consumption and emission rates for the facility.

Macroscopic models produce single fuel consumption and emission rates for each average speed input. These models assume that all vehicles pollute similarly for the average speed and vehicle-miles traveled considered and that variations in driver behavior can be neglected (An, Barth et al. 1997). This presents a problem when the drive cycles encountered in the field differ from those assumed within the models because estimated emission rates may not correspond to actual emissions. A particular problem occurs when comparing drive cycles to identical average speeds because identical emission rates are then estimated for all cycles despite differences in the second-by-second speed profiles.

There are two general approaches to overcome this limitation of current state-of-the-art procedures. One is a microscopic approach, and the other is a mesoscopic approach. The VT-Meso model was developed to estimate light-duty vehicle (LDV) fuel consumption and emission rates on a link-by-link basis based on average speed, number of vehicle stops per unit distance, and average stop duration. The model uses these variables to construct synthetic drive cycles with four operation modes: deceleration, idling, acceleration, and cruising. Within each mode of operation, fuel consumption and emission rates are determined using relationships derived from instantaneous microscopic energy and emission models. The model allows the user to calibrate typical deceleration and acceleration rates.

The objective of this paper is to validate the proposed VT-Meso model estimations against microscopic energy and emission estimates using simulated data. In a previous effort to validate the model, VT-Meso model estimations were compared against Environmental Protection Agency (EPA) field data (Rakha, Yue et al. 2006). The model was demonstrated to successfully predict absolute fuel consumption and HC, CO, CO_2, and NO_X emission rates for the 14 EPA drive cycles. This paper investigates the ability of the VT-Meso model to correctly predict changes in vehicle fuel consumption and emission rates across different drive cycle scenarios using the INTEGRATION microscopic simulation package.

The remainder of this paper is divided into four sections. The first section presents an overview of the INTEGRATION modeling framework. The second section provides an overview of the VT-Meso model structure. The third section describes the network construction and scenario development exercises. The fourth section presents the model's evaluation and results. Finally, the conclusions of the study and recommendations for further research are presented.

6.2 INTEGRATION Modeling Framework

The INTEGRATION software (Van Aerde and Yagar 1988; Van Aerde and Yagar 1988; Van Aerde, Hellinga et al. 1996; M. Van Aerde & Assoc. 2002; M. Van Aerde & Assoc. 2002) was employed for this study for several reasons. First, the software combines car-following, vehicle-dynamics, lane-changing, energy, and emission models. Thus, mobile-source emissions can be estimated from instantaneous speed and acceleration levels. Second, the traffic and emission modeling modules have been tested and validated extensively. For example, the software, which was developed over the past two decades, has not only been validated against standard traffic flow theory (Rakha and Van Aerde 1996; Rakha and Crowther 2002) but has also been utilized for the evaluation of real-life applications. Furthermore, the INTEGRATION software offers unique capability through the explicit modeling of vehicle dynamics by computing the tractive and resistance forces on the vehicle each deci-second (Rakha, Lucic et al. 2001; Rakha and Lucic 2002; Rakha, Snare et al. 2004). It should be noted that the procedures described in this paper are general and could be applied to other commercially available software applications if they combine the modeling of various resistance and tractive forces acting on a vehicle with accurate vehicle fuel consumption and emission models.

The INTEGRATION software uses car-following models to capture the longitudinal interaction of a vehicle and its preceding vehicle in the same lane. The process of car following is modeled as an equation of motion for steady-state conditions plus a number of constraints that govern the behavior of vehicles while moving from one steady state to another (decelerating or accelerating). The first constraint governs vehicle acceleration behavior, which is typically a function of vehicle dynamics (Rakha and Lucic 2002; Rakha, Snare et al. 2004). The second and final constraint ensures that vehicles maintain a safe position relative to the lead vehicle in order to ensure asymptotic stability within the traffic stream. A more detailed description of the longitudinal modeling of vehicle motion is provided by Rakha et al. (Rakha, Snare et al. 2004) In addition, lane-changing behavior describes the lateral behavior of vehicles along a roadway segment. Lane-changing behavior affects the vehicle car-following behavior, especially at high-intensity lane-changing locations such as merge, diverge, and weaving sections.

The software also models vehicle fuel consumption and emission rates using the VT-Micro framework (Rakha, Snare et al. 2004). The VT-Micro model was developed from experimentation with numerous polynomial combinations of speed and acceleration levels. Specifically, linear, quadratic, cubic, and quadratic terms of speed and acceleration were tested using chassis dynamometer data collected at the Oak Ridge National Laboratory (ORNL). The final regression model included a combination of linear, quadratic, and cubic speed and acceleration terms because it provided the least number of terms with a relatively good fit to the original data (R^2 in excess of 0.92 for all Measures of Effectiveness (MOE)). The ORNL data consisted of nine normal-emission vehicles, including six light-duty automobiles and three light-duty trucks (LDT). These vehicles were selected to produce an average vehicle consistent with average vehicle sales in terms of engine displacement, vehicle curb weight, and vehicle type. The data collected at ORNL contained between 1,300 and 1,600 individual measurements for each vehicle and MOE combination depending on the envelope of operation of the vehicle, which has a significant advantage over emission data collected from few driving cycles since it is impossible to cover the entire vehicle operational regime with only a few driving cycles. Typically, vehicle acceleration values ranged from −1.5 to 3.7 m/s^2 in increments of 0.3 m/s^2 (- 5 to 12 ft/s^2 in 1 ft/s^2 increments). Vehicle speeds varied from 0 to 33.5 m/s (0 to 121 km/h or 0 to 110 ft/s) in increments of 0.3 m/s (Ahn, Rakha et al. 2002; Ahn, Rakha et al. 2004; Rakha and Ahn 2004). In addition, the VT-Micro model was expanded by including data from 60 LDVs and LDTs. Statistical clustering techniques were applied to group vehicles into homogenous categories using Classification and Regression Tree algorithms. The 60 vehicles were classified into five LDV and two LDT categories. In addition, high-emission vehicle (HEV) emission models were constructed using second-by-second emission data. The HEV model was found to estimate vehicle emissions with a margin of error of 10% when compared to in-laboratory bag measurements (Rakha, Ahn et al. 2003; Ahn, Rakha et al. 2004).

The INTEGRATION software computes the effective tractive force as the minimum of two forces: the maximum engine tractive force (F_e) and the maximum frictional force that can be sustained between the vehicle wheels and the roadway surface (F_{max}) (Rakha, Dion et al. 2001; Ahn, Rakha et al. 2002; Rakha and Ahn 2004; Rakha, Ahn et al. 2004). The aerodynamic resistance (R_a), rolling resistance (R_{rl}), and grade resistance (R_g) are

also computed each deci-second. Subsequently, the maximum vehicle acceleration is then computed as

$$a = \frac{\min\left(F_e, F_{\max}\right) - \left(R_a + R_{rl} + R_g\right)}{m} \qquad [6\text{-}1]$$

6.3 Overview of the VT-Meso Model Framework

The VT-Meso model utilizes link-by-link average speeds, number of vehicle stops, and stopped delay as input parameters to construct a synthetic drive cycle and compute average link fuel consumption and emission rates (Rakha, Yue et al. 2006). Total link fuel consumption and emissions are then computed by multiplying the average fuel consumption and emission rates by its corresponding vehicle-kilometers of travel. Finally, system-wide parameters are estimated by summing across all links within a network. The first step involves the construction of a synthetic drive cycle that produces consistent average speed, number of vehicle stops, and stopped delay estimates. After constructing the drive cycle, the model estimates the proportion of time that a vehicle typically spends cruising, decelerating, idling, and accelerating while traveling on a link. A series of fuel consumption and emission models are then used to estimate the amount of fuel consumed and emissions of HC, CO, CO2, and NO_X emissions for each mode of operation. Subsequently, the total fuel consumed and pollutants emitted by a vehicle while traveling along a segment are estimated by summing across the different modes of operation and dividing by the distance traveled to obtain distance-based average vehicle fuel consumption and emission rates.

6.4 Scenario Development

In order to validate the VT-Meso model energy and emission estimates, four simulation networks were constrcuted. The INTEGRATION software was utilized to simulate these four networks considering 12 different vehicle types. Output from the INTEGRATION software, which include link specific average travel speed, traveled distance, stopped time, and number of stops were used as input to the VT-Meso model. The VT-Meso emission and fuel consumption estimates were compared to those computed by the INTEGRATION software based on second-by-second speed and acceleration measurementsin an attempt to validate the procedure.

6.4.1 Stop Sign Control Scenario

The objective of this scenario is to compare the VT-Meso and VT-Micro estimates for a stop-and-go condition. The simulation network is a 2-km, single-lane roadway with a single stop sign located after 1 km. This scenario involves vehicle deceleration and acceleration from a complete stop considering different cruising speeds. The cruising free-flow speeds are varied from 32 km/h (20 mi/h) to 64 km/h (40 mi/h) at increments of 8 km/h (5 mi/h) to analyze the impact of stop-and-go driving conditions on fuel consumption and vehicle emission rates for both models. The traffic volumes used for this scenario include a single vehicle vehicle and a demand of 300 veh/h.

6.4.2 Signal Control Scenario

This scenario compares the VT-Meso and VT-Micro estimates for different traffic signal offsets. The network used in this analysis is composed of three signalized intersections along a 2-km roadway segment. Signalized intersections are located after 500 m, 1,000 m, and 1,500 m. The cycle length at each of the three intersections is set at 60 s with offsets varying from 0 to 50 s at 10-s increments. All three signals are controlled by two-phase timings with a 70:30 phase split (east/west versus north/south), and only eastbound traffic exists. The free-flow speed of the network is 64 km/h (40 mi/h) with a lane saturation flow rate of 1,600 veh/h. Traffic demands of this simulation scenario include a single vehicle scenario and a demand of 800 veh/h.

6.4.3 Partial Stop Scenario

Partial stops have a large impact on vehicle fuel consumption and emission rates. The objective of this scenario is to test how the VT-Meso model performs for driving cycles with partial stops. The fuel consumption and emission rates estimated by the model are compared against the rates estimated by the VT-Micro model. The simulation network is a 2.5-km roadway. The first 1-km segment and the last 1-km segment has the same speed limit of 110 km/h, and the 0.5-km segment in the middle has a lower speed limit. The decrease in speed limit varies from 10 km/h to 50 km/h in increments of 10 km/h. A single vehicle and 900 veh/h were simulated for this scenario.

6.4.4 Weaving Segment Scenario

Weaving volume and weaving section length have significant impacts on the performance of a weaving section. This scenario simulates a Type A weaving section for different weaving volumes and weaving section lengths. The Weaving volume varies from 0 to 2,500 veh/h in increments of 500 vehicles, and the weaving section length varies from 150 m to 450 m in increments of 50 m. The free-flow speed at the ramp section and weaving section is 80 km/h (50 mi/h) and 112 km/h (70 mi/h), respectively.

6.5 Results

This section describes the fuel consumption and vehicle emission rate comparison for the four simulation scenarios. This comparison starts with the stop sign control scenario followed by the partial stop scenario, the signal control scenario, and the ramp scenario.

6.5.1 Stop Sign Control Scenario

This section describes the results for the stop sign scenario for both normal- and high-emitting vehicles. The scenario tests the performance of the VT-Meso model for conditions involving vehicle stop-and-go maneuvers. As discussed earlier in the methodology section, five different speed limits are considered in this scenario. The speed limits are varied from 32 km/h (20 mi/h) to 64 km/h (40 mi/h) at increments of 8 km/h (5 mi/h).

In the case of normal light-duty vehicles, Figure 6-1 illustrates the speed profile and emission comparison for the single-vehicle scenario for LDV1s. Figure 6-2 illustrates the

average travel speed and emission comparison for the 300-veh/h scenario for LDV1s. The total fuel consumption, HC, CO, and CO_2 emission rates are higher at lower speeds while the NO_X emission rates shows a slight increase when the free-flow speed increases. Given that a vehicle traveling at lower speeds spends more time traveling the 2-km roadway section, despite the lower time-based fuel consumption and emission rate, the total fuel consumption and emissions are higher at lower speed levels. As a vehicle's speed increases, the time-dependent rate also increases, though more slowly than the travel time rate of increase. Consequently, the distance-based fuel consumption and emission rate decreases until the rate of increase in the time-dependent rate exceeds the rate of decrease in time spent in the system. A more detailed description and explanation of these behaviors can be found elsewhere in the literature (Rakha, Ahn et al. 2004).

These figures also illustrate that HC and CO emission are more sensitive to travel speeds. Comparison between the single-vehicle scenario and the 300-veh/h scenario shows that vehicles consume more fuel and generate more emissions for the 300-veh/h scenario, which has a lower travel speed. Comparison between the single-vehicle scenario and 300-veh/h scenario also illustrates that the difference between VT-Micro and VT-Meso estimations is smaller for high traffic volumes because the vehicle interaction reduces the random variability.

Figure 6-3 illustrates the speed profile and emission comparison for the single-vehicle scenario for HEV1s, and Figure 6-4 illustrates the average travel speed and emission comparison for the 300-veh/h scenario for HEV1. The HEV1 shows a similar trend to the LDV1 except for the CO emissions. The result for CO emissions shows a bowl-shaped relationship with the minimum emission rate at 48 km/h (30 mi/h) while the CO emission for LDV1 has a minimum value at higher speeds. The absolute values of the HEV1 fuel consumption and CO_2 emission rates are close to those of the normal LDV1. In case of the NO_X emissions, the mass emissions for the HEV1 are significantly greater than those for the normal LDV. As is the case for the LDV1 vehicle, the 300-veh/h scenario results in a better VT-Meso estimate in comparison to the single-vehicle scenario.

6.5.2 Signal Control Scenario

This section describes the results for the signal control scenario for both normal- and high-emitting vehicles. The VT-Meso and VT-Micro model fuel consumption and vehicle emission estimates are varied as a function of the traffic signal offsets.

Figure 6-5 and Figure 6-6 illustrate the comparison of the VT-Micro and VT-Meso estimations as a function of signal offsets for LDV1s and HEV1s, respectively. As can be seen from these figures, higher average travel speeds are associated with a lower number of stops. The optimal offset for the 300-veh/h scenario is 40 s, and the worst offset is approximately 0 s regardless of the MOE that is considered in optimizing the signal offsets. The percentage changes in MOEs for optimal and worst offsets are calculated. The fuel consumption, HC, CO, NO_X, and CO_2 emissions for the worst offset are 17%, 18%, 25%, 4%, and 16% higher, respectively, than those of the optimal offsets. This result shows that the fuel consumption and vehicle exhaust emissions are generally low when the network is operating at the optimal signal offset. The figures demonstrate that

the VT-Meso model gives a good estimation for fuel consumption and CO_2 emissions. The estimations for HC, CO, and NO_X emissions are not as close as those for fuel consumption and CO_2 emission, but the VT-Meso model correctly predicts trends of increasing or decreasing HC, CO, and NO_X emissions. Specifically, the model produces the highest and lowest estimates for the same offsets for which the highest and lowest VT-Micro model estimates are obtained.

The variation in fuel consumption and emission rates for the HEV1 as a function of offsets is very similar to the LDV1 results. Similarly, the MOE rates are lowest at the optimal signal offsets. However, the differences in absolute values for the HEV1 are much greater than those of the normal LDV. The percentage changes in MOE for optimal and worst offsets are calculated. The fuel consumption, HC, CO, NO_X, and CO_2 emissions for the worst offset are 9%, 8%, 6%, 0%, and 9% greater, respectively, than those for the optimal offsets. As can be seen, the differences in fuel consumption and vehicle emissions are lower than those of the LDV1. Again the VT-Meso model produces similar trends to those produced using a microscopic model.

6.5.3 Partial Stop Scenario

The main objective of the partial stop scenario is to test the performance of the VT-Meso model for drive cycles with high speed variability. As discussed in the previous section, speed limit difference varied from 10 km/h to 50 km/h in increments of 10 km/h. The comparison between mesoscopic and microscopic models evaluates the effect of fractional stops on fuel consumption and vehicle emissions.

The analysis of LDV1s and HEV1s shows similar results. Figure 6-7 and Figure 6-8 illustrate the comparison of VT-Micro and VT-Meso estimations as a function of speed limit difference for LDV1 at different traffic volumes. As for the single-vehicle scenario, it is observed that the model currently tends to underestimate NO_X and CO emissions. Alternatively, the fuel consumption, HC emission, and CO emission appear to be fairly symmetric about the line of perfect correlation.

It is hypothesized that these differences are attributable to differences between the actual and constructed drive cycles. Further investigations of the test results indicate that the variability observed in each diagram could also be attributable to the way partial stops are converted into equivalent full stops when aggregating each drive cycle into an average speed, an average number of stops, and an average stop duration. Figure 6-9 compares a synthetic drive cycle to an actual drive cycle. Both cycles have the same average travel speed, deceleration time, acceleration time, and cruising time. This synthetic drive cycle will create problems for emissions that are more sensitive to high travel speed. Hence, this will cause the VT-Meso model to underestimate fuel consumption and emission rates for drive cycles with frequent partial stops.

As for the 1,100-veh/h scenario, it is also observed that the VT-Meso model provides a better match in terms of both absolute estimations and cyclic trends with the microscopic model estimates. This could be attributed to high traffic volume minimizing the high variability of the single vehicle. Also, high traffic volume is associated with lower travel

speed, and the lower travel speed will help better estimate emissions, which are more sensitive at high speeds.

6.5.4 Weaving Segment Scenario

This section compares the VT-Meso and VT-Micro models for a ramp scenario which entails aggressive accelerations at high speeds (i.e. high engine loads). Two independent variables were included in the weaving segment scenario: weaving section length and weaving volume. Weaving volumes varied from 0 veh/h to 2,500 veh/h in increments of 500 veh/h, and the weaving section length was varied from 150 m to 450 m in increments of 50 m. Input values of two independent variables ensured that the over-capacity condition and the steady-state condition were simulated.

The first plot in Figure 6-10 shows the average travel speed for different simulation conditions. When the weaving volume is lower than 1,500 veh/h, the simulation network is under capacity. Increasing the weaving volume and/or reducing the weaving section length reduces the weaving section capacity and thus results in over-saturated conditions; this can be seen from the difference in the average travel speed. As for the fuel consumption and vehicle emissions, the plots on the left side show the VT-Micro model estimations, and the plots on the right side show the VT-Meso model estimations. As can be seen from these plots, the VT-Meso model estimations have an excellent match both in terms of absolute values and cyclic trends for fuel consumption, HC, and CO_2 emissions and a good fit for NO_X emissions. The VT-Meso model tends to underestimate CO emission in terms of absolute values, however the trends are consistent.

6.5.5 Validation against MOBILE6 Estimation

This section validates the mesoscopic model by comparing the model outputs to outputs from the EPA MOBILE6 model. Average link travel speed and other adjustment input variables were used as input to the MOBLE6 model. It should be noted that the CO_2 emission estimate from MOBILE6 is unlike other MOBILE6 emission estimates. Specifically, the CO_2 emission rate is not affected by speed, temperature, and gasoline type. This rate is based on vehicle type only. The comparison was for four pollutants: HC, CO, NOx., and CO_2.

Figure 6-11 shows the comparison for the four stop sign control scenario for the LDV1 vehicle. This figure clearly shows that the CO_2 estimation from MOBILE6 is a constant value, and is not affected by the average travel speed and actual speed profile. Figure 6-12 shows the comparison for the signal control scenario using the LDV1 vehicle.

MOBILE6 uses an average vehicle travel speed to estimate vehicle emissions, which is not a very accurate predictor of vehicle emissions. The significant differences in emission rates between VT-Meso and MOBILE6 are NO_X and CO_2 emissions. As noted before, CO2 emissions from MOBILE 6 is not dependent variable on the average travel speed, this rate is affected by vehicle type only. For NO_X the emission difference is due to the fact that NO_X emission rates is both sensitive to vehicle speed and acceleration levels, MOBILE6 does not consider the effect of vehicle acceleration.

6.5.6 Overall Analysis

Table 6-1 summarizes the differences between the VT-Meso and VT-Micro model estimates. The table generally indicates that the mesoscopic model estimates appear to be consistent with the microscopic estimates. Most of the differences between VT-Meso and VT-Micro estimations are generally less than 10% for the stop sign and signal control scenarios. In these cases, the differences in results between the microscopic and mesoscopic estimates can be attributed to differences between the actual and constructed drive cycles. Other parameters that could affect the mesoscopic model estimates include the various assumptions made by the mesoscopic model when generating synthetic drive cycles, particularly regarding the assumed deceleration and acceleration rates. In general the mesoscopic model appears to estimate fuel consumption, HC, and CO_2 emissions consistently with the microscopic estimates; however, the model tends to underestimate NO_X emissions.

As for the partial stop scenario, the VT-Meso estimations are lower than those of the VT-Micro model. This underestimation is attributed to the higher fuel consumption usually required to increase the speed of a vehicle from 50 to 60 km/h than from, say, 30 to 40 km/h because accelerations at higher speeds usually result in higher loads being exerted on a vehicle's engine. Because of the nonlinearity of fuel consumption and emission rates as a function of speed, a series of partial stops will often produce higher fuel consumption and emission rates than a corresponding equivalent number of full stops.

6.6 Conclusions

This paper compares the VT-Meso and VT-Micro model fuel consumption and emission estimates for four simulation scenarios including stop sign, signal control, partial stop, and ramp scenarios. In additional, VT-Meso model was compared again EPA MOBILE6 model. The results demonstrate that the VT-Meso model provides an excellent match to the microscopic model estimates in terms of both absolute emission rates and cyclic trends. Specifically, this model provides close estimates for the stop sign, signal control, and ramp scenarios. On the other hand, the model predictions were less accurate in the partial stop scenario, especially in the case of CO emissions. The inaccuracies are partly attributed to the non-linear relationship between vehicle emissions and vehicle speed and errors in the construction of synthetic drive cycles.

The estimates from the VT-Meso model cannot be expected to always match estimates from microscopic models because of differences in the underlying drive cycles (the VT-Meso model constructs simplistic drive cycles). The model, however, constitutes an interesting alternative to existing models for cases in which detailed speed and acceleration data are not available. These results indicate that the VT-Meso model framework is sufficient for operational level comparisons. The study also demonstrates the need to perform additional tests to evaluate more precisely the effect of fractional stops on vehicle emissions or to more accurately convert partial stops into equivalent full stops for the purpose of estimating vehicle fuel consumption and emission rates.

Table 6-1: VT-Meso and VT-Micro Estimations Differences

Stop Sign Scenario

Speed Limit	HEV1					LDV1				
(km/h)	Fuel	HC	CO	NO_X	CO_2	Fuel	HC	CO	NO_X	CO_2
32	0.4%	-0.4%	2.3%	-2.3%	0.1%	1.4%	3.3%	3.1%	1.3%	1.2%
40	-0.1%	-0.6%	3.5%	-1.6%	-0.4%	1.1%	3.8%	3.8%	2.0%	0.9%
48	-1.4%	-1.3%	4.2%	-2.3%	-1.7%	0.4%	4.5%	4.5%	1.3%	0.1%
56	-2.5%	-1.4%	2.7%	-2.4%	-2.9%	-0.7%	3.4%	2.4%	-0.8%	-1.0%
64	-2.6%	-2.8%	3.6%	-0.2%	-2.8%	-0.2%	0.9%	1.6%	-2.0%	-0.5%

Signal Control Scenario

Signal Offset	HEV1					LDV1				
(s)	Fuel	HC	CO	NO_X	CO_2	Fuel	HC	CO	NO_X	CO_2
0	-6.9%	-3.6%	-0.2%	-5.8%	-7.3%	-3.5%	0.7%	1.1%	-1.8%	-4.0%
10	-5.9%	-3.0%	0.2%	-5.0%	-6.3%	-2.9%	1.0%	1.2%	-1.5%	-3.3%
20	-5.1%	-2.6%	-0.3%	-4.2%	-5.5%	-2.3%	0.7%	0.9%	-1.5%	-2.7%
30	-4.8%	-2.4%	-0.9%	-3.8%	-5.2%	-2.2%	0.2%	0.5%	-1.8%	-2.6%
40	-4.8%	-2.5%	-1.5%	-3.7%	-5.1%	-2.0%	-0.2%	0.2%	-2.2%	-2.4%
50	-6.6%	-3.5%	-1.1%	-5.3%	-7.1%	-3.3%	-0.1%	0.5%	-2.2%	-3.7%

Partial Stop Scenario (Single Vehicle)

Speed Limit Difference	HEV1					LDV1				
(km/h)	Fuel	HC	CO	NO_X	CO_2	Fuel	HC	CO	NO_X	CO_2
10	-2.7%	-5.5%	-12.2%	-4.6%	-2.3%	-3.7%	-10.7%	-7.1%	-0.8%	-2.6%
20	-6.0%	-5.9%	-12.1%	-7.9%	-5.7%	-7.0%	-15.2%	-13.8%	-10.2%	-6.1%
30	-5.5%	-0.4%	4.3%	-8.0%	-5.6%	-7.5%	-9.7%	-18.1%	-15.4%	-6.6%
40	-4.9%	2.6%	1.4%	-6.6%	-4.9%	-8.3%	-5.0%	-24.6%	-20.6%	-7.0%
50	-5.3%	1.5%	-13.7%	-4.1%	-4.6%	-8.7%	-6.4%	-30.5%	-25.6%	-7.1%

Partial Stop Scenario (1,100 veh/h)

Speed Limit Difference	HEV1					LDV1				
(km/h)	Fuel	HC	CO	NO_X	CO_2	Fuel	HC	CO	NO_X	CO_2
10	-4.7%	1.5%	17.4%	-3.9%	-5.4%	-5.8%	-4.6%	-11.5%	-14.7%	-6.1%
20	-2.9%	5.0%	28.1%	-2.8%	-3.9%	-5.0%	0.8%	-11.3%	-13.8%	-5.3%
30	-1.2%	6.9%	25.6%	-1.5%	-2.3%	-4.2%	4.5%	-12.1%	-13.4%	-4.3%
40	-0.9%	6.6%	13.2%	-0.5%	-1.8%	-4.1%	4.3%	-13.8%	-14.2%	-4.1%
50	-3.3%	3.2%	-2.9%	-0.7%	-3.7%	-5.7%	-0.5%	-17.0%	-16.9%	-5.6%

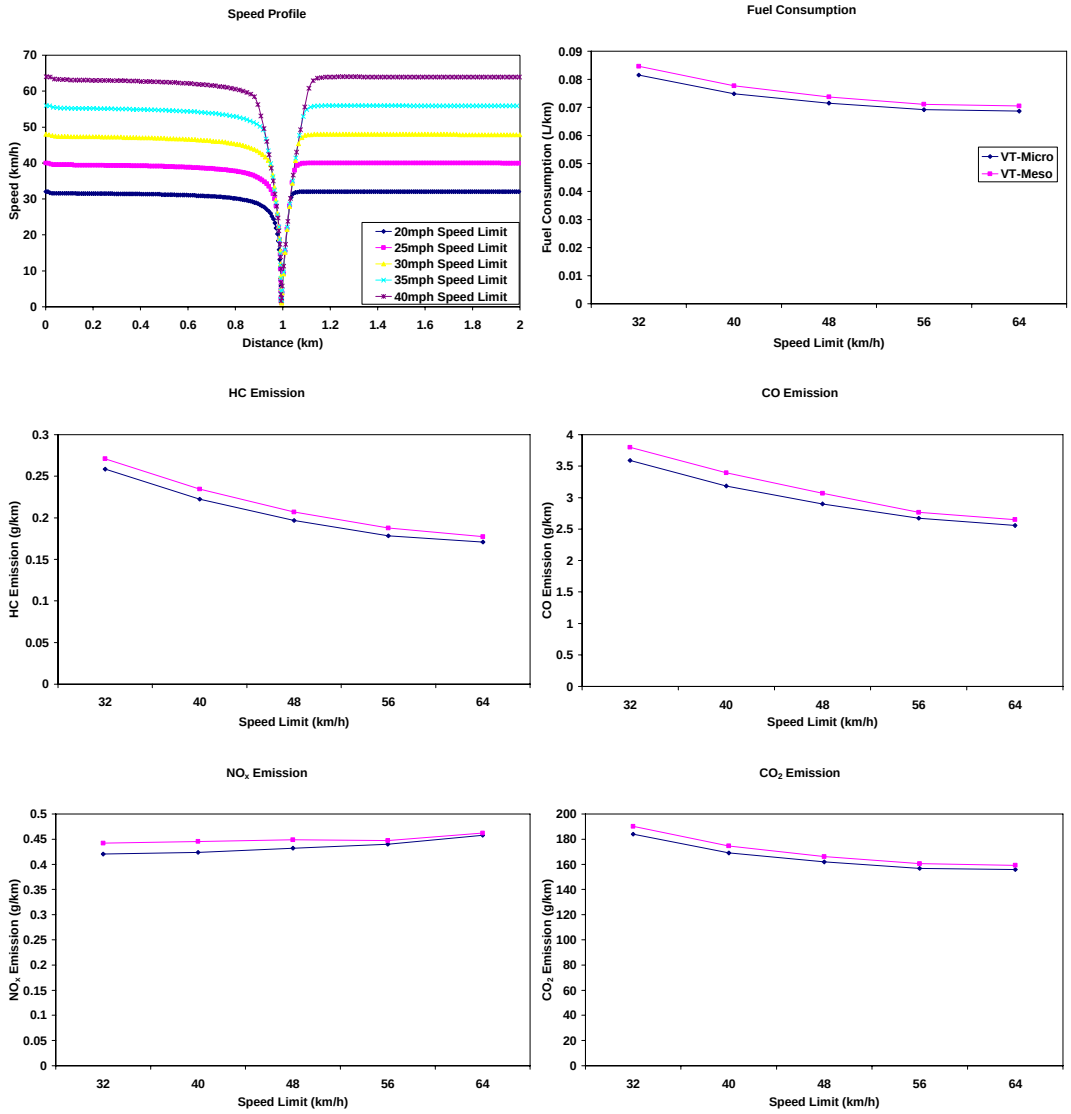

Figure 6-1: Signal LDV1 vehicle for Stop Sign Scenario

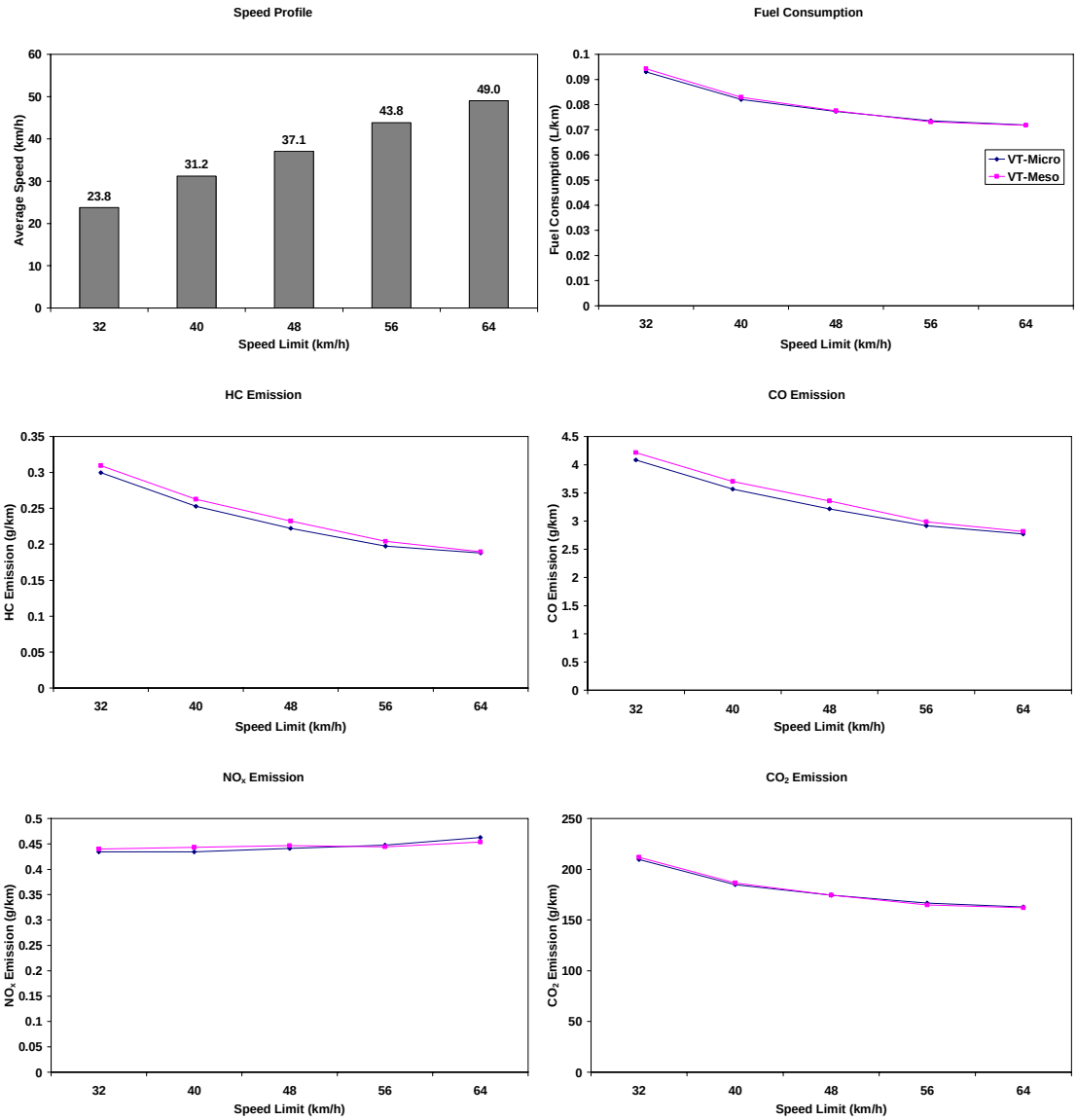

Figure 6-2: 300 veh/h LDV1 for Stop Sign Scenario

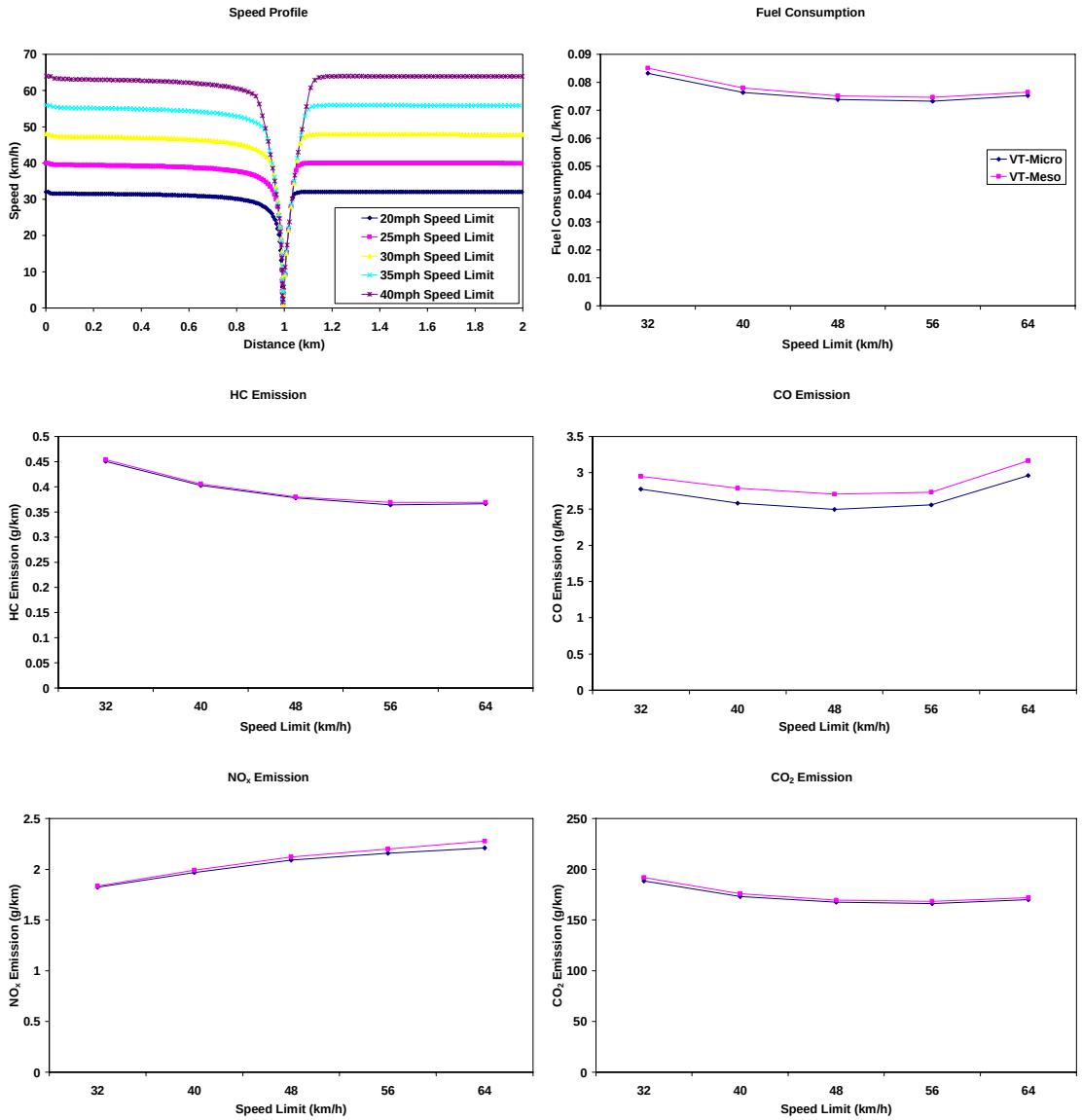

Figure 6-3: Signal HEV1 Vehicle for Stop Sign Scenario

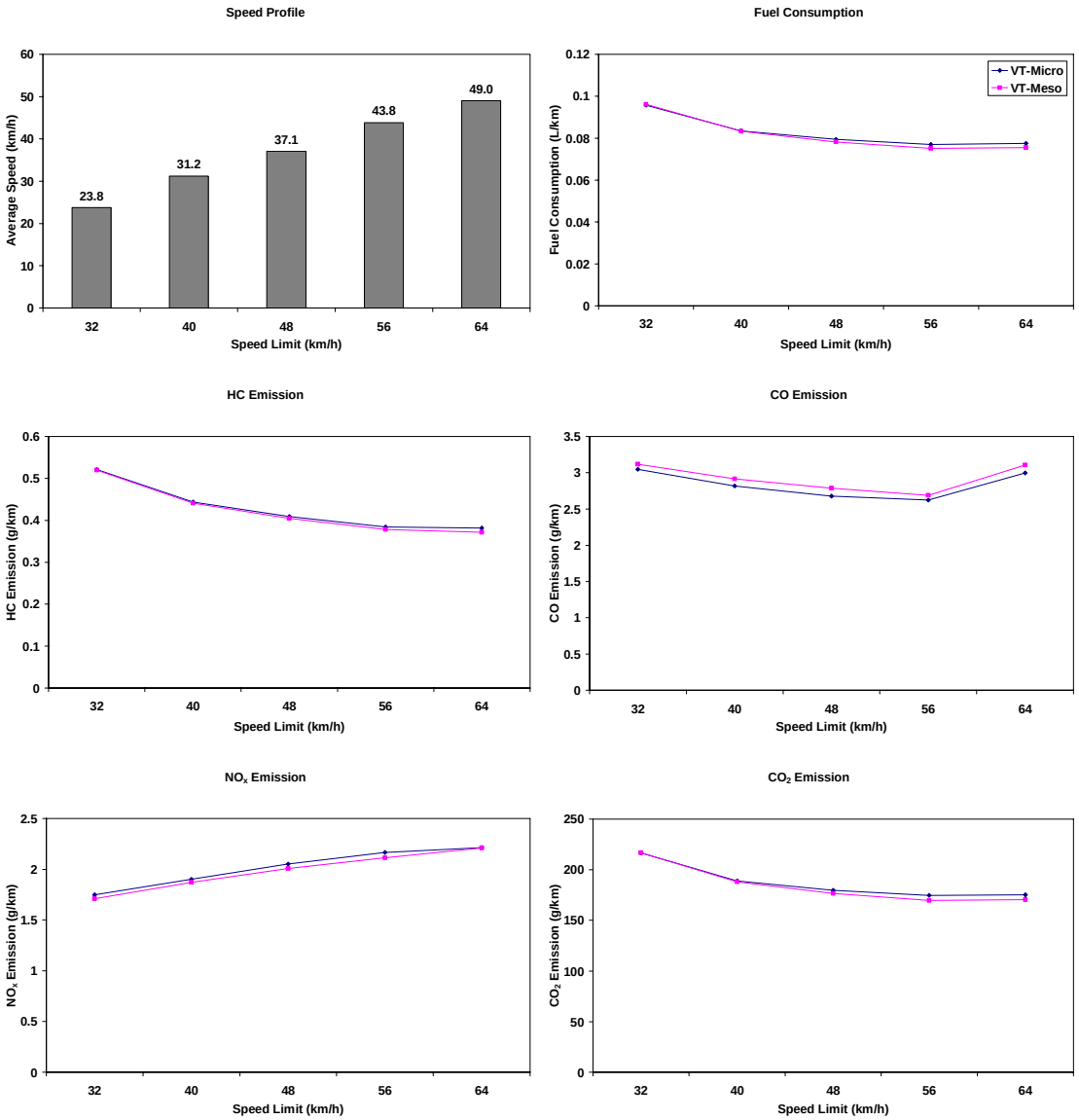

Figure 6-4: 300 veh/h HEV1 for Stop Sign Scenario

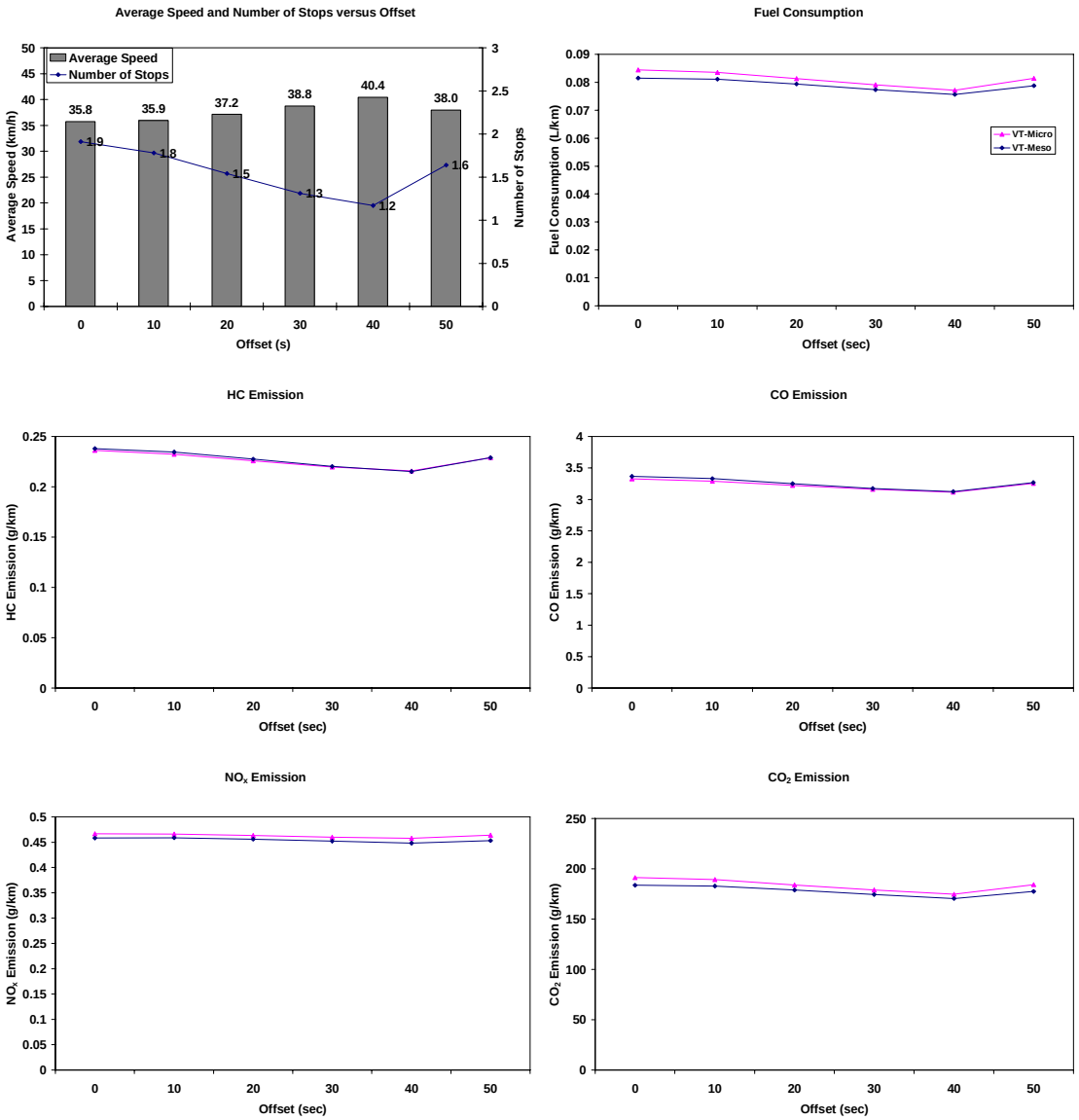

Figure 6-5: 800 veh/h LDV1 for Signal Control Scenario

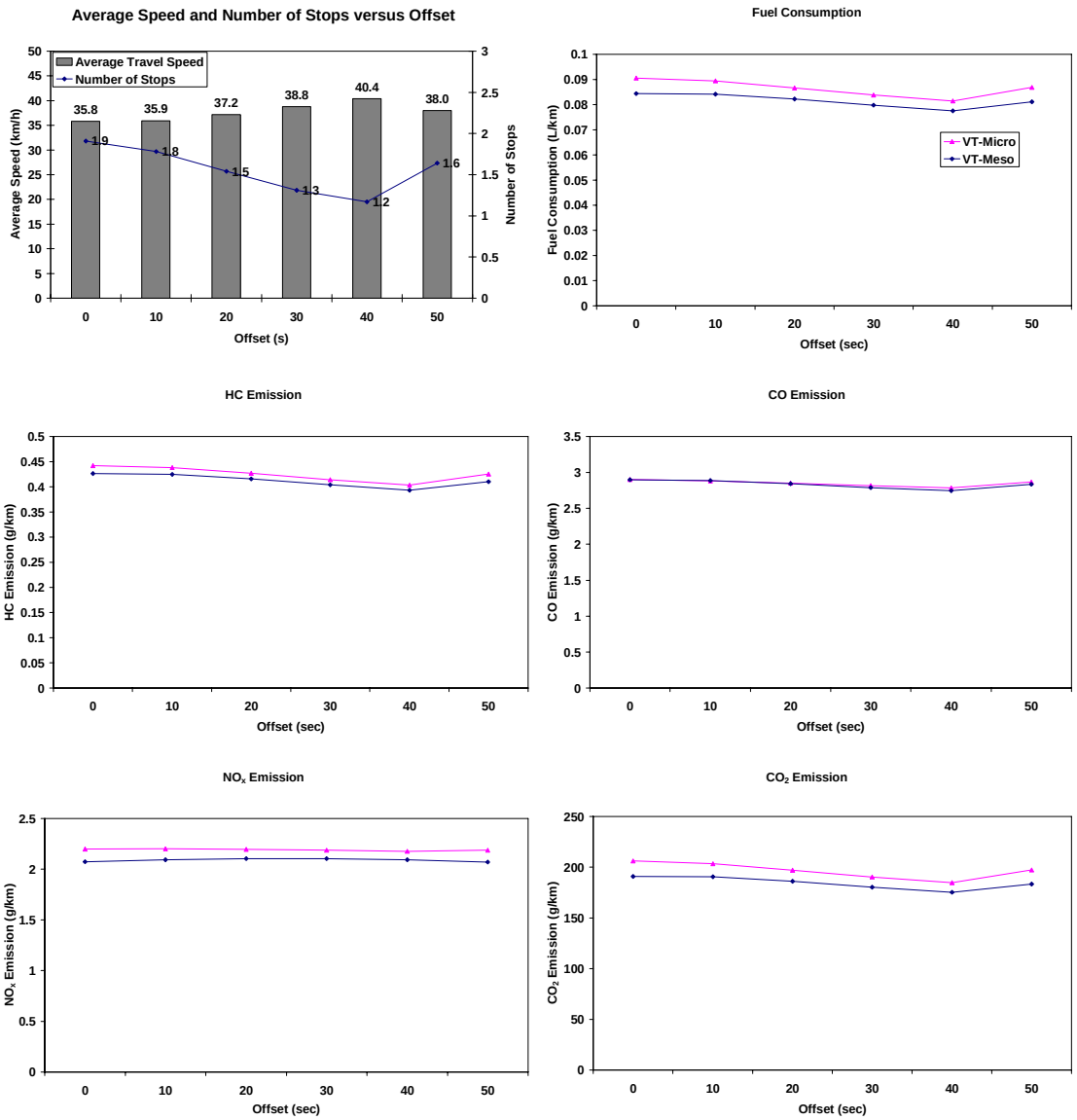

Figure 6-6: 800 veh/h HEV1 for Signal Control Scenario

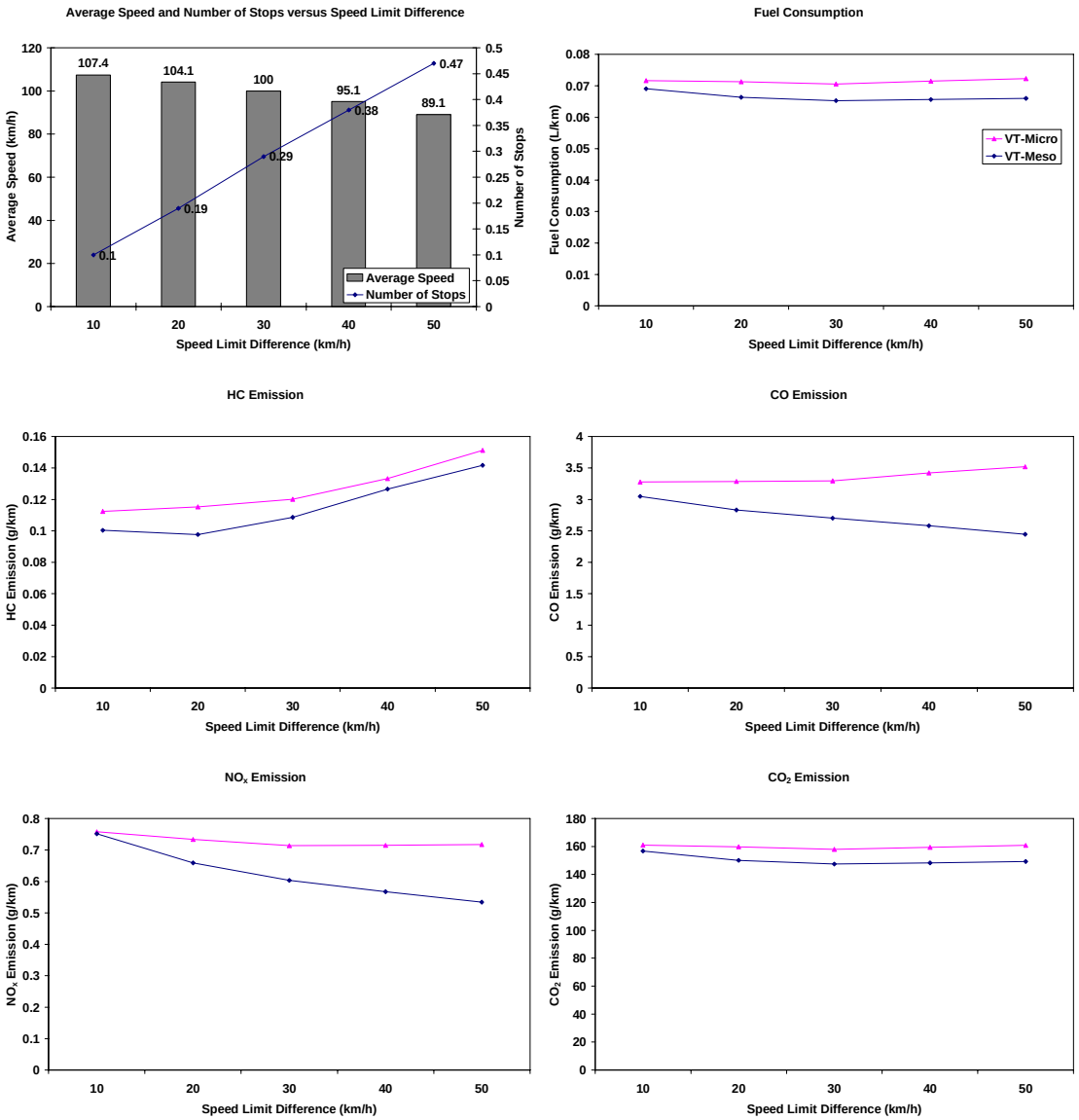

Figure 6-7: VT-Meso and VT-Micro Comparison for Partial Stop Scenario – Single LDV1

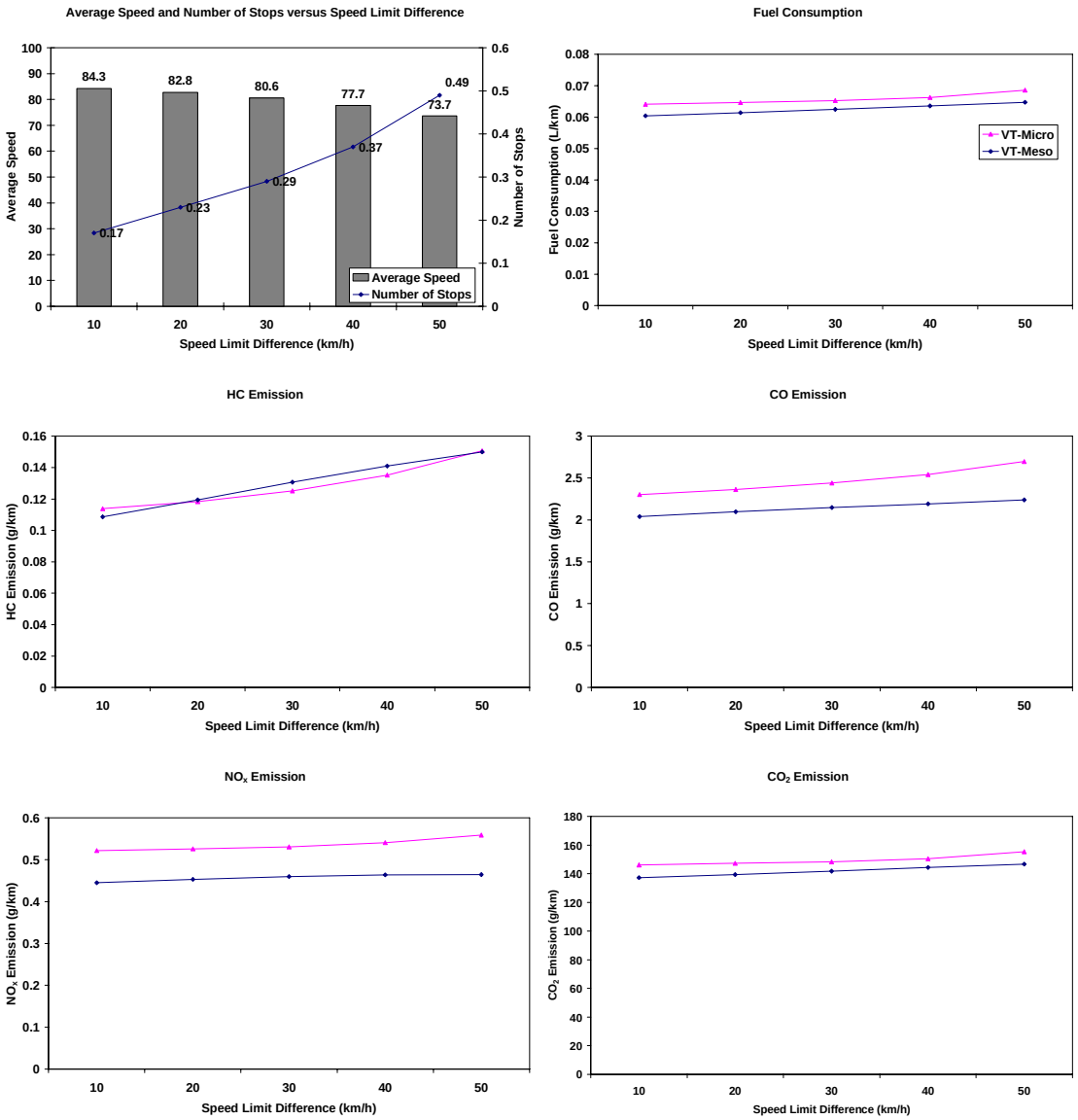

Figure 6-8: VT-Meso and VT-Micro Comparison for Partial Stop Scenario – 1,100 veh/h LDV1

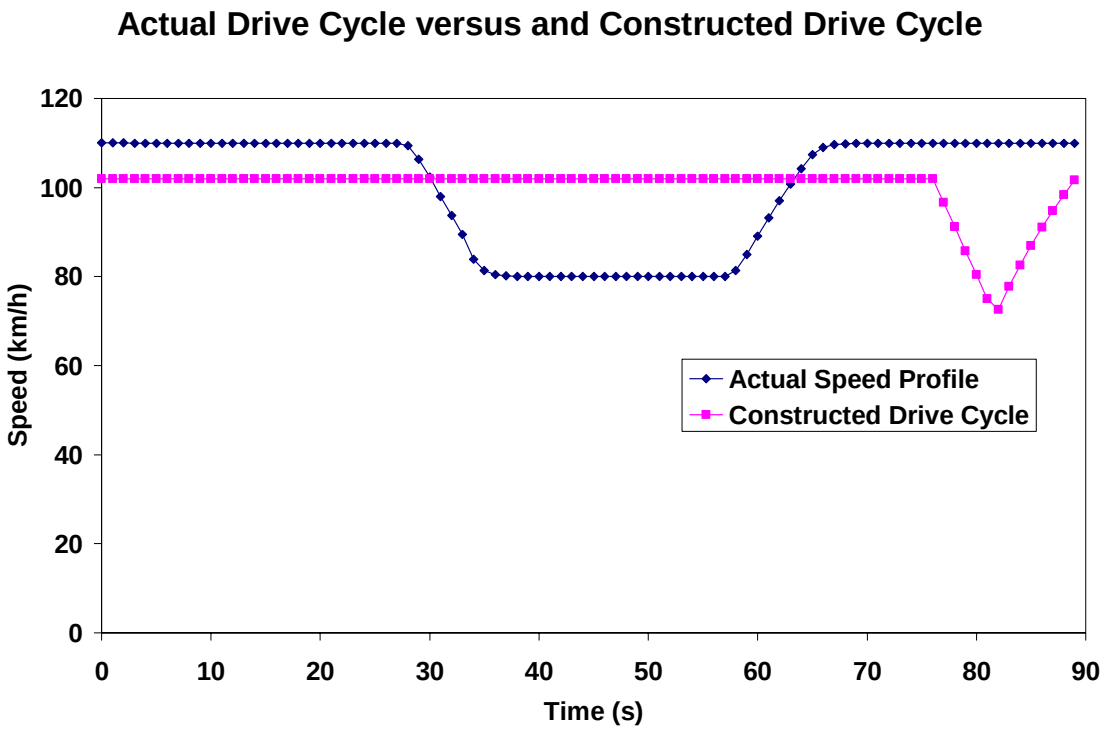

Figure 6-9: Comparison Between Synthetic Drive Cycle and Actual Drive Cycle

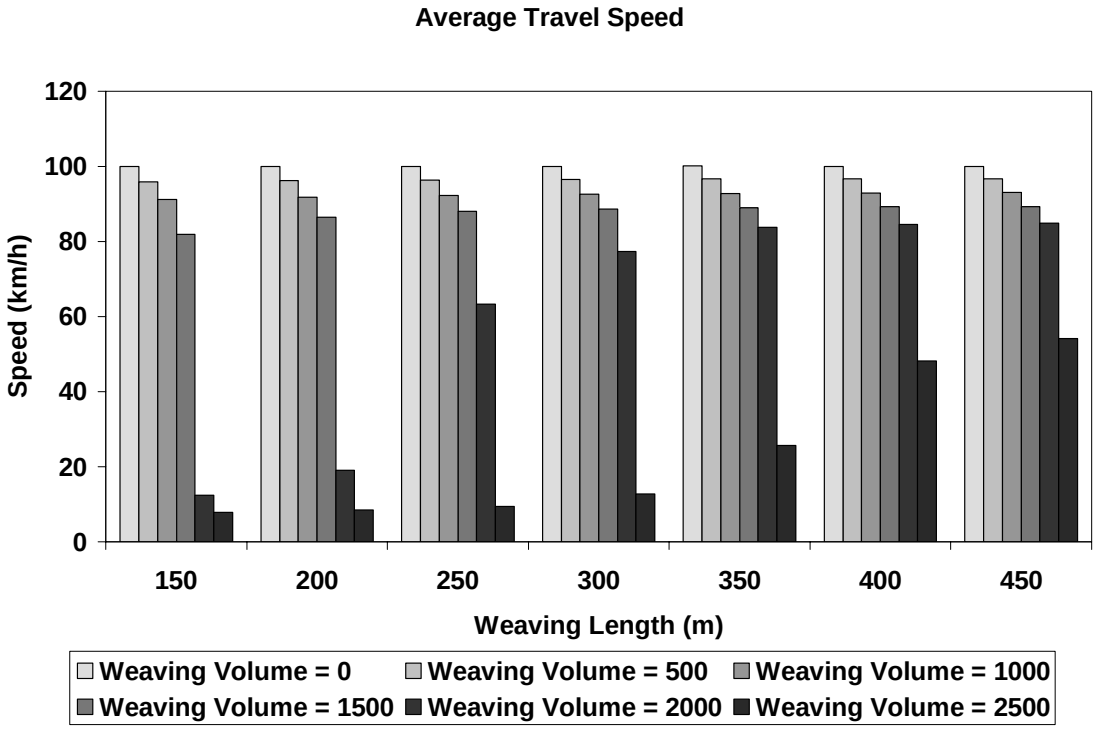
Average Travel Speed
Speed (km/h)
120
100
80
60
40
20
0
150
200
250
300
350
400
450
Weaving Length (m)
Weaving Volume = 0
Weaving Volume = 500
Weaving Volume = 1000
Weaving Volume = 1500
Weaving Volume = 2000
Weaving Volume = 2500

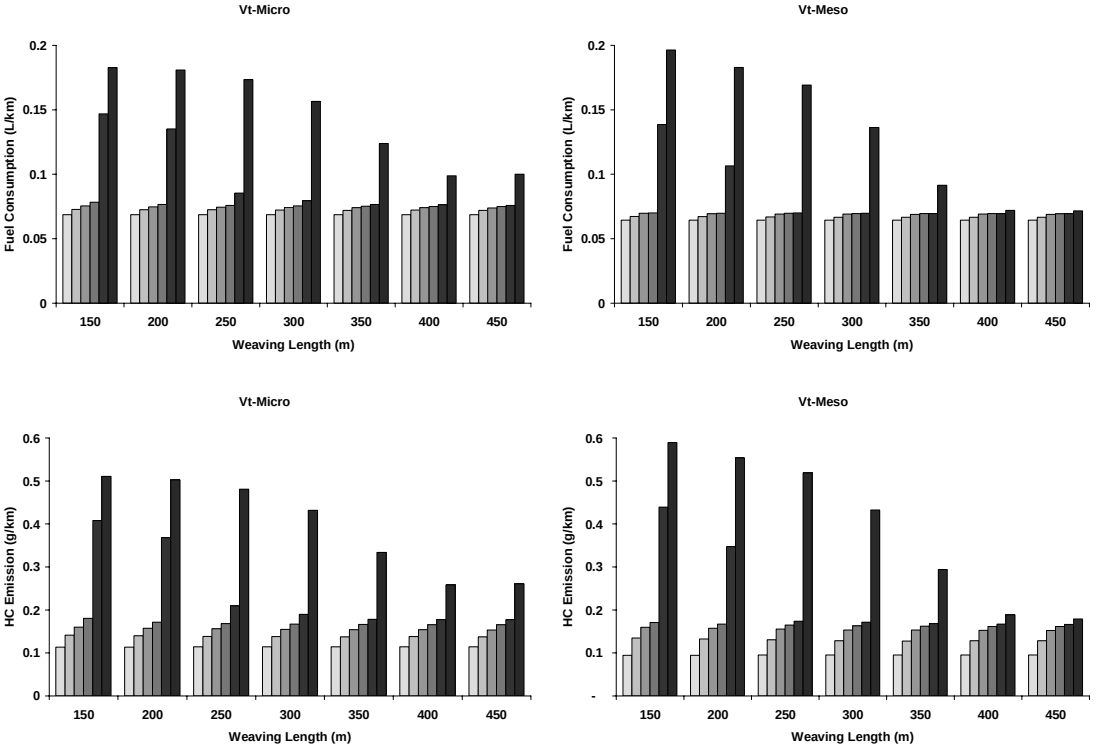
Vt-Micro
Fuel Consumption (L/km)
0.2
0.15
0.1
0.05
0
150
200
250
300
350
400
450
Weaving Length (m)
Vt-Meso
Fuel Consumption (L/km)
0.2
0.15
0.1
0.05
0
150
200
250
300
350
400
450
Weaving Length (m)
Vt-Micro
HC Emission (g/km)
0.6
0.5
0.4
0.3
0.2
0.1
0
150
200
250
300
350
400
450
Weaving Length (m)
Vt-Meso
HC Emission (g/km)
0.6
0.5
0.4
0.3
0.2
0.1
-
150
200
250
300
350
400
450
Weaving Length (m)

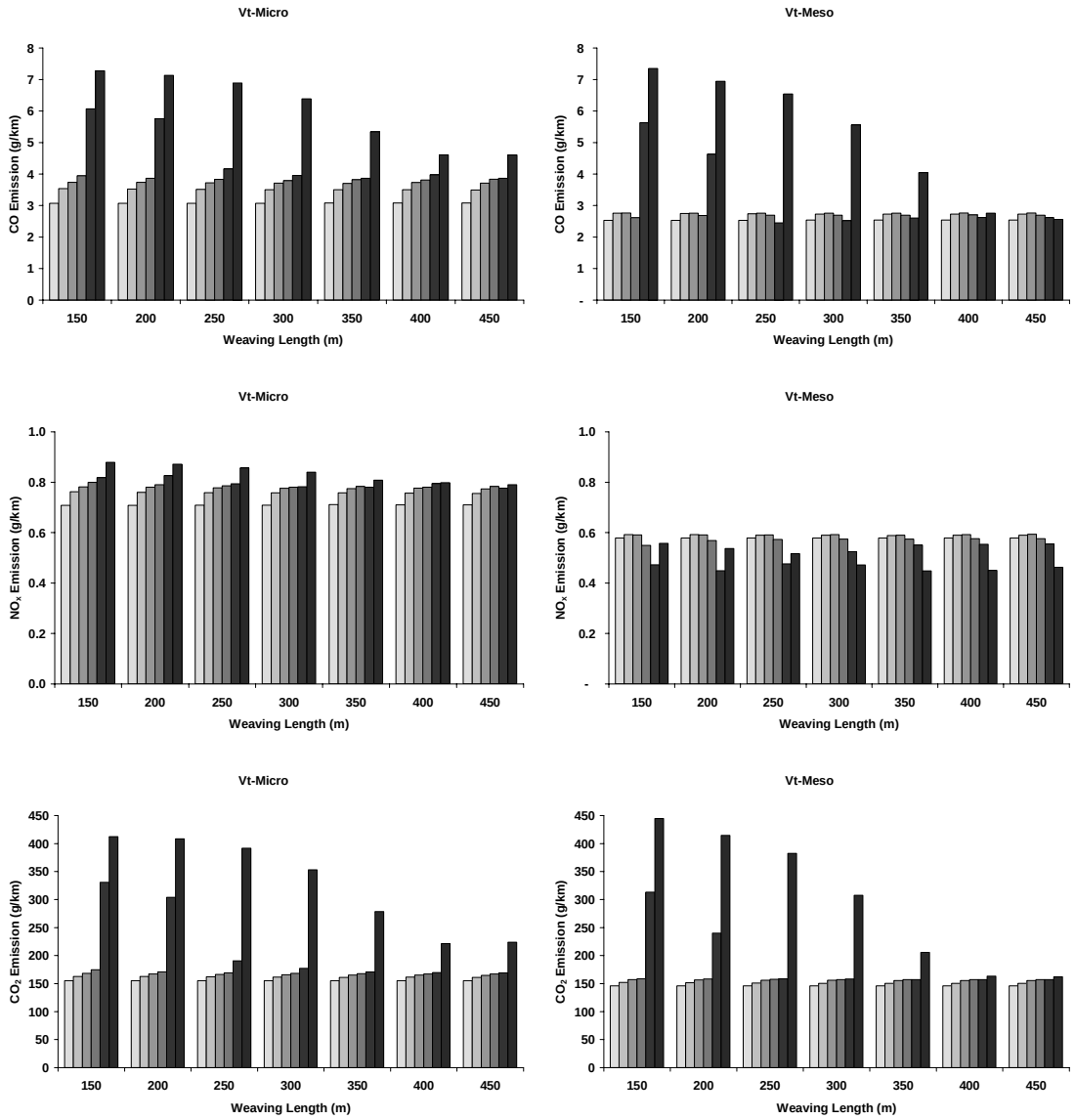

Figure 6-10: VT-Meso and VT-Micro Comparison for Ramp Scenario – LDV1

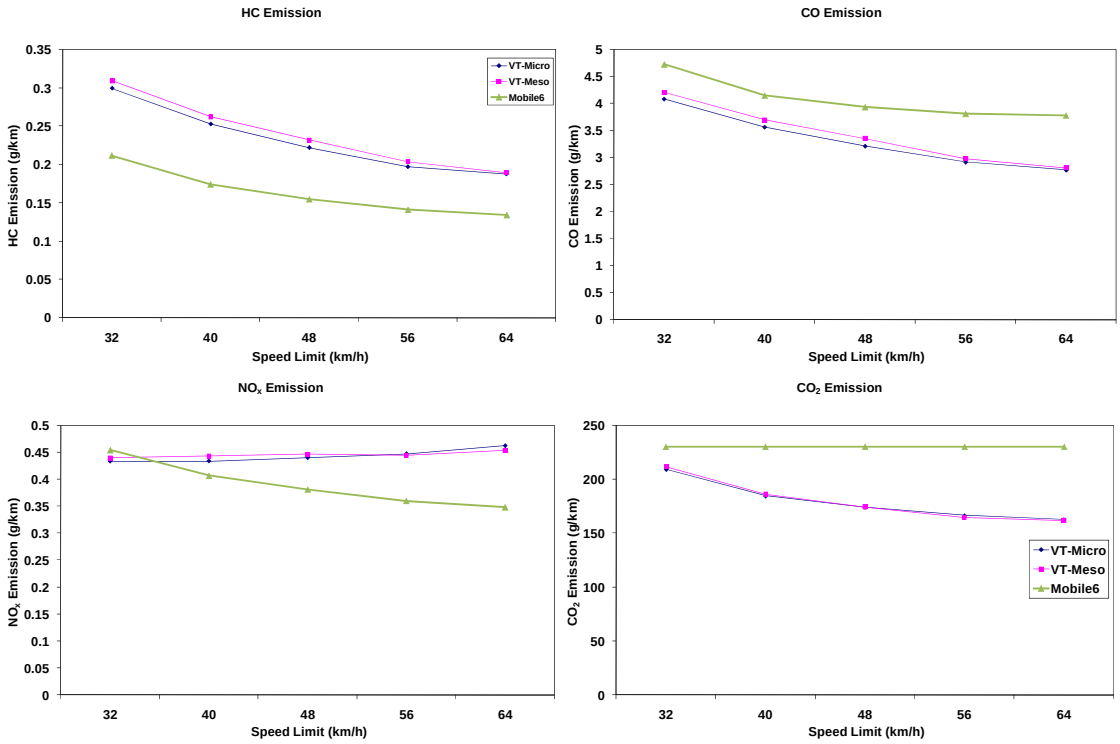

Figure 6-11: VT-Meso and MOBILE6 Comparison for Stop Sign Control Scenario – LDV1

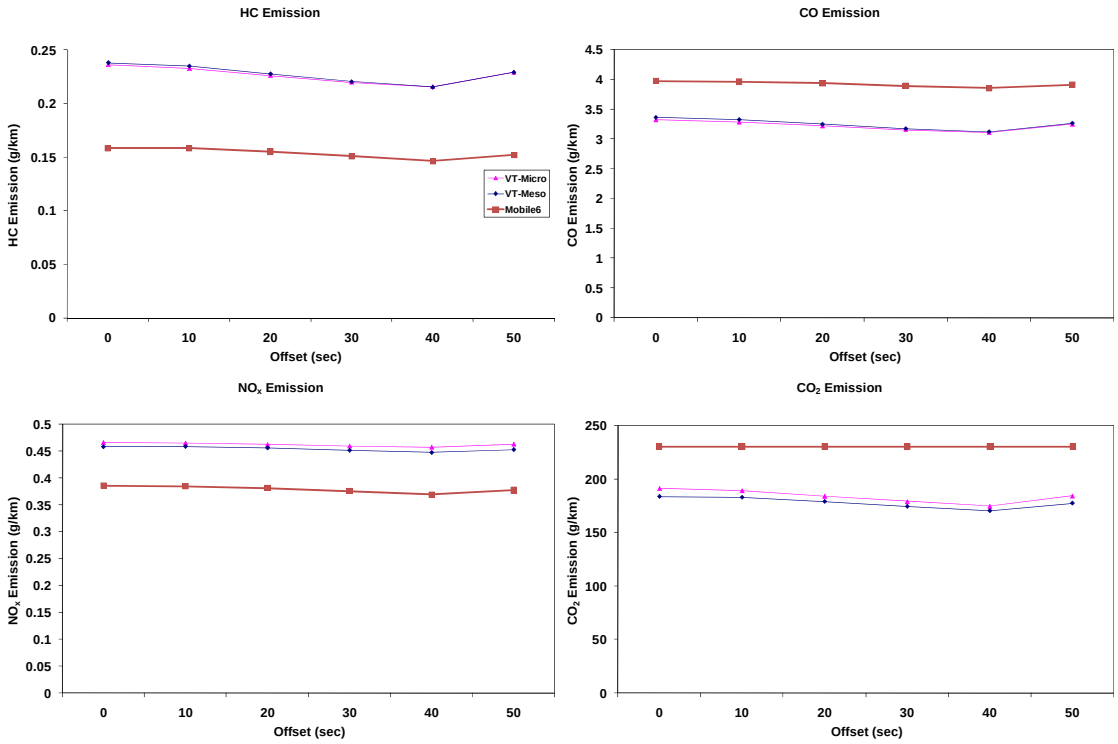

Figure 6-12: VT-Meso and MOBILE6 Comparison for Signal Control Scenario – LDV1

Chapter 7 : CONCLUSIONS AND RECOMMENDATIONS FOR FURTHER RESEARCH

7.1 Conclusions

This dissertation presents the development of VT-Meso fuel consumption and emission model that can be used to enhance current state-of-the-art vehicle fuel consumption and emission estimation. The conclusions of this research work can be summarized in three categories: characterization of typical driver deceleration behavior, VT-Meso model framework, and VT-Meso model application.

7.1.1 Typical Driver Deceleration Behavior

This study characterizes the typical driver deceleration behavior. Summary conclusions are:

- The deceleration rate increases when the speed decreases; drivers tend to decelerate harder at the end of the deceleration event, and thus the deceleration rate is speed-dependent.
- The deceleration rate frequency distributions do not follow the normal distribution with a skewed distribution. Specifically, the deceleration rates of most drivers are typically greater than the mean rate.
- The average driver deceleration rate is around 1.50 m/s^2 and the use of a constant deceleration rate over the entire deceleration maneuver appears to be adequate for environmental modeling purposes.

7.1.2 VT-Meso Framework for Estimating Hot Stabilized Light-Duty and High-Emitting Vehicle Emission Rates

This study develops a framework for modeling vehicle fuel consumption and emission mesoscopically. The proposed model is intended for use as a post-processor of traffic simulation models for the estimation of energy and environmental impacts of traffic operational projects including intelligent transportation system (ITS) applications. The proposed model was validated against the VT-Micro model and laboratory measurements. The results demonstrate that:

- The model provides an excellent match both in terms of absolute emission rates and cyclic trends with the microscopic model estimates and laboratory measurements.
- An analysis of predicted fuel consumption and emission rates for various deceleration rates indicates very little sensitivity to changes in the deceleration rate. The main impact of considering varying deceleration rates is therefore not to improve predicted estimates, but to determine the feasibility of a given scenario as changes in deceleration rates affect the deceleration distance and the distance that can be used to accelerate.
- The results indicate that the model is sensitive to the vehicle acceleration rate that is assumed and thus should be calibrated to driver and facility specific conditions.

7.1.3 VT-Meso Model Validation

This study compare the VT-Meso and VT-Micro model fuel consumption and emission estimates for four simulation scenarios including stop sign, signal control, partial stop, and ramp scenarios. The results demonstrated that the VT-Meso model provides an excellent match to the microscopic model estimates in terms of both absolute emission rates and cyclic trends. Specifically, this model provides close estimates for the stop sign, signal control, and ramp scenarios. On the other hand, the model predictions were less accurate in the partial stop scenario, especially in the case of CO emissions. The inaccuracies are partly attributed to the non-linear relationship between vehicle emissions and vehicle speed and errors in the construction of synthetic drive cycles.

The estimates from the VT-Meso model cannot be expected to always match estimates from microscopic models because of differences in the underlying drive cycles (the VT-Meso model constructs simplistic drive cycles). The model, however, constitutes an interesting alternative to existing models for cases in which detailed speed and acceleration data are not available. These results indicate that the VT-Meso model framework is sufficient for operational level comparisons. The study also demonstrates the need to perform additional tests to evaluate more precisely the effect of fractional stops on vehicle emissions or to more accurately convert partial stops into equivalent full stops for the purpose of estimating vehicle fuel consumption and emission rates.

7. 2 Recommendations for Further Research

The following areas of research should be pursued to expand the current research work on mesoscopic fuel consumption and emission modeling.

- Future research is required to investigate the relationship between speed and deceleration rate. The variable deceleration rate can be used to construct more accurate synthetic driving cycle.
- Further research should be conducted to determine how speed variability can be accounted for in the fuel consumption and emission estimation processes without requiring second-by-second analysis of speed and acceleration profiles.
- Further research can also be conducted to characterize typical speed variability for different facility types (collectors, arterials and freeways) and different levels of congestion. Such research would in turn allow the development of improved factors or equations for converting speed variations, stop-and-go patterns, and partial stops into equivalent number of stops for the purpose of estimating vehicle fuel consumption and emissions.
- The existing model also requires further enhancement to include diesel vehicles, and to consider the impact of cold-starts on fuel consumption and emissions.

BIBLIOGRAPHY

Ahn, K., H. Rakha, et al. (2004). "Microframework for modeling of high-emitting vehicles." Transportation Research Record. n 1880 2004: 39-49.

Ahn, K., H. Rakha, et al. (2002). "Estimating vehicle fuel consumption and emissions based on instantaneous speed and acceleration levels." Journal of Transportation Engineering **128**(2): 182-190.

Ahn, K., A. Trani, et al. (1999). Microscopic fuel consumption and emission modeling. Presented at 78th Annual Meeting of the Transportation Research Board, Washington, D.C.

Akcelik, R. (1985). "An Interpretation of the parameters in the Simple Average Travel Speed Model of Fuel Consumption." Australian Road Research **15**: 46-49.

An, F., M. Barth, et al. (1997). "Development of a Comprehensive Modal Emissions Model: Operating Under Hot-Stabilized Conditions." Transportation Research Record (1587): 52-62.

An, F. and M. Ross (1993). Model of Fuel Economy with applications to Driving Cycles & Traffic Management. Presented at 72nd Annual Meeting of the Transportation Research Board, Washington, D.C.

Atkinson, R. (1990). "Gas-Phase Tropospheric Chemistry of Organic Compounds." Environ **24**: 1-41.

Bachman, W., W. Sarasua, et al. (1996). "Geographic information framework for modeling mobile-source emissions." Transportation Research Record (1551): 123-133.

Bachman, W., W. Sarasua, et al. (2000). "Modeling regional mobile source emissions in a geographic information system framework." Transportation Research Part C: Emerging Technologies **8**: 205-229.

Barth, M., F. An, et al. (2000). Comprehensive modal emission model (CMEM), version 2.0 user's guide. Riverside, CA.

Brackstone, M. A., B. Sultan, et al. (2000). "Findings on the approach process between vehicles." Transportation Research Record(1724): 21-28.

CARB (1991). Methodology to Calculate Emission Factors for On-Road Vehicle. Sacramento, CA, California Air Resource Board.

Chang, M., L. Evans, et al. (1981). "Trip Time Versus Stop Time and Fuel Consumption Characteristics in Cities." Transportation Science **15**(3): 183-209.

Ding, Y. and H. Rakha (2002). "Trip-based explanatory variables for estimating vehicle fuel consumption and emission rates." Journal of Water, Air, and Soil Pollution: Focus **2**(5-6): 61-77.

Dion, F., H. Rakha, et al. (2004). "Comparison of delay estimates at under-saturated and over-saturated pre-timed signalized intersections." Transportation Research Part B-Methodological **38**(2): 99-122.

EPA (1993). Federal Test Procedure Review Project: Preliminary Technical Report. Ann Arbor, Michigan, Office of Air and Radiation.

EPA (1994). User's Guide to MOBILE 5 (Mobile Source Emission Factor Model). Ann Arbor, Michigan.
EPA (1996). "High-Tech I/M Test Procedures, Emission Standard, Quality Control Requirements, and Equipment Specifications: IM240 and Functional Evaporative Systems Tests, Revised Technical Guidance (Draft)."
EPA (2002). User's Guide to Mobile 6, Mobile Source Emission Factor Model. Ann Arbor, Michigan.
Evans, L., L. Herman, et al. (1976). "Multivariate Analysis of Traffic Factors Related to Fuel Consumption in Urban Driving." Transportation Science **10**(2): 205-215.
Evans, L. and R. Herman (1978). "Automobile Fuel Economy on Fixed Urban Driving Schedules." Transportation Science **12**(2): 137-152.
Glover, E. L. and J. W. Koupal (1999). Determination of CO basic emission rates, OBD and I/M effects for tier1 and later LDVs and LDTs. Ann Arbor, Michigan, US EPA.
Hellman, K. H. and R. M. Heavenrich (2001). Light-Duty Automotive Technology and Fuel Economy Trends; 1975 through 2001, US EPA.
INRO Consultants (1996). EMME/2 User's Manual, Release 8. Montreal, CA, INRO Consultants.
Koupal, J. W. and E. L. Glover (1999). Determination of NOx and HC basic emission rates, OBD and I/M effects for tier1 and later LDVs and LDTs. Ann Arbor, Michigan., US EPA.
M. Van Aerde & Assoc., L. (2002). INTEGRATION release 2.30 for windows: user's guide - volume I: fundamental features.
M. Van Aerde & Assoc., L. (2002). "INTEGRATION release 2.30 for windows: user's guide - volume II: advanced features."
Nizich, S. V. and United States. Environmental Protection Agency. Office of Air Quality Planning and Standards. (1994). National air pollutant emission trends, 1900-1993. Research Triangle Park, NC, U.S. Environmental Protection Agency Office of Air Quality Planning and Standards.
NRC (1995). Expanding metropolitan highways : implications for air quality and energy use. Washington, D.C., Transportation Research Board National Research Council.
Rakha, H. and K. Ahn (2004). "Integration modeling framework for estimating mobile source emissions." Journal of Transportation Engineering **130**(2): 183-193.
Rakha, H., K. Ahn, et al. (2003). "Microscopic modeling of vehicle start emissions." Transportation Research Record. n 1842 2003: 29-38 03-2288.
Rakha, H., K. Ahn, et al. (2004). "Development of VT-Micro model for estimating hot stabilized light duty vehicle and truck emissions." Transportation Research, Part D: Transport & Environment **9**(1): 49-74.
Rakha, H., K. Ahn, et al. (2003). The VT-micro framework for modeling of hot stabilized light duty vehicle and truck emissions. 82nd Annual Meeting of the Transportation Research Board, Washington DC.

Rakha, H. and B. Crowther (2002). "Comparison of Greenshields, Pipes, and Van Aerde car-following and traffic stream models." Transportation Research Record. n 1802 2002: 248-262 02-2143.
Rakha, H. and Y. Ding (2003). "Impact of stops on vehicle fuel consumption and emissions." Journal of Transportation Engineering **129**(1): 23-32.
Rakha, H., F. Dion, et al. (2001). "Using global positioning system data for field evaluation of energy and emission impact of traffic flow improvement projects: Issues and proposed solutions." Transportation Research Record. n 1768 2001: 210-223 01-2427.
Rakha, H., Y.-S. Kang, et al. (2001). "Estimating vehicle stops at undersaturated and oversaturated fixed-time signalized intersections." Transportation Research Record. n 1776 2001: 128-137 01-2353.
Rakha, H. and I. Lucic (2002). "Variable power vehicle dynamics model for estimating maximum truck acceleration levels." Journal of Transportation Engineering **128**(5): 412-419.
Rakha, H., I. Lucic, et al. (2001). "Vehicle dynamics model for predicting maximum truck acceleration levels." Journal of Transportation Engineering **127**(5): 418-425.
Rakha, H., M. Snare, et al. (2004). "Vehicle dynamics model for estimating maximum light-duty vehicle acceleration levels." Transportation Research Record. n 1883 2004: 40-49.
Rakha, H., M. Van Aerde, et al. (2000). "Requirements for evaluating traffic signal control impacts on energy and emissions based on instantaneous speed and acceleration measurements." Transportation Research Record. n 1738 2000: 56-67 00-1133.
Rakha, H., H. Yue, et al. (2006). "VT-MESO MODEL FRAMEWORK FOR ESTIMATING HOT STABILIZED LIGHT DUTY VEHICLE FUEL CONSUMPTION AND EMISSION RATES." Transportation Research Board
Rakha, H. A. and M. W. Van Aerde (1996). "Comparison of simulation modules of TRANSYT and integration models." Transportation Research Record(1566): 1-7.
Richardson, A. J. and R. Akcelik (1981). "Fuel consumption Models and Data Needs for the design and Evaluation of Urban Traffic System." Australian Road Research Board **ARR 124**(September).
Snare, M. (2002). Dynamic model for predicting maximum and typical acceleration rates of passenger vehicles. Department of Civil and Environmental Engineering. Blacksburg, VA, Virginia Tech. **Master Thesis**.
The Seider Group (1997). MINUTP Technical User's Manual. Palo Alto, CA, The Seider Group.
The Urban Analysis Group (1992). TRANPLAN, Version 7.1. Danville, CA, The Urban Analysis Group.
Van Aerde, M., B. Hellinga, et al. (1996). INTEGRATION: an overview of traffic simulation features. 75th Transportation Research Board Annual Meeting, Washington, DC.

Van Aerde, M. and S. Yagar (1988). "Dynamic integrated freeway/traffic signal networks: a routing-based modeling approach." Transportation Research **22A**(6): 445-453.
Van Aerde, M. and S. Yagar (1988). "Dynamic integrated freeway/traffic signal networks: problems and proposed solutions." Transportation Research **22A**(6): 435-443.
Waston, H. C., E. E. Milkins, et al. (1980). "A Simplified Method for Quantifying Fuel Consumption of Vehicles in Urban Traffic." SAE-Austria **40**(1): 6-13.
West, B. H., R. N. McGill, et al. (1997). Development of data-based light-duty modal emissions and fuel consumption models. Proceedings of the 1997 International Fall Fuels & Lubricants Meeting & Exposition, Tulsa, OK, USA, General and Advanced Emissions SAE Special Publications. v 1296 Oct 1997. SAE, Warrendale, PA, USA.
Wolf, J., R. Guensler, et al. (1998). "High-emitting vehicle characterization using regression tree analysis." Transportation Research Record(1641): 58-65.